Effects of Low Magnitude High Frequency Vibration on Blood Flow and Angiogenesis during Fracture Healing in Normal and Osteoporotic Bones

SUN, Minghui

A Thesis Submitted in Partial Fulfillment

of the Requirements for the Degree of

Doctor of Philosophy

in

Orthopaedics and Traumatology

The Chinese University of Hong Kong

August, 2011

UMI Number: 3504731

UMI
Dissertation Publishing

ProQuest

Thesis/Assessment Committee

Professor Ling QIN   (Chair)

Professor Kwok-Sui LEUNG   (Thesis Supervisor)

Professor Wing-Hoi CHEUNG   (Thesis Co-supervisor)

Professor Kwok-Pui FUNG   (Committee Member)

Professor Yu HUANG   (Committee Member)

Professor Volker ALT   (External Examiner)

ACKNOWLEDGEMENT

study. I also thank my colleagues in the Affiliated Drum Tower Hospital of Nanjing University Medical School for their encouragement and help.

Last, I would like to acknowledge General Research Fund (Ref. No. 462708) from the University Grants Committee of Hong Kong.

ABSTRACT

INTRODUCTION

Bone fracture, especially osteoporotic fracture, has become a major health issue due to its increase in morbidity, mortality and the financial burden of medical care. More and more attention has been focused on the enhancement of fracture healing and new biophysical mechanical stimulation therapies have been given to the study of fracture healing in osteoporotic bone. Our previous studies confirmed low magnitude high frequency vibration (LMHFV) (magnitude=0.3g, frequency=35Hz), providing non-invasive, systemic mechanical stimulation, can promote both normal and osteoporotic fracture healing in rats, however, the mechanism of its positive osteogenic effect is still unclear.

It is indicated that a good blood supply is a prerequisite for initiating the fracture repair, and angiogenic response is demonstrated to be crucial yet impaired during the osteoporotic fracture healing. It was also reported whole body vibration was effective in enhancing peripheral blood circulation through increasing the muscle pump function. Therefore, we hypothesized LMHFV could enhance the blood flow of hind limb and promote the angiogenesis at the fracture site in both normal and osteoporotic rats, hence to accelerate the healing process.

MATERIALS AND METHODOLOGY

Nine-month-old ovariectomy-induced (OVX) and sham-ovariectomized (Sham) rats were created closed fractures on right femoral mid-shaft. Five days after fracture

surgery, totally 72 rats were randomized into LMHFV (Sham-V, OVX-V) (35Hz, 0.3g, 20min/day, 5days/week) and control (Sham-C, OVX-C) groups. The external callus width (CW) and callus area (CA) were measured by radiography weekly to monitor the status of fracture healing. At weeks 2, 4 and 8 post-treatment, pulsed-wave Doppler ultrasonography was utilized to measure the blood flow velocity of injured femoral artery. Three-dimensional high frequency power Doppler ultrasonography (3D-HF-PDU) was adopted for assessing the microcirculation at the fracture site. After that, the vascular system of each animal was perfused with Microfil contrast agent and the fractured femur was subjected to microCT scanning for osseous tissue and microvasculature analysis at the peri-fracture region. Immunohistochemistry was performed to evaluate the expression of vascular endothelial growth factor (VEGF) in external callus. One-way ANOVA were used for comparison among groups. Significance level was set at $p<0.05$.

RESULTS

(1) Vibration groups had larger CW and CA than the corresponding controls, and higher CW and CA was also observed in Sham-C than OVX-C. OVX-V had the largest CW and CA than other groups in the early phase of fracture healing.

(2) Pulsed-wave Doppler showed an increasing blood flow velocity of injured femoral artery from weeks 2 to 8. At each time point, it indicated a higher blood flow velocity in vibration groups than control ones (week 2: OVX-V > OVX-C, $p=0.030$; week 4: Sham-V > Sham-C, $p=0.020$; OVX-V > OVX-C, $p=0.012$). A lower flow

velocity was found in OVX rats as compared with Sham ones (week 8: Sham-V> OVX-V, p=0.006; Sham-C > OVX-C, p=0.005).

(3) 3D-HF-PDU demonstrated an enhanced blood volume at the fracture site by LMHFV treatment compared to the controls during the early phase of fracture healing (week 2: Sham-V > Sham-C, p=0.021). The microcirculation of OVX groups was inferior to the corresponding Sham ones.

(4) MicroCT-based microangiography also confirmed increased vascular volume (VV) of fracture site in vibration groups (week 2: OVX-V > OVX-C, p=0.009; week 4: OVX-V > OVX-C, p=0.034), and an inferior level of angiogenesis was found in OVX groups as compared with Sham groups (week 2: Sham-V > OVX-V, p=0.014; Sham-C > OVX-C, p=0.014). The ratio of vascular volume to total tissue volume (VV/TV) showed a similar trend as above. Quantitative analysis of TV, bone volume (BV), high-density bone volume (BV_h) and low-density bone volume (BV_l), indicated better callus formation and mineralization in vibration groups than in control ones. The capacity of osteogenesis (by TV, BV, BV_h, BV_h/TV) was impaired in OVX groups as compared with Sham ones. These findings were consistent with angiogenesis results. A linear positive correlation between TV and VV was detected, as well as BV and BV_l. A significant correlation was found between BV_l and VV (r=0.7738, p<0.01). Interestingly, A higher percentage of increase in microvasculature was observed in OVX groups (week2: +25.7%; week 4: +57.1%) than corresponding

Sham groups (week2: +13.2%; week 4: +2.2%). OVX-V also had a higher percentage of increase in TV than Sham-V.

(5) Immunohistochemistry assessment also indicated higher level of VEGF expressions in vibration groups than controls within external callus in the early phase of fracture healing, and the OVX groups had lower level of expressions as compared with Sham ones.

DISCUSSION

Ovariectomy-induced osteoporotic rats had suboptimal femoral blood supply than normal rats because estrogen deficiency would increase blood viscosity, thus decreased the blood flow velocity. LMHFV could reduce the peripheral resistance by widening small vessels in muscles, which resulted in an increase of blood flow velocity. Vibration also promoted angiogenesis in both normal and osteoporotic fractures. This might be vibration increased the blood flow shear forces at vascular endothelium, which augmented the functions of VEGF by up-regulating VEGFR-2. The percentage of increase in angiogenesis by LMHFV in OVX groups was higher than Sham ones, which suggested osteoporotic bone might have higher sensitivity of angiogenic response to mechanical stimulation. With the consistent findings between angiogenesis and osteogenesis and the significant positive linear correlation between VV and BV_1, it indicated angiogenesis was associated with osteogenesis of fracture healing process, especially in the early stage, which suggested LMHFV therapy should be applied from the early healing phase.

CONCLUSION

LMHFV can augment blood flow of fractured hind limb and enhance angiogenesis at the fracture site with different extent in normal and osteoporotic rats, which indicates the promotion of both systemic and local blood circulation is one of the mechanisms for LMHFV to accelerate the fracture healing.

中文摘要

引言

鉴于发病率、致死率及其医疗费用的不断增加，骨折，尤其是骨质疏松性骨折，已成为当今日益严峻的社会健康问题。开发促进骨折愈合的方案开始越来越多地受到关注。作为新型生物物理治疗，机械刺激已被运用到研究增进骨质疏松性骨折的愈合中来。我们的前期研究证实，低能高频振动（LMHFV）（振幅 0.3g，振动频率 35Hz）可提供非侵入性、全身性机械刺激，促进大鼠普通骨折及骨质疏松性骨折的愈合。然而，迄今关于其正性成骨作用的机理尚不明晰。

前人研究表明，良好的血供是启动骨折修复的必要条件，血管新生在骨折愈合中具有决定性作用。人们发现，骨质疏松性骨折的血管新生能力在一定程度上受损。同时，有报道显示全身振动可通过增强肌肉泵功能来促进外周血液循环。因此，我们提出假设，低能高频振动可以通过增进下肢血供与促进骨折段的血管新生，来加速普通骨折及骨质疏松性骨折的愈合。

材料与方法

本实验采用卵巢切除术来诱导骨质疏松性（OVX）大鼠模型，假切除组（Sham）作为正常骨量模型组。至 9 月龄，对两组大鼠行右侧闭合性股骨干骨折造模术。术后 5 日，将 72 只大鼠随机分成振动治疗组（Sham-V、OVX-V，振幅为 0.3g，频率为 35Hz，每日治疗 20 分钟，每周治疗 5 日）与假治疗对照组（Sham-C、OVX-C）。每周采集 X 线片，测量股骨骨折段外骨痂宽度（CW）及其面积（CA），观察骨折愈合进展。分别在开展治疗后第 2、4、8 周，采用脉冲多普勒超声检测大鼠伤侧股动脉血流速度。应用三维高频能量多普勒超声（3D-HF-PDU）评测骨折段微循环状况。随后，向大鼠血管系统灌注 Microfil

增强造影剂，取伤侧股骨标本行三维显微 CT 扫描，以评估骨折段骨组织与微血管形成情况。运用免疫组织化学技术测定外骨痂血管内皮生长因子（VEGF）的表达。本研究采用单向方差分析对各组间差异进行统计学分析，p 值小于 0.05 示为有显著性差异。

结果

(1) 振动治疗组骨痂宽度、面积较对照组增加，假卵巢切除对照组比卵巢切除对照组骨痂尺寸大。然而卵巢切除振动组在愈合早期骨痂宽度与面积均大于其他组。

(2) 脉冲多普勒超声检查显示从治疗后第 2 周至第 8 周，各组大鼠的股动脉血流速度逐渐增加。在各时间点，振动治疗组血流速度高于假治疗组（第 2 周：OVX-V > OVX-C，p=0.030；第 4 周： Sham-V > Sham-C，p=0.020；OVX-V > OVX-C；p=0.012）。卵巢切除大鼠血流速度低于假切除大鼠（第 8 周：Sham-V > OVX-V，p=0.006; Sham-C > OVX-C，p=0.005）。

(3) 三维高频能量多普勒超声评估显示，振动治疗组在愈合早期骨折段的血容量较对照组增高（第 2 周：Sham-V > Sham-C，p=0.021）。卵巢切除组骨折段微循环血量较相应假切除组为低。

(4) 显微 CT 微血管造影检查亦证实振动治疗组骨折段血管容积（VV）较对照组增加（第 2 周：OVX-V>OVX-C，p=0.009；第 4 周：OVX-V>OVX-C，p=0.034）。结果还发现，卵巢切除组骨折段血管新生水平较假切除组低（第 2 周：Sham-V>OVX-V，p=0.014；Sham-C>OVX-C，p=0.014)。血管容积与骨折段组织总体积的比率（VV/TV）亦呈类似趋势。骨折段骨组织定量（TV、BV、BVh、

BVl）表明，振动治疗对骨痂形成、矿化均较对照组增强，而卵巢切除组较假切除组各阶段成骨能力降低。骨组织定量变化与血管新生趋势保持一致。分析表明，TV、BV、BVl与VV均呈线性正相关，且BVl与VV有显著相关性(r=0.7738，p<0.01)。我们发现振动治疗后，卵巢切除组大鼠骨折端血管新生的增加比率（第2周：+25.7%；第4周：+57.1%）较假切除组（第2周：+13.2%；第4周：+2.2%）为高。同时，骨组织定量也有类似发现，卵巢切除组振动治疗后 TV 增长率比非卵巢切除振动组高。

(5) 免疫组织化学染色显示，在骨折愈合前期，振动治疗组骨折段血管内皮生长因子（VEGF）的表达较对照组升高，而卵巢切除组大鼠 VEGF 表达量较假切除组为低。

讨论

卵巢切除诱导骨质疏松的大鼠股动脉血供较非骨质疏松大鼠为低，可能是因为卵巢切除引起雌激素缺乏，导致血液粘稠度增加，从而使得血流速度下降。低能高频振动治疗可以通过扩张肌肉微血管，降低外周血管阻力，进而加快血流速度。振动治疗对非骨质疏松及骨质疏松性大鼠骨折段微血管新生均有促进作用，原因可能是振动刺激增强了血流在血管内皮处的剪切力，从而通过上调 VEGF-2 型受体，增进 VEGF 的成血管功能。振动治疗后，卵巢切除组血管新生增高比率较假切除组高，提示骨质疏松性骨折血管新生反应对机械刺激的敏感度可能较正常骨为高。鉴于骨折段成血管与成骨定量结果趋势基本一致，且新生血管容积与新生低密度骨具有显著正相关性，我们认为血管新生在骨折愈合过程中与成骨密切相关，尤其在愈合早期阶段，提示振动治疗应及早施行。

结论

在正常非骨质疏松性及骨质疏松性骨折愈合过程中，低能高频振动可以不同程度地增强骨折下肢的血供，并能促进骨折段血管新生。本研究表明，对全身及局部循环的促进作用可能是低能高频振动治疗加速骨折愈合的重要机制之一。

PUBLICATIONS

Papers:

1. Sun MH, Leung KS, Zheng YP, Huang YP, Wang LK, Qin L, Leung AH, Chow SK, Cheung WH. Three-dimensional High Frequency Power Doppler Ultrasonography for the Assessment of Microvasculature during Fracture Healing in a Rat Model. J Orthop Res. 2011. [Epub ahead of print]

2. Cheung WH, *Sun MH, Zheng YP, Chu CW, Leung HC, Qin L, Wei FY, Leung KS. Low Magnitude High Frequency Vibration Promotes Fracture Healing through Stimulating Angiogenesis at the Fracture Site in a Rat Model. (2011, submitted)

3. Cheung WH, Chow SK, Sun MH, Qin L, Leung KS. Low-intensity pulsed ultrasound accelerated callus formation, angiogenesis and callus remodeling in osteoporotic fracture healing. Ultrasound Med Biol. 2011. 37(2):231-8.

4. Fung CH, Cheung WH, Sun MH, Pounder NM, de Ana FJ, Leung KS. Fracture within the Mid-Near Field of Low Intensity Pulsed Ultrasound (LIPUS) Heals Better. (2011, submitted)

Co-first author and co-corresponding author

Conference Oral Presentations:

1. <u>Sun MH</u>, Leung KS, Chu CW, Zheng YP, Qin L, Wei FY, Cheung WH. Stimulatory Effects of Low Magnitude High Frequency Vibration on Blood Flow and Angiogenesis at Fracture Site in Rat Model. The 57th Annual Meeting of the Orthopaedic Research Society (ORS). 2011. Long Beach, CA, USA.

2. Wei FY, Leung KS, Qin L, <u>Sun MH</u>, Cheung WH. Low Intensity Pulsed Ultrasound Increases Stormal cell-derived Factor 1 Signaling in Rat Mesenchymal Stem Cells. The 57th Annual Meeting of the Orthopaedic Research Society (ORS). 2011. Long Beach, CA, USA.

3. <u>Sun MH</u>, Leung KS, Zheng YP, Qin L, Wei FY, Cheung WH. Low Magnitude High Frequency Vibration Promotes Fracture Healing by Stimulating Angiogenesis in a Rat Model. The 5th International Congress of Chinese Orthopaedic Association (COA). 2010. Chengdu, China.

4. <u>Sun MH</u>, Cheung WH, Chu CW, Leung KS. Low Magnitude High Frequency Vibration Augments Blood Flow and Angiogenesis at Fracture Site. The 4th International Congress of Chinese Orthopaedic Association (COA). 2009. Xiamen, China.

Conference Poster Presentations:

1. Sun MH, Leung KS, Zheng YP, Huang YP, Wang LK, Qin L, Cheung WH. Use of Three-dimensional High Frequency Power Doppler Ultrasonography for Assessing Angiogenesis during Fracture Healing in Rats. The 5th International Congress of Chinese Orthopaedic Association (COA). 2010. Chengdu, China.

2. Wei FY, Leung KS, Qin L, Sun MH, Cheung WH. Low Intensity Pulsed Ultrasound Promotes Mesenchymal Stem Cells Homing through SDF-1/CXCR4 Pathway. The 5th International Congress of Chinese Orthopaedic Association (COA). 2010. Chengdu, China.

3. Cheung WH, Leung KS, Chu CW, Qin L, Sun MH. Low Magnitude High Frequency Vibration Accelerates Fracture Healing Through Enhancing Angiogenesis at Fracture Site. The 7th Combined Meeting of the Orthopaedic Research Societies (CORS). 2010. Kyoto, Japan.

4. Sun MH, Leung KS, Chu CW, Qin L, Cheung WH. Stimulating Effect of Low Magnitude High Frequency Vibration on Angiogenesis during Fracture Healing in Rat Model. International Society for Fracture Repair (ISFR) 12th Biennial Conference. 2010. London, UK.

5. Sun MH, Cheung WH, Chu CW, Qin L, Leung KS. Low Magnitude High Frequency Vibration Therapy Augments Blood Flow and Angiogenesis at Fracture Site in Rat Model. The 56th Annual Meeting of the Orthopaedic Research Society (ORS). 2010. New Orleans, LA, USA.

6. <u>Sun MH</u>, Cheung WH, Qin L, Leung KS. Vibration Enhances Blood Flow and Angiogenesis at Fracture Site in Rat Model. The 29th Annual Congress of the Hong Kong Orthopaedic Association (HKOA). 2009. Hong Kong SAR, China.

LIST OF ABBREVIATIONS

2-D	Two-dimensional
3-D	Three-dimensional
3D-HF-PDU	Three-dimensional high frequency power Doppler Ultrasonography
ANOVA	Analysis of variance
A-P	Anterioposterior view
BMC	Bone mineral content
BMD	Bone mineral density
BMP	Bone morphogenetic proteins
BV_h	Volume of high-density bone
BV_l	Volume of low-density bone
BV	Total bone volume
CA	Radiographic callus area
Cl.Ar	Callus area in immunostaining sections
CUHK	The Chinese University of Hong Kong, Hong Kong SAR, China
CW	Radiographic callus width
DAB	Diaminobenzidine tetrahydrochloride
ECM	Extracellular matrix
ECs	Endothelial cells
EPCs	Endothelial progenitor cells
FGF	Fibroblast growth factor
HIF	Hypoxia-inducible factor
IGF	Insulin-like growth factor
IHC	Immunohistochemistry
K-wire	Kirschner wire
L_5	The fifth lumbar vertebra
LASEC	The Laboratory Animal Services Center of CUHK
LIPUS	Low-intensity pulsed ultrasound
LMHFV	Low-magnitude high-frequency vibration

Micro-CT	Micro-computed tomography
MMPs	Matrix metalloproteinases
MRI	Magnetic resonance imaging
mRNA	Messenger ribonucleic acid
MSCs	Mesenchymal stem cells
OVX	Ovariectomy
OVX-C	Control group of osteoporotic rats
OVX-V	Vibration group of osteoporotic rats
PBS	Phosphate buffered saline
PDGF	Platelet-derived growth factor
PEMF	Pulsed electromagnetic field
PECAM-1	Platelet endothelial cell adhesion molecule-1
pO_2	Partial pressure of oxygen
PTH	Parathyroid hormone
PWH	The Prince of Wales Hospital, Hong Kong SAR, China
ROI	Region of interest
RFH	Right femoral head
RFS	Right femoral shaft
SD	Standard deviation
SD rat	Sprague-Dawley rat
Sham-C	Control group of non-osteoporotic rats
Sham-V	Vibration group of non-osteoporotic rats
TGF-β	Transforming growth factor-beta
TV	Total tissue volume
USA	The United States of America
VEGF	Vascular endothelial growth factor
VEGF.Ar	Area of VEGF expression in external callus
VOI	Volume of interest
VV	Vascular volume

INDEX FOR FIGURES

INDEX FOR TABLES

TABLE OF CONTENTS

CHAPTER 1

INTRODUCTION AND LITERATURE REVIEW

Bone is characterized physically by the fact that it is a hard, rigid and strong tissue, and microscopically by the presence of relatively few cells and much intercellular substance composed of collagen fibers and stiffening substances. All bones have a mechanical function providing attachment to various muscle groups. In addition, in some parts of the body, bones provide a protective function to vital structures - skull (brain), ribs (lungs, heart) and pelvis (bladder, pelvic viscera). Some bones retain their haematopoietic function in adults - vertebrae, iliac crests, proximal parts of femur and humerus. All bones serve as a reservoir of calcium and actively participate in calcium homeostasis of the body (1,2).

A bone fracture is defined as a break in the continuity of the bone. It can be the result of high force impact or stress, or trivial injury as a result of certain medical conditions that weaken the bones, such as osteoporosis, bone cancer, or osteogenesis imperfect (3-6). Both local and systemic variables influence the rate and degree of fracture healing. If the healing rate is slower than usual, it will result in delayed union. A complete cessation of the healing process, in which fibrous tissue is never replaced by bony matrix, is termed non-union. To promote the fracture healing has long been one of the major goals for orthopaedic surgeons and scientists.

In recent decades, with the penetrating scientific understandings on bone fractures, advances of managements to accelerate fracture healing have been largely developed and improved, concerning biological (7), mechanical (8,9) and biophysical (10-12) enhancements. Presented in this thesis are the studies on the effects and the probable action mechanisms of low magnitude high frequency vibration (LMHFV), a

novel noninvasive and systemic biophysical intervention, on normal and osteoporotic fracture healing. Introduction and literature review on the crucial concepts are provided in the first place, out of which come with the hypotheses and the study plan.

1.1 Fracture and Fracture Healing

1.1.1 Structural Types of Bone

Bone is a specialized type of connective tissue consisting of cells and an intercellular matrix. There are three cell types: (1) osteoblasts, the bone forming cells, (2) Osteocytes, the most abundant cell in bone, are actively involved in the routine turnover of bony matrix. (3) Osteoclasts, removes bone tissue which is known as bone resorption. The bone matrix is composed of: (1) organic matter, consisting of type I collagen fibres and glycoproteins, and (2) inorganic matter, made up of stiffening substances to resist bending and compression. The bone mineral is an analogue of crystals of calcium phosphate-hydroxyapatite $Ca_{10}(PO_4)_6(OH)_2$ (13-16).

Macroscopically, there are two types of bones: cortical (compact) bone and cancellous (spongy or trabecular) bone (13-16). Cortical bone is made up of a structure of Haversian systems or Osteons. Cancellous bone consists of a series of interconnecting plates of bone - the trabeculae. The surfaces of bone are covered by a layer of bone-forming cells and the following connective tissues: periosteum (outer layer) and endosteum (inner layer) The periosteum consists of an outer fibrous layer consisting of collagen fibers and fibroblasts, as well as an inner cambium layer composed of flattened cells - the osteoprogenitor cells. The endosteum lines the internal surface of bone. It is composed of osteoprogenitor cells and small amount of connective tissue. Bone marrow is the organ of haematopoiesis, containing connective tissue, blood vessels and numerous "marrow cells" - myelocytes, erythroblasts, giant cells and some fat cells (15). (Figure 1.1.1)

4

1.1.2 Blood Supply of Long Bone

The vascular anatomy of long bones is complex and reorganizes throughout growth until closure of the growth plate when it assumes its final form. A given long bone is supplied by 6 groups of arteries: (1) proximal epiphyseal arteries; (2) proximal metaphyseal arteries; (3) diaphyseal nutrient arteries singly or in pairs; (4) distal metaphyseal arteries; (5) distal epiphyseal arteries; and (6) periosteal arteries. (17,18) Branches of these are anastomosed so profusely with adjacent groups that they can substitute for each other and protect against infarction caused by failure of a single arterial pedicle. (Figure 1.1.2)

Nutrient arteries branch from the major systemic arteries, enter the diaphyseal cortex through the nutrient foramen, and then go into the medullary canal, branching into ascending and descending small arteries. These branch into arterioles in the endosteal cortex and supply at least the inner 2/3 of the mature diaphyseal cortex via vessels in the Haversian system. Metaphyseal-epiphyseal system arises from the periarticular vascular plexus. Periosteal system is composed primarily of capillaries that supply the outer 1/3 (at most) of the mature diaphyseal cortex. (19-21)

In bone, the volumetric capacity of the venous system is six- to eightfold greater than that of the arterial system. Blood is drained by perforating veins that empty into deep veins of the extremities. There are six major veins organized with the groups of arteries, and the large central venous sinus and its tributaries are drained by the nutrient vein. (17,18)

The vasculature of bone plays a prominent role in fracture healing. (17,19)Most

Haversian canals contain a single capillary, as do the cutting cones that mediate the remodeling of adult bone. The integrity of the capillary and sinusoidal networks of diaphyseal and metaphyseal marrow is essential for the orderly release of the cellular components of blood. (22-26)
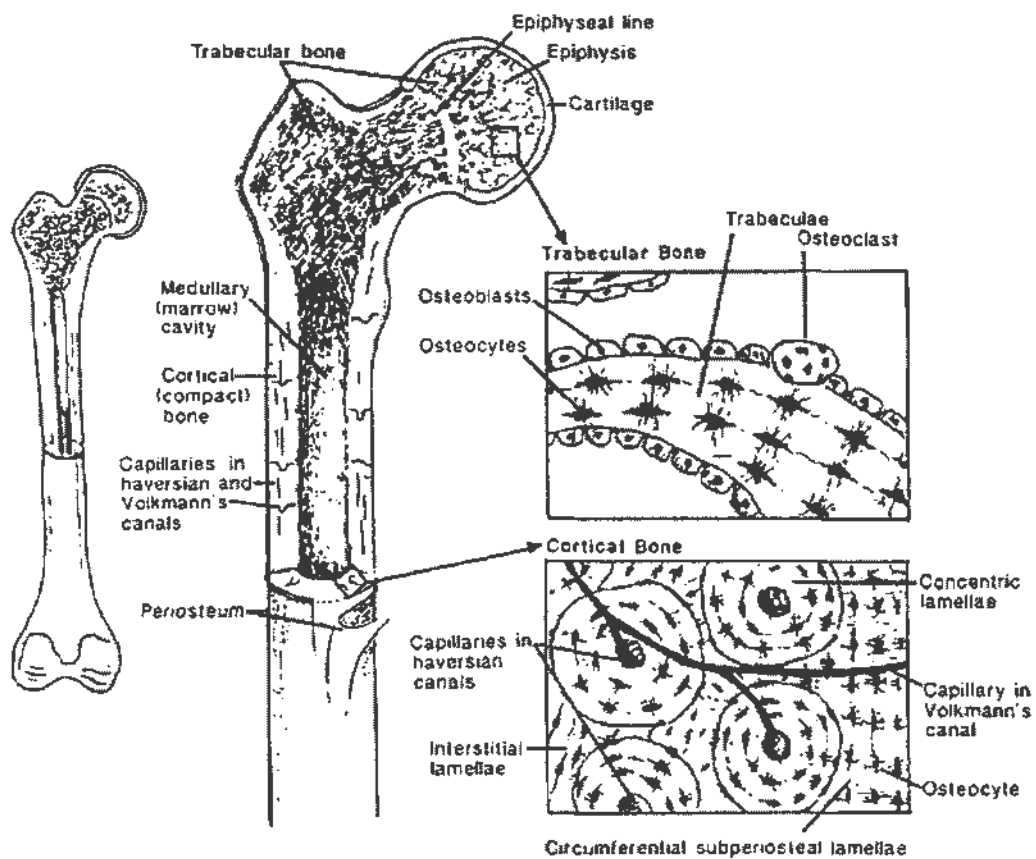
Figure 1.1.1 Sketch of the structure of a long bone (femur). Cortical bone consists of tightly packed osteons. Cancellous bone consists of a meshwork of trabeculae. Cortical bone resides in the diaphyses, while trabecular bone presents at the metaphyses and epiphyses. *(From Hayes W C , 1991 Biomechanics of cortical and trabecular bone: implications for assessment of fracture risk In: Mow VC, Hayes WC Basic Orthopaedic Biomechanics. Raven Press, New York, pp. 93–142.)*
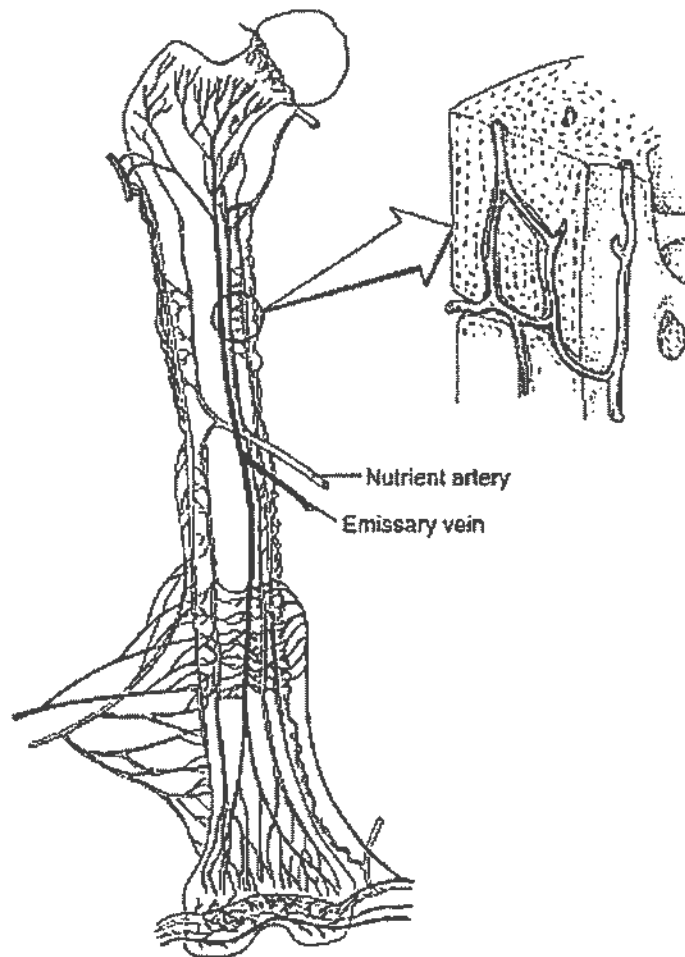
Figure 1.1.2 Blood supply to long bone. Bone receives 5-10% of the cardiac output. Long bones receive blood from three systems: (1) nutrient artery; (2) metaphyseal-epiphyseal artery; and (3) periosteal artery. *(From Brinker MR, Miller MD: Fundamentals of Orthopaedics, p4. Philadelphia, WB Saunders, 1999.)*

1.1.3 Mechanism of Fracture Healing

1.1.3.1 Histological and Cellular Changes during Fracture Healing

Fracture healing is a highly orchestrated process comprising a series of biological repair stages intimately linked with one another.

Primary fracture healing involves anatomic reduction of the fracture fragments, optimization of the strain environment, and a biological response in which the cortex directly attempts to reestablish its own continuity. These are remodeling units consisting of osteoclasts that resorb cortical bone, thereby permitting angiogenesis and stem cell deposition into the fracture site, and progenitor cells differentiate into osteoblasts that secrete matrix and bridge the fracture gap. This process enlists minimal participation from the periosteum, external soft tissues, and the bone marrow (3,4).

If rigid internal fixation is not provided and micromotion exists at the fracture site, secondary fracture healing occurs (3,27-31). The response of the periosteum and adjacent soft tissues to bony injury forms the basis of secondary fracture healing. It involves both intramembranous and endochondral ossification that proceed concurrently.

Within the first 7 days after fracture, an inflammatory response takes place at the fracture site as demonstrated by the invasion of macrophages, polymorphonuclear leukocytes, and lymphocytic cells (3,4,30,32). These cells secrete proinflammatory cytokines including interleukin-1 (32), interleukin-6 (33,34), and tumor necrosis factor-α (TNF-α) (35,36). At the same time, peptide signaling molecules such as

members of the transforming growth factor-beta (37-39) super gene family, including all of the bone morphogenetic proteins (BMPs) (40-45), as well as platelet-derived growth factor (PDGF), are triggered (4,30,46). (Figure 1.1.3.1-A)

The first 7 to 10 days of healing involve a process of chondrogenesis in which two major biochemical constituents are secreted: type II collagen and a variety of proteoglycans. Type II collagen provides the initial structure of the fracture callus while the proteoglycans mediate hydration of the newly formed tissue and control the rate and physical chemistry of the mineralization process (47,48). By 14 days, protein synthesis is complete and hypertrophic chondrocytes release calcium into the extracellular matrix in order to precipitate with (49-52). Preliminary fracture callus is composed largely of cartilage, and once enough cartilaginous callus is formed, mineralization takes place. (Figure 1.1.3.1-B)

By 3 to 4 weeks after fracture, the callus is composed mostly of calcified cartilage. This tissue becomes a target for chondroclasts, multinucleated cells specialized in the resorption of calcified tissues. The chondrocytes undergo apoptosis during endochondral fracture healing and this process is identical to that occurred in the lower hypertrophic zone of the growth plate (53,54). As chondroclasts remove the calcified cartilage, blood vessels penetrate the tissue and bring perivascular mesenchymal stem cells that differentiate into osteoprogenitor cells and then osteoblasts (55-60). This remodeling of the primary soft callus to woven bone results in fracture union by approximately 28 to 35 days (61-65). At this time, osteoclasts populate the tissue and remodel the callus, converting it to lamellar bone. (Figure

1.1.3.1-C)

1.1.3.2 Molecular Mechanism of Fracture Healing

The events of fracture healing involve a well-coordinated series of events leading to chondrogenesis, the removal of calcified cartilage, its replacement with bone, and the remodeling of that bone to a lamellar bone structure with the capacity to support mechanical loads. Several growth factors and cytokines are involved in the process of bone repair and remodeling. The function of these growth factors is to interact in a coordinated fashion and to influence each other's expression. While the molecular basis for fracture healing is far from understood, key regulators such as angiogenic factors (VEGF and HIF-1α) (45,66-70), the chondrogenic and osteogenic factors (BMPs and GDFs) (40,43,71-74), and the regulators of bone remodeling (members of the TNF-α family) (75) are involved in a coordinated manner. The ability to further elucidate these mechanisms and to develop technologies to control their function could play an important role in the future of fracture management.

Torn periosteum
Haematoma
Necrotic marrow
Dead bone
Intact periosteum
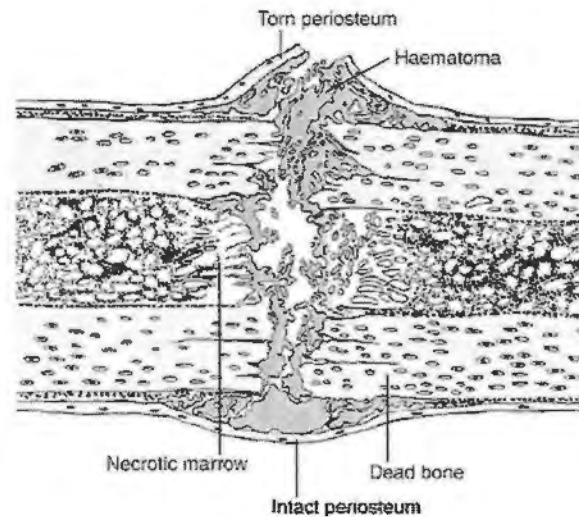
A: Initial events following fracture of a long bone diaphysis (3 days post-fracture). A hematoma accumulates beneath the periosteum and between the fracture ends. There is necrotic marrow and cortical bone close to the fracture line.

Organized haematoma
(cartilage and bone)
Granulation tissue
Early new bone formation
Cartilage
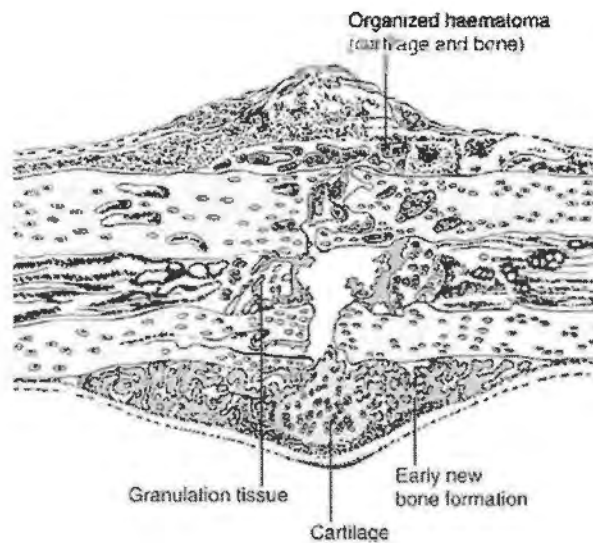
B: Early repair of a diaphyseal fracture of a long bone (9 days post-fracture): the organization of the hematoma, early woven bone formation in the subperiosteal regions, and cartilage formation in inter-fragment region. Periosteal cells contribute to healing this type of injury.

Persistent cartilage

Revascularizing cortical bone
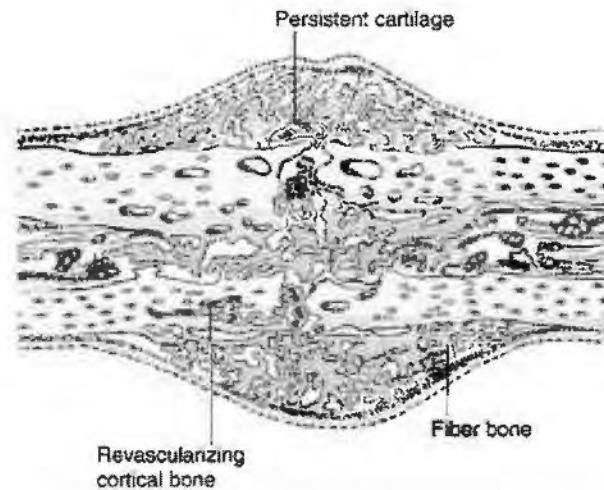
Fiber bone

C: Progressive fracture healing by fracture callus (21 days post-fracture): woven or fiber bone bridging the fracture gap and uniting the fracture fragments. Cartilage remains in the region most distant from ingrowing capillary buds. In many instances, the capillaries are surrounded by new bone. Vessels revascularize the cortical bone at the fracture site.

Figure 1.1.3.1 Histological changes during long bone fracture healing. *(From Einhorn TA. The cell and molecular biology of fracture healing. Clin Orthop Relat Res 1998;335 Suppl:S7-21.)*

1.1.4   Osteoporosis and Osteoporotic Fracture

1.1.4.1 Epidemiology of Osteoporotic Fracture

Osteoporosis is a systemic skeletal disease characterized by low bone mass and microarchitectural deterioration of bone tissue, with a consequent increase in bone fragility and susceptibility to fracture (76-79).

Worldwide, 100-200 million people are at risk of an osteoporotic fracture each year. Statistics predict that by the year 2012, 25% of the European population will be over the age of 65 and by the year 2020, 52 million will be over 65-years-old in the USA (80,81). In Hong Kong SAR, three typical osteoporotic fractures - fractures of hip, distal forearm and vertebral body - presented incidence of 4.59/1000/year (82), which was 4.9% in Beijing, China (2000) (83). The combined risk for the three typical fractures was reported about 40%, which was almost equivalent to the risk of cardiovascular diseases (81,84). Facing so high fracture risk, orthopaedic surgeons are coming to understand that treatments of patients with osteoporotic fractures need to address the underlying osteoporosis in order to reduce the incidences of further fractures.

1.1.4.2   Osteoporotic Fracture Healing

Normal fracture healing is a specialized process in which structural integrity is restored through the regeneration of bone. Fracture healing traditionally proceeds through the stages of intramembranous and endochondral bone formation, which was described above (3,4,29,30). The angiogenesis, callus formation, mineralization and

remodeling, are clearly susceptible to alteration in osteoporotic patients and animals (78,85-88).

The synthesis of bone and its mineralization depend on the calcium environment. Osteoporotic patients have a diminished pool of rapidly soluble calcium, inadequate dietary calcium, and a deficient structural calcium bone reserve (79,89-92). Calcium mineralization is subject to delay, and the stage of remodeling is prolonged because of competition for ionized calcium with the rest of the body. Also, substances that may have been mobilized to maintain systemic calcium homeostasis (PTH and vitamin D) may compromise the latter stages of fracture repair (79,90,93-96). In addition, up to 40 percent of elderly patients are mildly to moderately malnourished, and this condition compromises bone collagen synthesis (85,97). Bone scans remain positive (indicating continued metabolic remodeling) well into the third year after fracture in elderly persons, and union cannot be fully ascertained until that time. Studies have demonstrated that osteoporotic rats have delayed healing (78,88). It is uncertain whether it is the osteoporosis or the estrogen deficiency that compromises fracture repair.

The decline in the capacity for fracture repair has been shown to be age related (98-101). Disturbance of the development of strength within fracture calluses in the elderly has been shown in experimental rat models, but little is known about the causes of osteoporosis and its effect on the fracture repair process in humans.

The relationship between fracture healing and osteoporosis is complex. The etiology may related to aging (98-101), hypogonadism (102-105), rheumatism

(106,107) and thyroid and parathyroid disorders (108,109), and the therapies commonly used for osteoporosis (estrogens, vitamin D, bisphosphonates, exercise and passive mechanical stimulation) may all potentially affect fracture healing.

1.1.5   Enhancement of Fracture Healing and Limitations

Despite the improvements in surgical tools and technique (lag screws, plates, interlocking intramedullary fixation, etc), the healing and recovery of fractures still require a long period. In osteoporotic fractures, it takes up even longer time to heal. It will take up around 4~8 months for an osteoporotic hip fracture healing (110). The prolonged healing process not only delays the functional rehabilitation, but also lengthens the bed-rest period which may increase the risk of pulmonary embolism or decubitus, consequently leads to raise up the fracture mortality (111).

Facing these problems in delayed fracture healing, the enhancement modalities are imminently needed. Currently, the managements for healing enhancement can be broadly classified into biological and physical modalities. Biological stimulation involves the introduction of osteoinductive, osteoconductive, or osteogenic factors into the local environment, whereas biophysical interventions include pulsed electromagnetic fields (PEMF) (112,113), ultrasound (9,114-117) and shockwave (118) therapies at the fracture site.

1.1.5.1 Biological Methods

The use of bone grafts for the treatment of bone defects is increasing, and the

indications are growing with rising numbers of spinal fusions, primary and revision arthroplasties, and periprosthetic fractures (7). Autogenous bone graft provides the basic components required to stimulate skeletal repair, including osteoinductive factors, an osteoconductive extracellular matrix, and osteogenic stem cells present in the form of bone marrow elements (119,120). However, the morbidity associated with graft harvesting, such as donor site pain, nerve or arterial injury, and infection rates (8%~10%) (121,122) have prompted extensive research into alternatives.

1.1.5.2 Biophysical Enhancement

The mechanical environment has a direct impact on fracture healing. Direct mechanical perturbation as well as biophysical modalities such as electromagnetic, ultrasound or shockwave has been shown to affect fracture healing.

There are numerous clinical reports to support effectiveness of biophysical stimulation on fresh fracture, delayed union, and bone lengthening Several prospective, randomized clinical studies have shown the efficacy of low intensity pulsed ultrasound (LIPUS) in stimulating bone formation after fracture (114,117,123-125), non-union (126-128), and bone lengthening (129,130). Pulsed electromagnetic fields (PEMF) stimulation has been in clinical use for nearly 30 years on patients with delayed fracture healing and non-union and demonstrated its effect in a multitude of clinical case reports (112,113). Double-blinded studies confirmed the clinical effectiveness of pulsed electromagnetic fields stimulation on osteotomy healing (131-133) and delayed union fractures (134,135). Brighton et al conducted

multicenter study of the non-union and reported an 84% clinical healing rate of non-union with direct current treatment (136). Schaden et al. reported 76% of non-union or delayed union patients treated with one time extracorporeal shock wave therapy resulted in bony consolidation with a simultaneous decrease in symptoms (137). However, LIPUS, PEMF and shock wave therapy can just provide localized osteogenic enhancing effect, and the induction of systemic response to fracture healing should be limited.

The studies in our laboratory had proven that low magnitude high frequency vibration (LMHFV), a novel biophysical intervention therapy, could significantly accelerate and enhance the fracture healing in both normal and osteoporotic bones (10,11). Besides, LMHFV is also effective in improving bone mineral density (BMD) (138-142), augmenting blood flow (143-146), enhancing muscle properties (147-153), stimulating neuromuscular efficiency (154-161) and increasing the production of growth hormones (162), etc

Based on these findings of LMHFV, it would strongly support the efficacy of biophysical stimulation as a systemic therapeutic modality in bone fracture repair and tissue regenerate augmentation. However, the mechanism of the beneficial effects of LMHFV is still unclear. More investigations need to be performed to consummate our knowledge of this novel physiological mechanical therapy

1.2 Low Magnitude High Frequency Vibration Therapy

1.2.1 Wolff's Law

Wolff's law is a theory developed by a German anatomist/surgeon Julius Wolff (1836-1902) in the 19th century that states that bone in a healthy person or animal will adapt to the loads it is placed under. If loading on a particular bone increases, the bone will remodel itself over time to become stronger to resist that sort of loading. The internal architecture of the trabeculae undergoes adaptive changes, followed by secondary changes to the external cortical portion of the bone, perhaps becoming thicker as a result. The converse is true as well: if the loading on a bone decreases, the bone will become weaker due to turnover, it is less metabolically costly to maintain and there is no stimulus for continued remodeling that is required to maintain bone mass (163-165).

1.2.2 Low Magnitude High Frequency Vibration (LMHFV)

Low magnitude, high frequency vibration treatment is a non-invasive biophysical intervention that provides whole-body vibration stimulation. It has been reported to be effective in maintaining BMD (138-142), enhancing muscle strength (147-153), improving the balance capacity (149,166-168), altering blood circulation (143-146), and promoting fracture healing (10,11). However, the mechanism of these beneficial effects by LMHFV is still poorly understood.

1.2.2.1 Effects on Osseous Tissue

Vibration is reported to be beneficial in maintaining and/or enhancing the bone mass in individuals such as the elderly (169), postmenopausal women (170-172), and adolescents (173). Rubin et al. demonstrated a significant increase (34%) in femoral trabecular bone mass in adult ewes after 1-year vibration treatment (174). Vibration applied at increasing accelerations (0.1, 0.3, and 1.0g) enhanced trabecular bone volume >30% in a non-dose-dependent fashion in the proximal tibia of adult mice (12). Trabecular bone formation rate to bone surface ratio (BFR/BS) and mineralizing surface to bone surface ratio (MS/BS) were enhanced in female mice following 3 weeks of vibration.

The effects of vibration has been examined in ovariectomized (OVX) young (175,176) and mature (177,178) animals. Results indicated that hip density, muscle strength, and postural control were enhanced in postmenopausal women, following 6 months of vibration treatment. (172). Another study showed trabecular BFR/BS increased 159% following 28 days of vibration in 8-month-old OVX rats (178). However, ex vivo cross-sectional pQCT analysis demonstrated that vibration (3.0g) augmented total cortical and medullary areas in the tibial diaphysis. It also enhanced periosteal and endosteal perimeters (176). Investigations conducted on young women with low BMD showed enhanced cancellous bone in the spine and increased cortical bone area in the femur following 1 year of vibration treatment (30Hz, 0.3g, 10min/day) (179).

Plenty of studies have shown that low magnitude high frequency vibration

stimulated new bone formation in intact bone. Furthermore, Leung KS et al. indicated that LMHFV (0.3g, 35Hz, 20min/day, 5days/week) could accelerate the callus formation, mineralization in closed femoral shaft fractured rats (10). Shi HF et al. found LMHFV could also be beneficial for the osteoporotic fracture healing enhancement in adult rats (11). Chow HK et al. confirmed LMHFV could enhance bone remodeling, in which LMHFV was shown to partially reverse the inhibition of ibandronate on bone remodeling (180).

1.2.2.2 Effects on Blood Flow

Investigators have been increasingly intrigued by the physiological response of humans to vibration for some time, and recently in relation to its potential as a non-pharmacological means to improve peripheral blood flow.

Kerschan-Schindl et al. examined the circulatory responses of participants who stood on a platform vibrating at 26 Hz (3×3 min sets) (145). Despite the brief duration of the exposure, mean blood velocity to the quadriceps and gastrocnemius muscles was doubled. Further, the resistive index of the popliteal artery was decreased compared with resting levels. According to the authors, the imposed vibration (amplitude = 3 mm, peak acceleration = 78 m^{-1} s^{-2}) evoked rhythmical muscle contractions which caused alterations in peripheral circulation without significant cardiovascular changes as indicated by a lack of change in HR and blood pressure.

Helmkamp et al. acknowledged that the health effects of occupational vibration were heavily dependent on the characteristics of the vibration exposure (e.g. vibration

frequency, direction and amplitude) (181). Indeed, brief exposure to low-magnitude mechanical vibration may have a number of benefits particularly with respect to enhancing local muscle blood flow.

Zhang et al. used a brief (3 min) vibratory stimulus that emitted random acceleration of constant power density between 5 and 2000 Hz. Six healthy participants rested their foot against a vibrating plate and blood flow to the tibialis anterior muscle was quantified using photoplethysmography. Local muscle blood flow was increased by an average of 20% as a consequence of the brief vibration stimulus (182).

In a similar study, Stewart et al. provided additional evidence that localized vibration could be effective for the augment of leg blood flow in postmenopausal women (146). In their study, 18 women, (aged 46-63 years), placed their right foot on a vibrating customized foot plate apparatus, whilst in a supine position with a 35° upright tilt. The plate was attached to an actuator which delivered sinusoidal vertical displacements of up to 2 mm. A vibration frequency of 45 Hz for 5-7 min was sufficient to result in significant increases in calf blood flow up to 46% as measured by strain gauge plethysmography. It was argued that plantar vibration enhances venous drainage as well as peripheral blood flow and lymphatic flow.

Plenty of previous studies indicated that vibration had benefit in improving the peripheral blood flow. However, the effects of revascularization and blood perfusion in fracture callus by vibration have not been studied yet. This investigation may be of help to demonstrate the influence of microcirculatory regeneration by LMHFV at the

peri-fracture region hence to partially clarify the mechanism of the osteogenic

promoting effect by vibration.

1.3 Angiogenesis and Fracture Healing

1.3.1 Angiogenesis

Angiogenesis, the sprouting of new capillaries from the pre-existing vessels, is a complex process that encompasses activation, migration, and proliferation of endothelial cells (ECs). This process is essential for reproduction, development and tissue repair (183-187).

Angiogenesis requires extensive interactions between a variety of cells and molecules and is controlled by various peptides and other modulating factors. In order for vascular sprouting to occur, a cascade of events must be completed (Figure. 1.3.1). First, basement membrane dissolution must occur, a process that is facilitated by proteases. Next, chemoattractants and mitogens are activated in order to facilitate EC migration and proliferation, respectively. Finally, tube formation occurs requiring inhibitory signals as well as those that facilitate formation of junctional complexes and reconstitution of a basement membrane. Formation of the basement membrane, which signals the onset of vessel maturation, involves recruitment by EC of pericytes (adventitial cells) that embed within the basement membrane (188). If this microvessel is to become a larger vessel with a medial layer, then appropriate signals are required for the recruitment of smooth muscle.

A large number of local and circulating angiogenic factors are known to be involved in the angiogenic process, including VEGF, angiopoietins, and basic fibroblast growth factor (bFGF) (183-187,189-196). VEGF is the most important angiogenic factor induced by local hypoxia. VEGF induces various functions on

endothelial cells by interacting with high affinity tyrosine kinase receptors. VEGF and VEGF receptors (VEGFR) are therefore considered as potential targets for angiogenesis imaging (183-187).

1.3.2 Angiogenesis in Bone Repair

Bone fracture results in disruption of the marrow architecture and blood vessels within and around the fracture site, which leads to acute necrosis and hypoxia of the surrounding tissue. During bone repair, the three components of the normal bone blood supply - medullary, periosteal, and osseous - can be enhanced according to physiological need (60,197). Increased vascular permeability leads to higher exudation of plasma, one of the initial and essential parts of angiogenesis, and the subsequent formation of osteogenic matrix. Due to the hypoxia, local VEGF will release to herald vessel formation by causing endothelial cells to migrate at the tips of capillary sprouts where they proliferate and form tubular structures (198,199). Further neovessel maturation with adjacent pericytes and smooth muscle cells alters microcirculatory properties such as permeability. Chemoattraction of pericytes and smooth muscle cells help to stabilize capillary network formation and arborization by a PDGF-BB-controlled process (200-202). After vascularization, osteoblastic cells proliferate and with the production of an osteogenic matrix, endocondral bone formation can begin. The newly generated blood supply to the callus and cortical bone appears to persist until the medullary blood supply is fully regenerated. The heterogeneity in vascularity after bone damage could help to explain local differences

in bone formation in normal, delayed and non-unions (60,197). (Figure.1.3.2)

Many growth factors/cytokines induced in response to injury are believed to have a significant role in the process of repair (60,197). These include members of the fibroblast growth factor (FGF), transforming growth factor (TGF), bone morphogenetic protein (BMP), insulin-like growth factor (IGF) and platelet derived growth factor (PDGF) families, as well as vascular endothelial growth factor, VEGF (203,204). These factors are produced by and/or responded to by many cell types present at the fracture site. Besides recruitment of osteoprohenitor cells and osteoblasts, recently, VEGF has also been reported playing an important role in promoting osteoclastic bone remodeling by mediating osteoblasts (205-207). Other angiogenic (60,197) and anti-angiogenic factors (208), such as those expressed in the growth plate of developing bones, might similarly be expressed and active in the fracture callus during endochondral ossification. Skeletal injury in humans is characterized by local (injury site) and systemic angiogenic responses. Accordingly, systemic factors - such as parathyroid hormone (PTH), growth hormone, steroids, calcitonin and Vitamin D - can also modulate bone metabolism and vascularity (60,197).

Based on previous findings above, reestablishment of vascularity is a crucial event in fracture healing. The applications to promote angiogenesis at the fracture site should be considered as an essential strategy on fracture healing enhancement.

1.3.1 Angiogenesis in the Fracture Healing of Elderly

Impaired angiogenesis will decrease bone regeneration, regardless of age. Changes in angiogenesis that occur with aging have been noted at the molecular, cellular, and physiologic levels of regulation.

A decrease in endothelial cells, the hemostatic cascade, neurochemical mediators, and growth factors and their cognate receptors has been observed. Also, alterations in the structural and regulatory components of the matrix contiguous to forming vessels in aged tissues could influence bone healing in elderly patients (209, 210). Age is a major limiting factor for mobilization of EPCs. In vitro studies revealed that young bone marrow-derived EPCs recapitulated the cardiac myocyte-induced expression of PDGF-BB, whereas EPCs from the bone marrow of aging mice did not express PDGF-BB when cultured in the presence of cardiac myocytes (209-211).

Together, the age-related changes provide mechanistic insights into the diminished angiogenesis and vasculogenesis in ischemia-reperfusion models. Although there is no direct evidence till now, decreased blood vessel formation may contribute to the age-related delay of osteoporotic fracture healing. Therapeutics that support blood vessel formation will be essential to enhance osteoporotic fracture healing in the elderly patients.

1.3.4 Mechanical Loading and Angiogenesis

Several clinical and animal model investigations provide evidence that angiogenesis is stimulated by mechanical loading (212,213). Exercise training and blood volume augment have been linked with coronary microvascular angiogenesis

(214). Increased blood flow and pressure could be underlying mechanical stimuli. Other possible stimuli are the extravascular stretch stimulus due to forced expansion of end diastolic dimensions from volume overload and stretch of the capillary abluminal surface (215-218).

The physical environment of ECs (shear stress, transmural pressure and cyclic stretch) can activate mechanotransduction mechanisms mediated by integrins and associated GTPases (219,220). The signal transduction pathways stimulated act through phosphorylation of kinases. Some studies attempted to unravel the complex metabolic and mechanical stimuli inherent in exercise and proposed that elevated shear stress resulting from functional hyperaemia and stretch of the endothelium as part of the duty cycle may promote angiogenesis in different ways (215-218). It was shown that mechanical stimuli may induce capillary growth in normal mature cardiac and skeletal muscle.

In EC cultures, elevated shear stress leads to higher rates of EC division and, in vivo, the site and extent of angiogenesis appears to be closely related to the level of tissue hyperaemia, i.e. an elevated microvascular shear stress. High shear stress may increase ECs production of MMPs in culture. In vivo levels of MMPs are upregulated in EC during flow-induced arterial remodeling (215), but not with pharmacologically induced hyperaemia, whilst inhibition of their activity during increased muscle activity prevented angiogenesis. One important response is the apparent upregulation of eNOS mRNA and protein expression, possibly leading to angiogenesis via the promotion of VEGF expression. As with signaling induced by high flow in arteries,

shear stress induced by adrenoreceptor antagonism (prazosin) elicited increases in VEGF associated with capillary angiogenesis, and electrical stimulation led to a rapid increase in capillary-located VEGF-A expression that matched ECs proliferation at these sites (221). Interestingly, vasodilatation invoked by various vasodilator compounds failed to increase the expression of VEGF, FGF-2 or TGFβ (222), despite similar treatments being effective in inducing angiogenesis. Neither flow-mediated increases in VEGF nor angiogenesis was induced in hyperperfused dog muscle in the absence of contractions (215,223), which suggests that, for blood flow to induce angiogenesis, it must be coupled with other changes, e.g. altered tissue pO_2, metabolites, etc. Importantly, imposition of elevated shear stress may induce signaling through VEGFR in the absence of ligand binding (224), offering yet another potential avenue in the increasingly complex network of angiogenesis control.

As mentioned above *(see chapter 1.2)*, vibration treatment, providing biophysical mechanical stimuli, was also reported augmented blood flow of lower extremities, which was supposed to increase the shear stress at the endothelium to stimulate angiogenesis. However, whether vibration can enhance flow-induced angiogenesis in bone fracture healing is still unknown.

1.3.5 Assessing Angiogenesis during Fracture Healing

The ability to image neovascularization is an attractive strategy that represents a novel approach to noninvasively monitor angiogenesis and to assess the efficacy of therapies directed at modulation of the angiogenic process. Several imaging

modalities are currently used or under development. X-ray micro-computed tomography (microCT) (225,226) and ultrasound (e.g. power Doppler) (227-230)approaches provide primarily anatomical information at high spatial resolution. Recently, efforts have focused on the development of ultrasound probes to monitor biochemical processes including angiogenesis. Magnetic resonance (MR) imaging is another popular imaging modality that offers superior spatial resolution and penetration depth and provides both anatomical and functional information (231-234). In addition, the nuclear imaging techniques based on positron emission tomography (PET) (235) or single-photon emission computed tomography (SPECT) (225,236) offer favorable sensitivity and resolution for in vivo tomographic imaging.

Due to the advantages of high imaging resolution and 3D anatomic visualization, microCT is attracting more and more attention to be utilized in microvasculature assessment. With the development of ultrasound imaging technique, transducers with high frequency (> 20 MHz) has been adopted in the evaluation of small vessels with low flow velocity. It was indicated that at a center frequency of 50 MHz, the detection of vessels by power Doppler could be down to 15-20 μm in diameter in the mouse ear, and a wider range of velocities (1-25 mm/s) of blood flow was able to be assessed in superficial tissues or organs (237,238). Given the advantages of non-invasion, real-time monitoring, less angle-dependence, and high sensitivity to low velocity flow, we tried to develop a three-dimensional (3D) imaging technique by using power Doppler to obtain the spatial anatomic and quantitative volumetric information of blood perfusion within the callus during fracture healing.
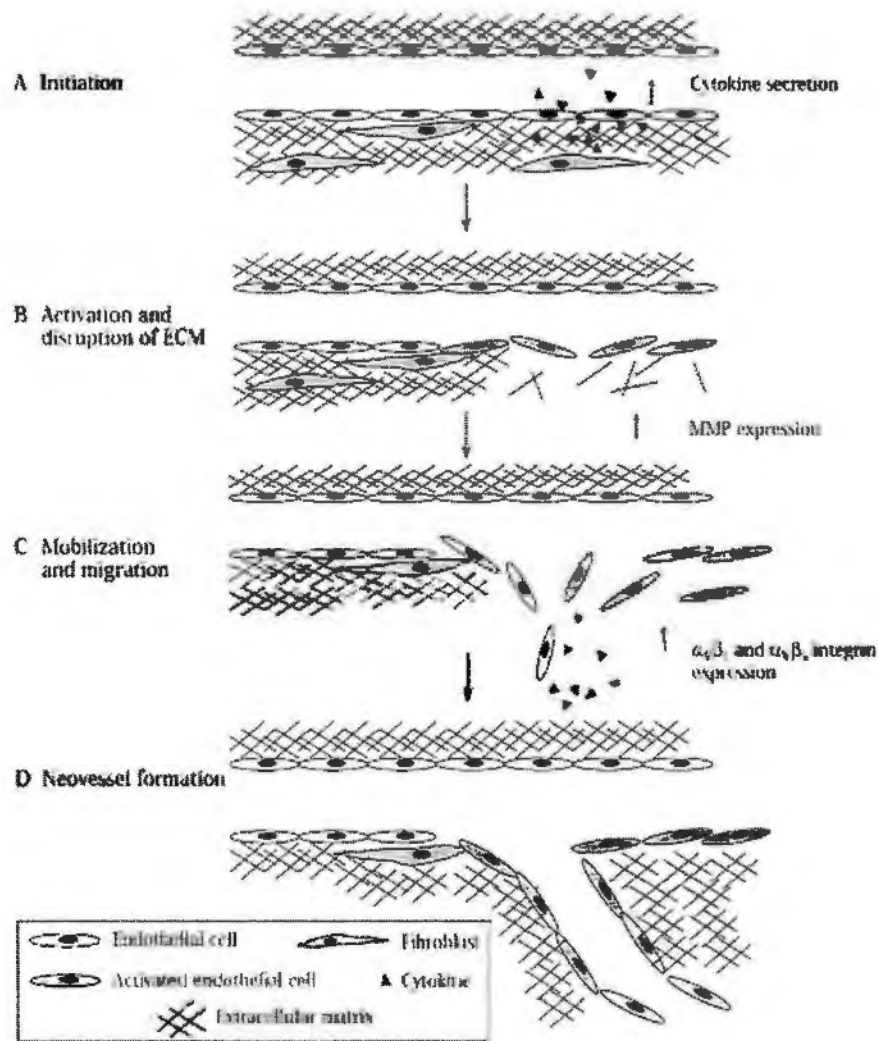
Figure 1.3.1 Sequential events in angiogenesis. **A.** Angiogenesis is initiated by release of angiogenic cytokines from platelets, monocytes, and fibroblasts. **B.** Activated endothelial cells (ECs) subsequently disrupt their interactions with neighboring ECs, digest the basement membrane, and digest other extracellular matrix (ECM) components (by releasing matrix metalloproteinases (MMPs). **C.** Activated ECs and fibroblasts (plus platelets, smooth muscle cells, and monocytes/macrophages) subsequently release the necessary angiogenic cytokines that allow the local, resident ECs to invade and migrate through the ECM and proliferate. **D.** These form new immature tubules. *(From Bauer SM et al Angiogenesis, Vasculogenesis and Induction of Healing in Chronic Wounds Vasc Endovascular Surg 2005;39(4):293-306.)*
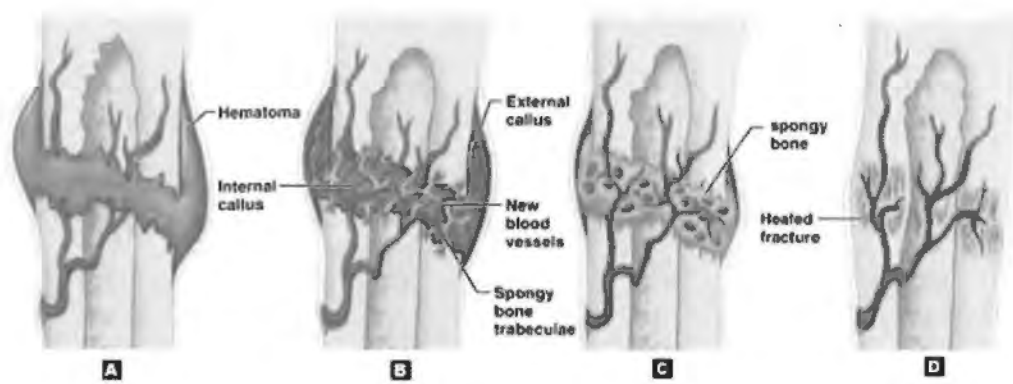
Figure 1.3.2 Sketch of the four classic histological stages of secondary fracture healing, including hematoma formation and inflammation, angiogenesis, soft callus formation, bony callus formation and bone remodeling. *(From Human Anatomy & Physiology, Benjamin Cummings, 2006)*

1.4 Hypotheses

As described above, a good blood supply is a prerequisite for initiating the fracture repair, and angiogenic response is reported crucial throughout the fracture healing, including hematoma, inflammation, endochondral ossification and remodeling (60,197). Our previous studies confirmed LMHFV (0.3g, 35Hz) could promote both normal and osteoporotic fracture healing in rats (10,11). Other studies reported vibration could promote peripheral blood flow through enhancing the functions of muscle pump (143,145,146). Therefore, **the first hypothesis of this study was that LMHFV (0.3g peak-to-peak, 35Hz) could enhance the blood flow of ischemia hind limb and promote angiogenesis at the fracture site in both normal and osteoporotic rats, hence to accelerate the healing process.**

In osteoporotic condition, Griffith et al found that ovariectomy could reduce the bone perfusion, which was associated with a decreased BMD. They suspected it could be caused by the reduction of erythropoetic marrow amount and endothelial dysfunction (239). Ding et al. also documented a reduced local blood supply and VEGF expression at the tibial metaphysis of ovariectomized rats (240). Due to the reduced blood perfusion of bone and poor capacity of vessel formation in osteoporotic condition (209-211), **the second hypothesis of this study was that the angiogenic response in osteoporotic fracture was diminished as compared with non-osteoporotic fracture, which might result in the prolonged healing process in osteoporotic condition.**

1.5 Study Plan

To testify the hypotheses described above, the whole study was designed as follows:

Nine-month-old ovariectomy-induced (OVX) and sham-ovariectomized (Sham) rats were created closed femoral fractures according to our established protocol. The fractured rats were randomly divided into either treatment or control groups. LMHFV at 0.3g, 35Hz with 20min/day and 5days/week was provided for treatment groups 5 days after fracture creation, while control groups underwent the same procedures except without vibration.

Radiography was taken weekly after treatment to monitor the status of bone healing. At weeks 2, 4 and 8 post-treatment, pulsed-wave Doppler ultrasound was utilized to measure the blood flow velocity of femoral artery at the fracture side. Three-dimensional high frequency power Doppler ultrasonography (3D-HF-DPU) was adopted for assessing the microcirculation at the fracture site. After that, the vascular system of each animal was perfused with Microfil contrast agent and the fractured femur was subjected to microCT scanning for microvasculature analysis of fracture site. Immunohistochemistry was performed to evaluate the expression of vascular endothelial growth factor (VEGF) signals in external callus.

1.6 Objectives

The objectives of this study are listed as follows:

1. To investigate the effects of LMHFV treatment on angiogenesis of fracture site and the blood flow of hind limb in both normal and osteoporotic rats;

2. To demonstrate the mechanism of the promoting effect of LMHFV on osteogenesis in conjunction with the microcirculation alteration;

3. To study the differences in angiogenesis and the possible causes of delayed fracture healing in osteoporotic bone.

4. To establish a novel in vivo imaging methodology by 3D Doppler sonography for assessing the microvasculature of superficial tissues in small animals.

FLOWCHART OF STUDY DESIGN

Osteoporotic Model	6-month-old Female S/D Rat	→ OVX *or* Sham-OVX →	9-month-old Female S/D Rat

↓

Closed Fracture Model of Femoral Mid-shaft	Intramedullary fixation → Fracture Creation

↓

LMHFV Treatmenat & Fracture Healing

LMHFV *(Sham-V, OVX-V)*　　0.3g, 35Hz, 20min/d, 5d/wk ⟶

Control　*(Sham-C, OVX-C)*　　Power Off, 20min/d, 5d/wk ⟶

Start　　Week 2　　Week 4　　Week 8

↓

Angiogenesis and Osteogenesis Assessments

- X-ray Radiography
- MicroCT
- Pulsed-wave Doppler
- 3D High Frequency Power Doppler
- MicroCT-based Microangiography
- Immunohistochemistry

↓

Statistical Analysis

CHAPTER 2
MATERIALS AND METHODOLOGY

2.1 Establishment of Animal Models

2.1.1 Osteoporotic and Non-osteoporotic Rat Model

The osteoporotic rats were established in 6-month-old female Sprague-Dawley (SD) rats (200 to 250 grams, retired breeders) by bilateral ovariectomy (OVX), and housed to 9-month-old for induction (241,242). After anesthesia (sodium pentobarbital, 60 mg/kg, i.p., SIGMA, St. Louis, MO, USA), shaving on the back, and asepsis preparation (0.5% Hibitane in 70% ethanol), the rat was in prone position with bilateral ovaries approached through two 8 mm dorsal incisions (Figure 2.1.1-1 A). After dissection of the posterior abdominal wall, the ovaries were identified. Then the ovaries, part of the oviducts, concomitant vessels and some visceral fat were ligated (3-0 sutures, Mersilk, Ethicon Ltd., Belgium) and resected following careful stanching (Figure 2.1.1-1 B, C). The abdominal wall and the skin were then stitched with 3-0 sutures. Following surgery, buprenorphine in 0.03 mg/kg, s.c. (Temgesic, Schering-Plough, NJ, USA) was given 3 times every 24 hours for analgesia. The rats were allowed free cage movement with standard diet during the following 3-month induction. The establishment of osteoporosis by OVX was confirmed by bone mineral density (BMD) measurement at the 5th lumbar vertebra (L5, 5 sections above iliac crest), the right femoral head (RFH, 3 sections) and the right femoral shaft (RFS, 4 sections superior and distal to ischial tuberosity) by XtremeCT (Scanco Medical, Brüttisellen, Switzerland) (Figure 2.1.1-2).

38
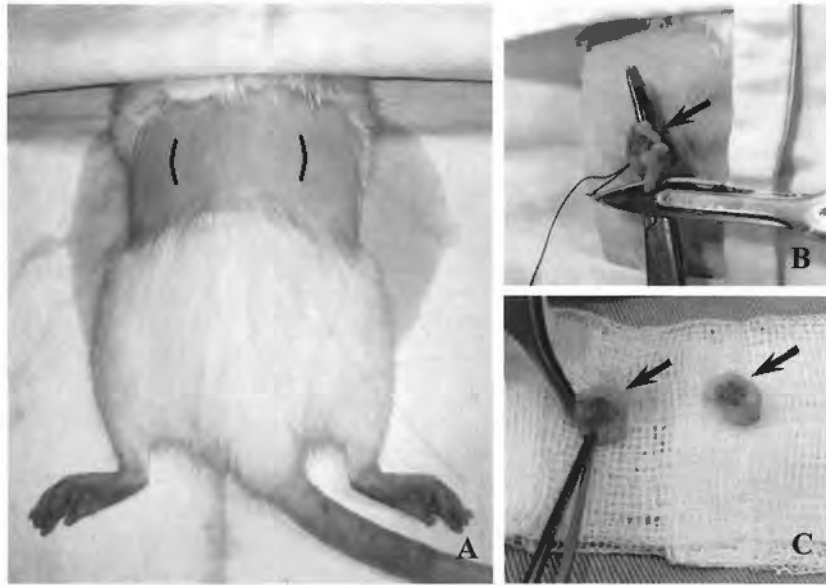
Figure 2.1.1-1 The surgical procedure of bilateral ovariectomy in rats. **A:** Two dorsal incisions to approach bilateral ovaries at the posterior abdominal wall. **B:** Expose and resect the ovary (black arrow) surrounded by visceral fat. **C:** The resected ovaries (black arrows) with some visceral fat.
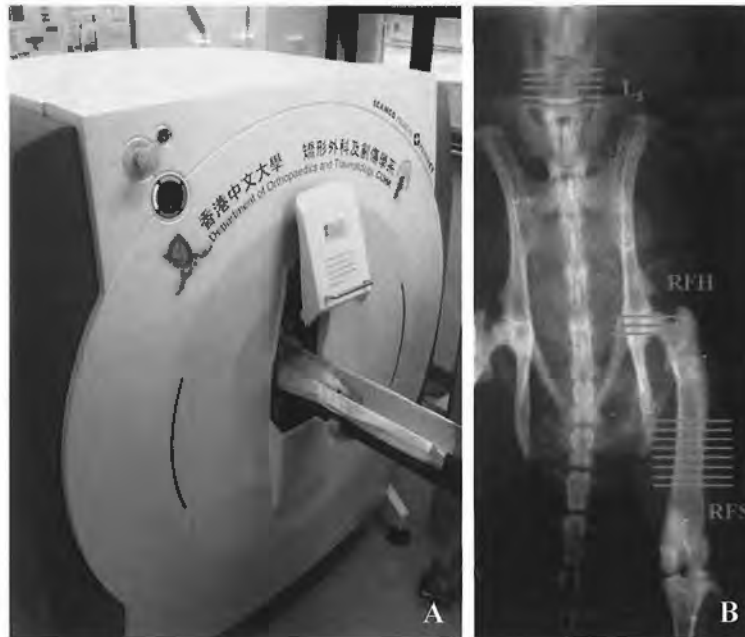
Figure 2.1.1-2 BMD measurement to confirm the efficacy of ovariectomy. **A:** Xtreme-CT scanning. **B:** Use radiograph to locate the regions of interest (ROI) including L_5 (5 sections above iliac crest), RFH (right femoral head, 3 sections), and RFS (right femoral shaft, 8 sections).

2.1.2 Closed Femoral Shaft Fracture Model in Rats

The closed fracture model was performed following our established protocol modified from Bonnarens's study (10,11,243). Nine-month-old rats were generally anesthetized and prepared for intramedullary pinning of the right femur. After shaving and cleansing of the right leg, the rat was placed supine on the operating table. The right knee was completely fixed and a 8mm longitudinal incision was made just medial to the patella. After the dissection of the joint capsule, the patella was dislocated laterally, exposing the articular surface of the femoral condyles (Figure 2.1.2-1A). The canal was reamed with an 18 gauge needle inserted between the condyles (Figure 2.1.2-1B). A sterile Kirschner wire (K-wire, $\emptyset$ 1.2 mm, Sanatmetal Ltd., Eger, Hungary) was then introduced into the medullary canal through the entry point. The K-wire retrograded up the shaft and perforated the proximal femur through the piriformis fossa. An incision was made over the greater trochanter to gain access to the proximal end of the pin. The tip of K-wire was 180° bended and it was cut so as to leave a 3 mm handle, which was subsequently buried beneath muscle to prevent distal migration (Figure 2.1.2-1C). The distal end of the K-wire was cut flush with the cortex of the patellofemoral groove (Figure 2.1.2-1D) and buried beneath the articular surface so as to allow free knee motion. After irrigation, the patella was put back with the joint capsule and the skin stitched with 5-0 sutures (Mersilk, Ethicon Ltd., Belgium), and a radiograph was taken to confirm the pin placement.

With the rat supine, the pre-pinned femur was placed in abduction and external rotation and the mid-shaft was positioned over the animal support stage of a

customized 3-point-bending apparatus (Figure 2.1.2-2 A, B). A metal blade (weighted 500 grams) was dropped from a height of 35 cm to create mid-shaft transverse fracture on the right femur (Figure 2.1.2-2 C). A radiograph was taken to document the fracture, configuration and to measure any angulation in the pin. No obvious fracture gap (< 0.5 mm) or displacement (< 0.5 mm) was confirmed as a successful model by anteroposterior (A-P) and lateral radiographies (Figure 2.1.2-2 D), which was done with the rat prone and with both legs fully abducted.

After waken up, buprenorphine was given during the first 24 hours for analgesia. The rats were allowed unrestricted cage activities after surgery.

2.2 Grouping of Animals

Seventy-two fractured rats were randomly divided into four groups: normal control group (Sham-C), normal vibration group (Sham-V), ovariectomized control group (OVX-C) and ovariectomized vibration group (OVX-V). Each group was subdivided into three time points (n=6): 2, 4 or 8 weeks after vibration treatment. (Table 2.2) The time points for sampling were selected according to our previous study which represented 3 stages of fracture healing respectively in in 9-month-old ovariectomized rats. The most active changes of callus formation occurred in the first 4 weeks (11).
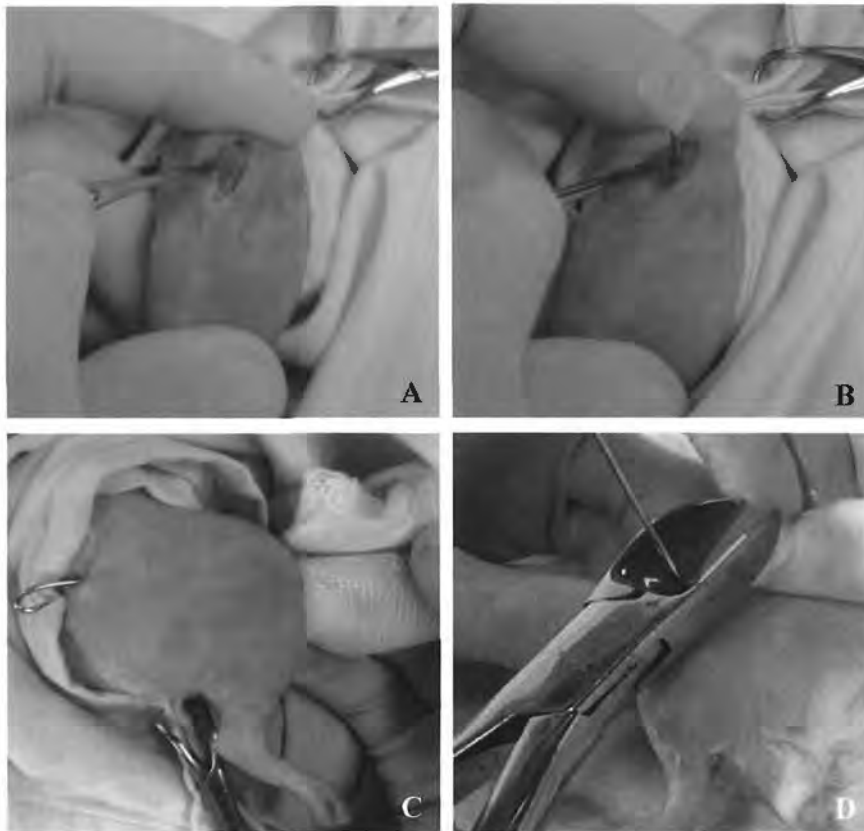
Figure 2.1.2-1 The surgical procedure of intramedullary fixation. **A:** To dissect the joint capsule of the right knee, then to dislocate the patella laterally to expose the articular surface of the femoral condyles. **B:** Intramedullary drilling and reaming with an 18 G needle at the intercondylar notch. **C:** Insert the K-wire into the medullary canal through the entry point of intercondylar notch. The proximal end of K-wire was 180° bended and buried beneath muscle to prevent distal migration. **D:** The distal end of the K-wire was cut flush with the cortex of the patellofemoral groove.
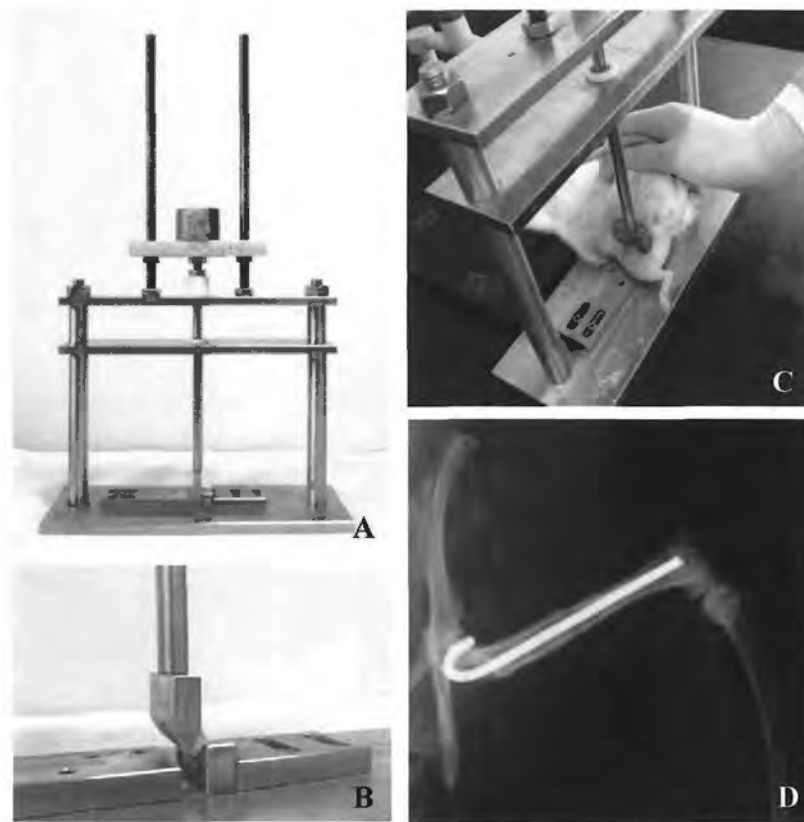
Figure 2.1.2-2 The procedure of closed fracture at the right femoral mid-shaft in rats. **A:** Three-point-bending apparatus for fracture creation with adjustable dropping weight and height. **B:** The detail of the 3-point-bending settings with an arc support designed to position the rat thigh. **C:** The rat was positioned supinely on the apparatus to create transverse fracture at the mid-shaft of right femur with the dropping metal blade. **D:** The efficacy of fracture creation was confirmed by radiography after surgery.

2.3 Low Magnitude High Frequency Vibration Therapy

Treatment started at 5 days after fracture creation, when the rats were able to bear the full body weight (11). For treatment groups, rats were housed individually in standard bottomless, compartmented cage and placed on a custom-designed (patent-pending) vibration platform (Figure 2.3 A). Low magnitude high frequency vibration (LMHFV) treatments oscillating vertically at 35Hz with a peak-to-peak acceleration of 0.3g (g = gravitational acceleration) (Figure 2.3 B, C) was provided for 20 minutes/day and 5 days/week. The rats of Sham-C and OVX-C groups stood on the vibration platform with power switch off as sham treatment under the same regime.

Table 2.2-1 Animal Grouping for Fracture Healing Study

Groups	Week 2	Week 4	Week 8
Non-osteoporotic Control (Sham-C)	6	6	6
Non-osteoporotic Vibration (Sham-V)	6	6	6
Osteoporotic Control (OVX-C)	6	6	6
Osteoporotic Vibration (OVX-V)	6	6	6

Table 2.2-2 Schedule of the treatment and sampling

Groups					1st week post-treatment						2nd week post-treatment						3rd week post-trea
Sham-V	F				V	V	V	V	V^a		V	V	V	V	V^{ab}		V	V	V
Sham-C	F				C	C	C	C	C^a		C	C	C	C	C^{ab}		C	C	C
OVX-V	F				V	V	V	V	V^a		V	V	V	V	V^{ab}		V	V	V
OVX-C	F				C	C	C	C	C^a		C	C	C	C	C^{ab}		C	C	C

Groups					5th week post-treatment						6th week post-treatment						7th week post-tre
Sham-V	F				V	V	V	V	V^a		V	V	V	V	V^a		V	V	V
Sham-C	F				C	C	C	C	C^a		C	C	C	C	C^a		C	C	C
OVX-V	F				V	V	V	V	V^a		V	V	V	V	V^a		V	V	V
OVX-C	F				C	C	C	C	C^a		C	C	C	C	C^a		C	C	C

F: surgery of fracture creation.

V: LMHFV treatment (magnitude=0.3 g, frequency=35 Hz, 20 min/day, 5 days/week).

C: sham treatment for control (stand on vibration platform with power off, 20 minutes/day, 5 day

a: radiography taken for callus size measurement.

b: six rats were performed pulsed-wave Doppler, 3D high-frequency power Doppler evalua micro-CT and immunohistochemistry assessments.

47
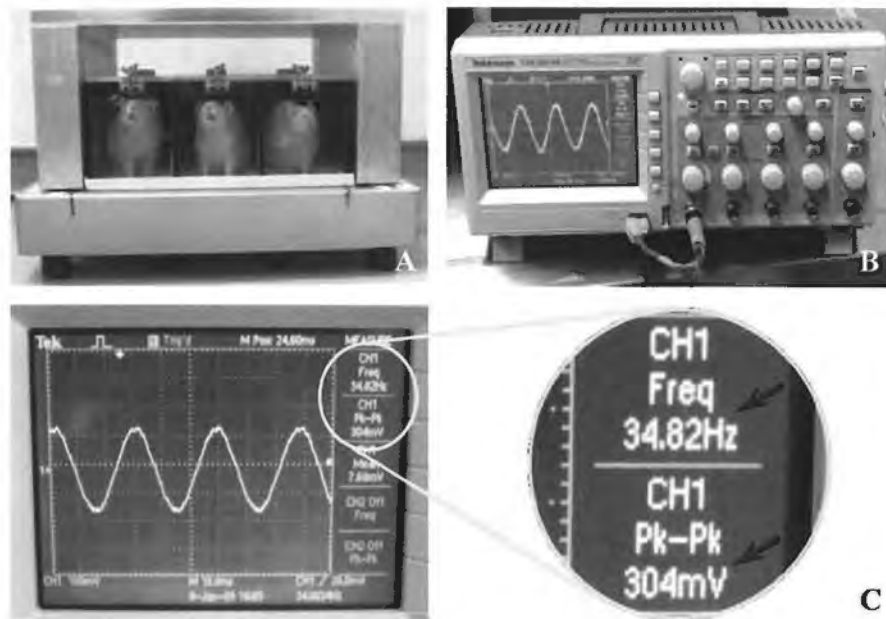
Figure 2.3 Calibration of the LMHFV platform. **A:** Rats were housed individually and placed on the vibration platform. **B:** Calibration of the LMHFV platform with an oscilloscope. **C:** The calibrated vibrational signal - frequency=35 Hz (upper arrow), magnitude=0.3 g (lower arrow) - shown on the oscilloscope monitor.

2.4 Radiographic Analysis

Radiography was used to monitor and to assess the status of fracture healing in vivo. After general anesthesia, the rat was pronely positioned and both legs were fully abducted, radiographies were taken weekly (3 sec exposure time at tube voltage of 60kVp,) to document the lateral view of rat femur by a cabinet X-ray apparatus (Faxitron X-ray system model 43855C, Wheeling, Illinois, USA) (Figure 2.4-1 A). On each radiograph, an aluminum wedge calibrator was used as reference (Figure 2.4-1 B). Fracture healing status was monitored through the measurement of callus width (CW) and callus area (CA) from the lateral radiography.

The x-ray films were digitized with a scanner (Epson Perfection 4990 Photo Scanner, Japan) (Figure 2.4-1 C). Callus width was defined as the maximal outer diameter of the mineralized callus (d2) minus the outer diameter of the femur (d1) (Figure 2.4-2 A). Callus area was calculated as the sum of the areas of the external mineralized callus around the fracture site (Figure 2.4-2 B) (8,10). Images were then measured by the software of ImagePro-Plus (Version 5.0, Media Cybernetics, Inc., Bethesda, MD, USA), the data of CW and CA were compared among different groups.
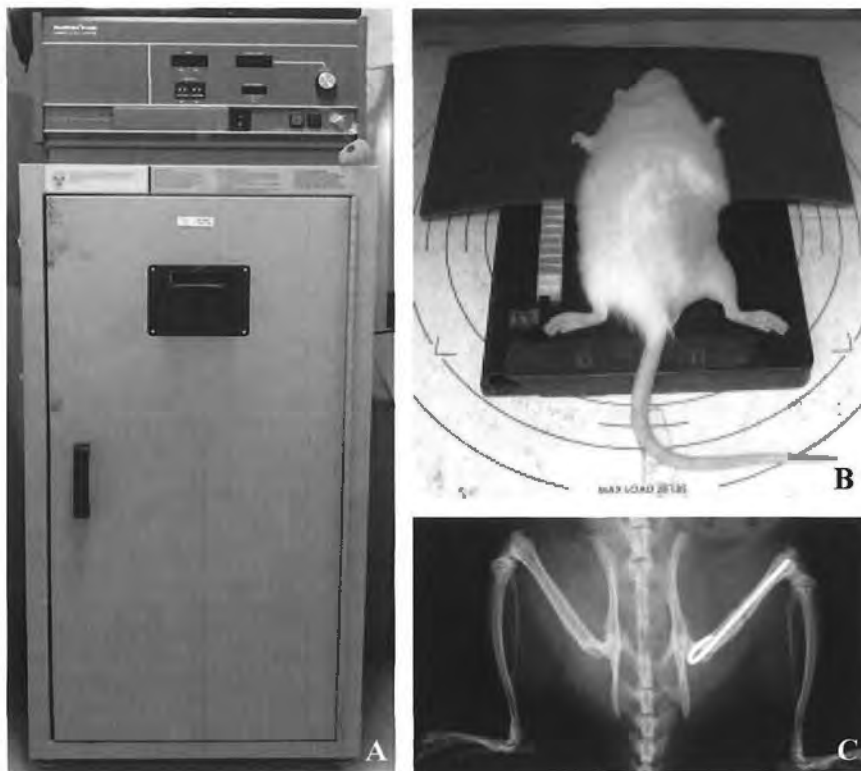
Figure 2.4-1 The procedure of radiography taken. **A:** The cabinet X-ray apparatus (Faxitron X-ray system model 43855C, Wheeling, Illinois, USA) **B:** Pronated position of the rat for lateral radiography. **C:** Digitalized lateral radiograph of rat femur with intramedullary fixation.
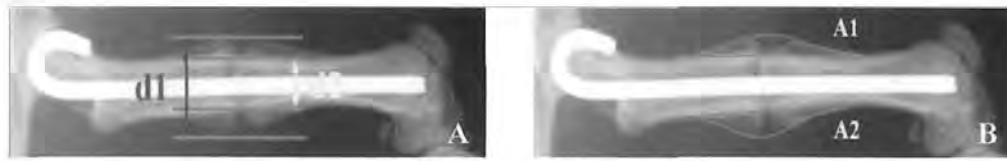
Figure 2.4-2 External callus width (CW) and callus area (CA) measurements on the digitized lateral radiograph. **A:** CW was defined as the maximal outer diameter of the external callus (d1) minus the outer diameter of the femur (d2). **B:** CA was calculated as the sum of the areas of the external callus.

2.5 Pulsed-wave Doppler Ultrasonography

At each time point, blood flow of femoral artery at the fractured side was measured in the pulse-wave Doppler mode using Voluson 730 Expert System (General Electric Company, USA). After general anesthesia, shaving the hind limb, the rat was supinely positioned. Five minutes later, color-Doppler mode was used to find the femoral artery and femoral vein at transverse view, then the transducer (center frequency: 16MHz) was turned 90° into the longitudinal view (Figure 2.5). The peak systolic flow velocity of femoral artery was collected by 5 times within 10 minutes 5mm downstream to the fracture gap. At each data collection period, the average of five blood flow readings was used to measure mean blood flow velocity (244,245).
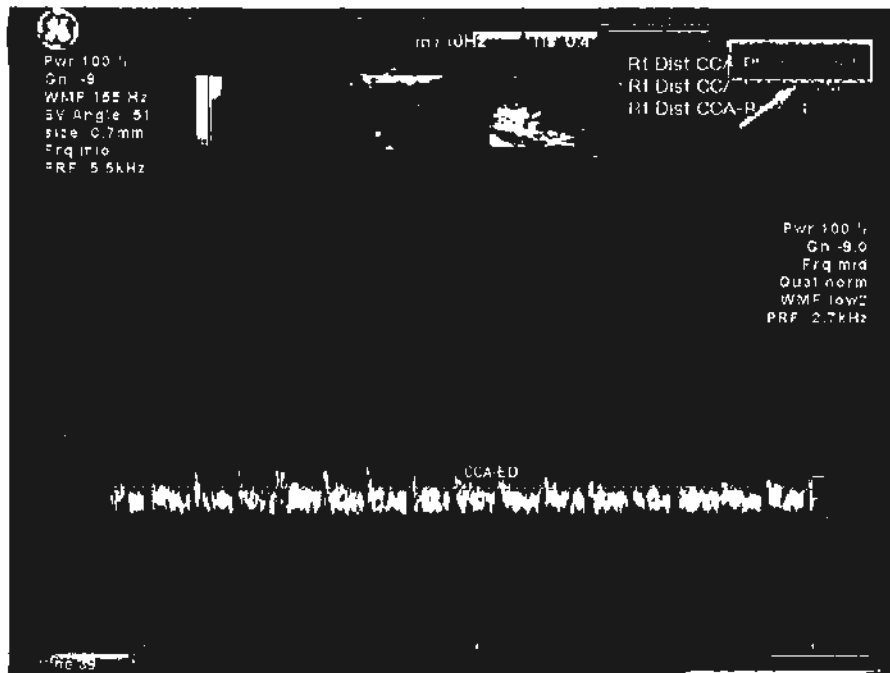
Figure 2.5 Measurement of blood flow velocity of femoral artery by pulsed-wave Doppler. The peak systolic flow velocity (white arrow) of femoral artery was collected by 5 times within 10 minutes to take average.

2.6 Three-dimensional High Frequency Power Doppler Ultrasonography (3D-HF-PDU)

The rats received three-dimensional high frequency power Doppler ultrasonography (3D-HF-PDU) assessment (246-251) at the fracture site using Vevo-770 high frequency In-Vivo Micro-Imaging System (VisualSonics, Toronto, Ontario, Canada) (Figure 2.6-1 A). The rat was positioned pronely on a flat, heated pad with the body temperature maintained at 37°C (Figure 2.6-1 B). The extremities were secured and coupling gel was loaded to cover the exposed callus region (Figure 2.6-2 A). 2D real time B-mode scanning was chosen to visualize the femur and the scanning window was centered at the fracture line, with a 7.4 mm × 7.0 mm field of view. The ultrasound transducer (center frequency: 55 MHz), held by a hand-free stand, was positioned 4.5 mm above the center portion of external callus so as to match the focal zone. Then the device was switched to the 3D power Doppler mode (gain: 20 dB; pulse repetition frequency: 5 kHz; wall filter: 2.5 mm/s) and the scanning was constructed by a linear translation of the transducer along an axis (the femur) which is perpendicular to the single plane of 2D imaging. The translation rate was set at 0.05 mm/s. A scanning step of 0.05 mm (Figure 2.6-1 C) was used with a scanning range of 10.0 mm. After lateral side scanning of the fracture site, the rat was turned to the supine position for medial side scanning of the fracture site (Figure 2.6-2 B), following the same procedures as above. In total, 200 images for each side were collected within 30 minutes after induction of anesthesia. A rectangular region of interest (ROI) was manually outlined on the 100th slice (Figure 2.6-3 A) by a single

investigator. The height of ROI was set from the exterior margin of the external callus to the medullary cavity, and the length of ROI was 7.40 mm, i.e. the length of scanning window. The same ROI selection was performed automatically in the remaining 2D slices by a custom-designed script of Matlab (Version7.0, The MathWorks, Inc., Natick, MA, USA). The color voxel ($0.016 \times 0.016 \times 0.050$ mm^3) number was obtained by counting the color pixels within ROI in each slice. Then we calculated the volume of color voxels in each image to represent the vascular volume in each slice volume and added them together (Figure 2.6-3 B). Therefore, the total vascular volume at the fracture site was the sum of the volume of both lateral and medial sides. The customized script was used to discriminate and filter signals from large vessels: for an intra-linked region of flow signal displayed in the 2D image, the first criterion assessed was the area it covered. If the area was large than 1.3 mm^2, a second criterion was set by observing the short axis of a regressed oval for this region. If the short axis was also larger than a critical value (0.35 mm), this region was then judged as a large vessel and was then excluded in the calculation. Vascular volume at the fracture site was then calculated as the sum of the color voxel volumes of both lateral and medial sides. Mean signal intensity of blood flow was evaluated as the average amplitude of color voxels converted to a relative value from 0 to 255 (Figure 2.6-4). The relative number of moving erythrocytes around the fracture site was then calculated by the formula: relative number of erythrocytes = (number of color voxels of lateral side × mean intensity of color signals at the lateral side) + (number of color voxels of medial side × mean intensity of color signals at the medial side).

Figure 2.6-1 The procedure of 3D-HF-PDU scanning. **A:** Vevo-770 high frequency In-Vivo Micro-Imaging System. **B:** The rat was prone positioned on a flat with the extremities secured. Coupling gel was loaded to cover the exposed callus region for linear scanning. **C:** The step size of scanning was set at 0.05 mm (black arrow).
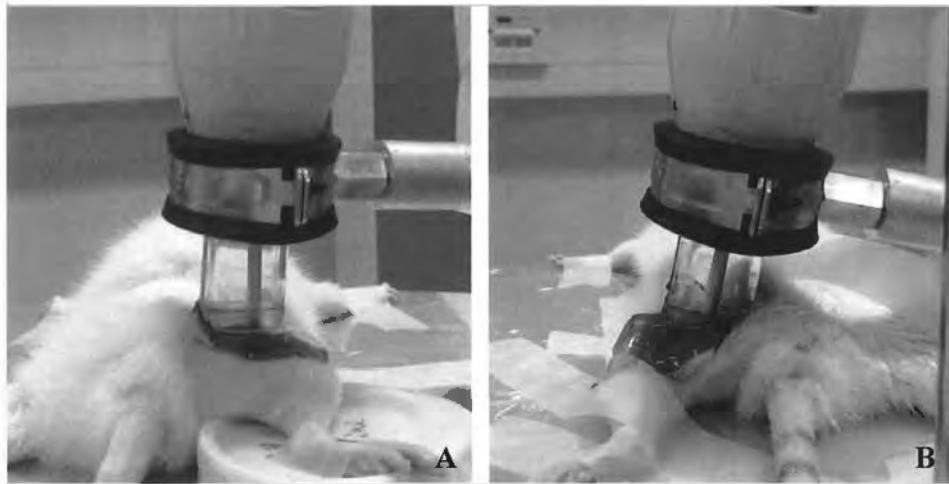
Figure 2.6-2 Positioning the rat for bifacial scannings of the callus region. **A:** Lateral side scanning. **B:** Medial side scanning.
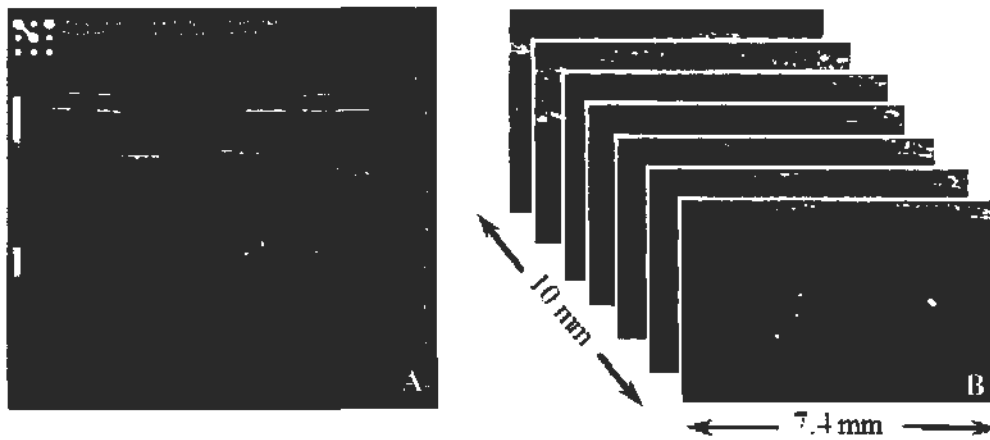
Figure 2.6-3 Region of interest (ROI) selection for blood volume calculation. **A:** A rectangular ROI was manually outlined (in red) on the 100th slice. The height of ROI was set from the exterior margin of the external callus to the medullary cavity, and the length of ROI was the length of scanning window (7.4 mm). The same ROI selection was performed automatically in the remaining 2D slices by a custom-designed script of Matlab. **B:** 200 images for each side with a scanning range of 10.0 mm were collected for color pixel volume calculation.
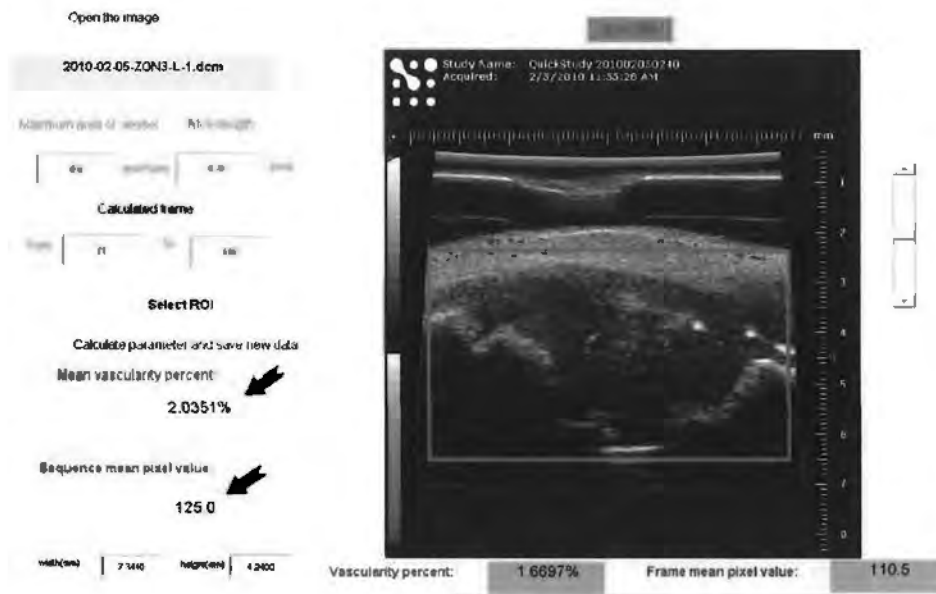
Figure 2.6-4 Calculation of blood volume and flow intensity. A custom-designed script of Matlab was used to analyze and to present the percentage of color voxels (upper arrow) within the volume of interest, thus the blood volume could be calculated. Mean signal intensity of blood flow (lower arrow) was evaluated as the average amplitude of color voxels converted to a relative value from 0 to 255.

2.7 MicroCT-Based Microangiography

After the measurement of 3D-HR-PDU, the abdomen cavity of the rat was cut open and the abdominal aorta was separated carefully from the vessel sheath (Figure 2.7-1 A). The aorta was then ligated and the distal aorta was gently clamped by a bulldog clamp. After that, a scurf-needle with its sharp needlepoint smoothly cut was inserted into the aorta between the clamp and ligation points, and the bulldog clamp was loosened to make sure that the needle was in the aorta, then the needle was fixed with aorta using 3-0 silk (Figure 2.7-1 B). The inferior vena cava was cut to allow outflow of the perfusate and 10 mL of pre-warmed heparinized 0.9% saline (50 IU/ml) was injected. The vascularity was then flushed continuously by using pre-warmed 100ml saline at flow speed of 20ml/min until the outflow from the inferior vena cava was limpid. 10 ml of pre-warmed formalin was injected to fix the skeletal specimen. 9 ml Microfil contrast agent (MV Diluent-MV 117 Orange-MV Curing Agent, Flow Tech, Carver, MA, USA), a radiopaque silicone rubber compound containing lead chromate, was rapidly injected as soon as they were mixed. The animals were then euthanized with an overdose of pentobarbital. The cadaver was stored at room temperature for 1 hour and then at 4°C overnight to ensure polymerization of the contrast agent (226,252). The efficacy of Microfil contrast agent perfusion was then preliminarily examined by radiography (Figure 2.7-1 C, D).

The fractured femur was then dissected from the surrounding musculature carefully (Figure 2.7-2 C_1) and a high-resolution (8-36 μm isotropic voxel size) micro-CT imaging system (VivaCT 40, Scanco Medical, Bassersdorf, Switzerland)

(Figure 2.7-2 A) was used to perform osseous tissue scanning and produce 3D vasculature images. The scanner was set at a voltage of 70 kVp and a current of 102 μA and the resolution was set to medium, which creates a 1024 × 1024 pixel image matrix. The femur was fixed in a plastic tube (20.3 mm in diameter) with its long axis perpendicular to the bottom of the tube (Figure 2.7-2 B). The scan was initiated 3.7 mm proximal to the fracture line, with an entire scan length of 7.4 mm (Figure 2.7-2 D_1).

The scan was carried out with isotropic voxels. The callus was contoured with ROI iteration to define the outer surface of the callus and a 3D reconstruction was performed using a low-pass Gaussian filter (sigma = 0.8; support = 1).

In the following analysis, to differentiate the newly formed mineralized callus from the old cortices, the low- and high-density mineralized tissues were reconstructed using different thresholds (high attenuation = 350, low attenuation = 165) defined in 2-D images according to established evaluation protocols (10,11,86,253). The thresholds were further conformed by a series of 2- and 3-D evaluations. The high-density tissues represent old cortices and newly formed, highly mineralized callus while the low-density tissues represent newly formed callus. To compare the morphologic characteristics between groups, the reconstructed fracture segments were shown in transparent-view 3-D images. The high-density bone (threshold > 350) was shown in dark color, while the low-density bone (threshold 165 - 350) was shown in transparent light color. The unmineralized tissue (threshold < 165) was not shown. Quantitative analysis was performed covering the 350 slices of the

2-D images with the low- and high-density mineralized tissues evaluated separately. Morphometric parameters used for evaluation included total tissue volume (TV, mm^3, calculated from the contoured ROI in 2-D images), volume of high-density bone (BV_h, mm^3), volume of low-density bone (BV_l, mm^3), total bone volume (BV, mm^3, i.e. equivalent to $BV_h + BV_l$, or TV − interstitial space) and normalized BV/TV, BV_h/TV as well as BV_l/TV.

After microCT scanning, the specimens were fixed by 10% neutral buffered formalin for 24 hours, and then were decalcified by 9% formic acid for 7 days. Anteroposterior-view radiographs were taken to confirm the success of decalcification by using the cabinet X-ray system under an exposure condition of 60 kV/3 sec.

The decalcified femur (Figure 2.7-2 C_2) underwent a second microCT scanning with the same ROI as above, i.e. 3.70 mm proximal and distal to the fracture line (Figure 2.7-2 D_2). For segmentation of blood vessels from the background, the noise was removed using a low-pass Gaussian filter (sigma = 0.8, support = 1) and the blood vessels were defined at a threshold of ≥100. The semi-automatically built-in contouring program was used to draw contours at each 2D section for an automatic reconstruction of 3D vascular images in the decalcified sample. Subsequently, a black-white scale to the surface of the 3D images was mapped to produce a visual representation of the vessel tree, and total vessel volume (VV, mm^3), volume fraction (VV/TV, VV/BV) were documented for quantitative analysis (226,252).
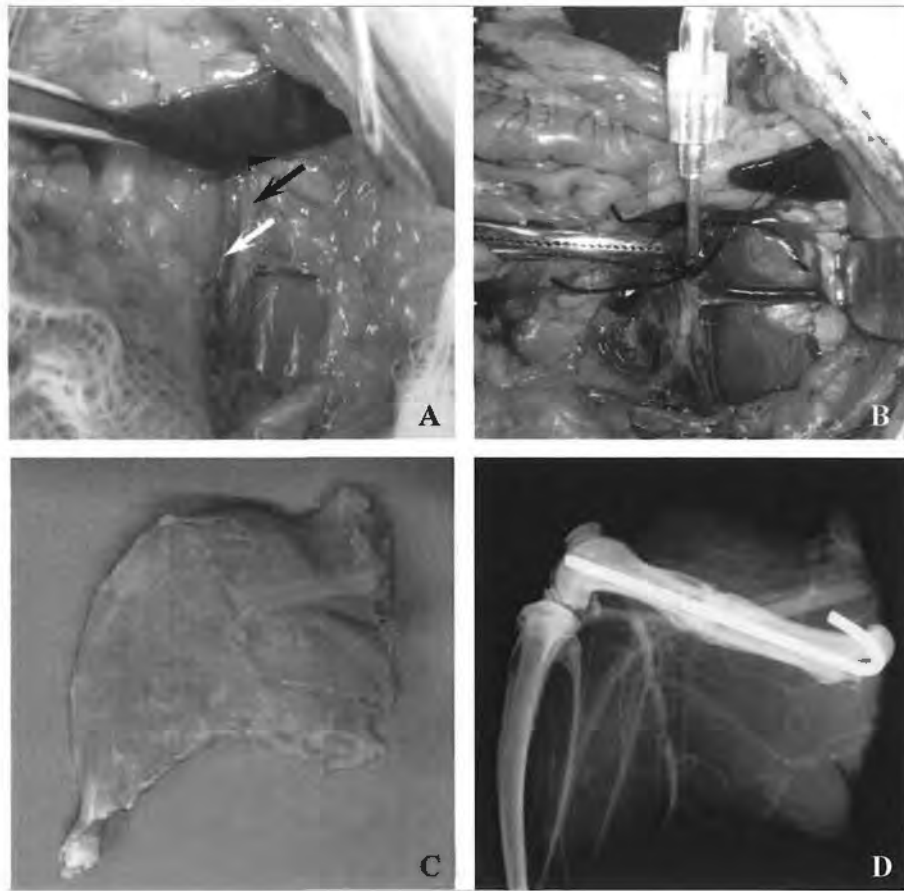
Figure 2.7-1 The procedure of Microfil perfusion. **A:** Cut open the abdomen cavity of the rat and expose the abdominal aorta (black arrow) and inferior vena cava (white arrow). **B:** Insert a scurf-needle with its sharp needlepoint smoothly cut into the aorta. Cut the inferior vena cava to allow outflow of the perfusate. **C, D:** The efficacy of Microfil contrast agent perfusion was preliminarily examined by radiography. The radiograph showed a continuous vasoganglion, which represented a well-perfused vascularity system by Microfil.
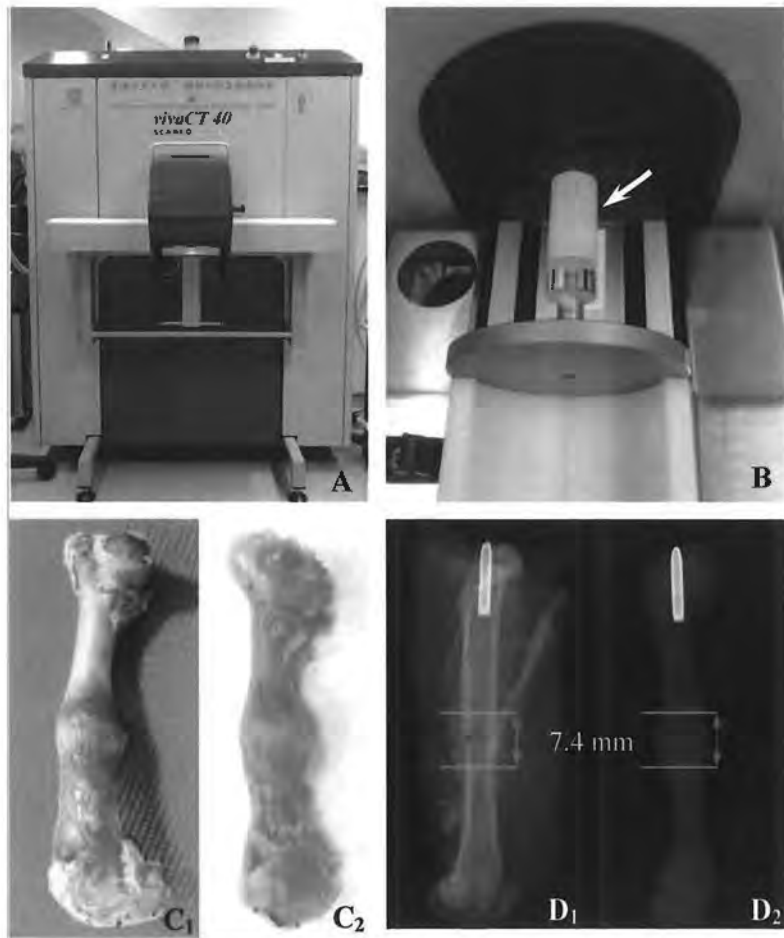
Figure 2.7-2 The procedures for the microCT scanning of osseous tissue and microvasculature at the fracture site. **A:** High-resolution micro-CT imaging system (VivaCT 40, Scanco Medical, Bassersdorf, Switzerland). **B:** The femur was fixed in a plastic tube (20.3 mm in diameter, white arrow) with its long axis perpendicular to the bottom of the tube. **C$_1$:** Undecalcified femur for osteogenesis assessment. **C$_2$:** Decalcified femur for angiogenesis assessment. **D$_1$, D$_2$:** ROI selection for microCT scanning pre- and post- decalcification, respectively. Both were 3.7 mm proximal and distal to the fracture line with a total range of 7.4 mm.

2.8 Immunohistochemistry

After microCT scanning, the decalcified femurs were embedded in paraffin. The specimens were cut longitudinally into 7-μm thick sections and transferred to poly-lysine-coated slides. The mid-sagittal sections were immunostained with specific reagents for vascular endothelial growth factor (VEGF) identification at the fracture site (59,254). Following deparaffinization and rehydration, the sections were washed with phosphate buffered saline (PBS). Endogenous peroxidase activity was blocked by immersing sections in 3% hydrogen peroxide in methanol for 20 minutes, and rinsing in PBS. Antigens were retrieved with 2mg/ml protease (Merk KGaA, Darmstadt, Germany) at 37°C for 1 hour. Nonspecific antigen binding was blocked by 5% goat serum (Millipore Corporation, Billerica, MA, USA) in 1% bovine serum albumin (Sigma-Aldrich, St. Louis, MO, USA)/PBS (BSA/PBS) solution for 20 minutes. The sections were then incubated with antibodies against VEGF (1:100, Sc-7269, Santa Cruz Biotechnology, Inc., Santa Cruz, CA, USA) at 4°C overnight. After washing in PBS, nonspecific antigen was blocked again with 5% goat serum in 1% BSA/PBS, and the sections were then incubated with horseradish peroxidase (HRP)-conjugated anti-mouse IgG (Millipore Corporation, Billerica, MA, USA) at room temperature for 1 hour. For negative controls, primary antibody was replaced by blocking solution. Samples from each group were stained in the same batch with the same incubation time and conditions. The rat kidney tissue for VEGF immunostainings was used as a positive control. The immunoreactivity in specimens was demonstrated with diaminobenzidine tetrahydrochloride (DAB, Dako North

America Inc, Carpinteria, CA, USA) and the sections were counterstained with haematoxylin. The temporal and spatial expression of VEGF in the sections were then localized and analyzed using the Leica microscope system (DMRXA2, Leica Microsystems GmbH, Wetzlar, Germany). The ROI was evaluated in the slides covering 1.5mm proximal and distal to the fracture line in the captured 100× images. The area of external callus (Cl.Ar) involved in the ROI was measured using Image-Pro Plus software. Immuno-activities of VEGF were quantified as the area of immunohistochemically stained signals (VEGF.Ar) in brown color in each of 10 sections from the same specimen. The percentage of VEGF expression area (VEGF.Ar/ Cl.Ar) in callus area was also calculated for comparison (255).

2.9 Statistical Analysis

All quantitative data were expressed as mean ± standard deviation (SD) and analyzed with SPSS version 16.0 software (SPSS Inc, Chicago, IL, USA). One-way ANOVA was used to compare among different groups at each time point. Significant difference was set at a probability level of 95% ($p < 0.05$).

CHAPTER 3
RESULTS

3.1 Establishment of the Animal Models

3.1.1 Osteoporotic Rat Model

Totally 43 rats were used to establish the osteoporotic model; 44 rats were performed the sham OVX surgery. The average time for the surgical procedures of bilateral ovariectomy was around 20 minutes, with no significant bleeding occurred during the surgery. After that, no postoperative complications like wound infection or abdominal infection were observed. No sudden death occurred during the three months of inducement following OVX or sham OVX surgery. BMD dropping was observed after three months of inducement in the OVX group. At the 5th lumbar vertebra (L_5), the right femoral head (RFH) and the right femoral shaft (RFS), BMD dropped by 9.9%, 9.3%, and 7.1% respectively.

The rats in the OVX group gained 59.1% higher body weight after three months of inducement of ovariectomy, while the rats in the sham-OVX group gained only 28.3% higher body weight. Three months after the inducement, mean body weight of OVX group was significantly higher than those in Sham group (p = 0.002).

3.1.2 Closed Femoral Shaft Fracture Model

All 87 rats (Sham-OVX, OVX) were used to create the closed mid-shaft fracture model at the right femur. The average time for the surgical procedures of internal fixation was around 15 minutes, during when no significant bleeding occurred. The successful rate to achieve a transverse fracture at the femoral shaft within 0.5 mm fracture gap (confirmed by lateral and A-P radiographies) by the 3-point-bending fracture-making apparatus was 87.4% (76 out of 87). Those rats (n = 11) with non-transverse fractures were excluded from the further study. Single dose of buprenorphine (0.03 mg/kg, s.c., Temgesic, Schering-Plough, NJ, USA) was given during the first 24 h for analgesia. All rats were allowed free cage movement, and *ad libitum* access to standard rat diet and tap water. After fracture, the movements and activities of the rats were carefully monitored during the first few days. The rats were found to use the fractured limb to bear weight on the next day after surgery. One rat got beaten at the wound by others on the next day after the fracture creation, and was excluded from our study. Another three rats died unexpectedly due to the anesthetic accident during the further monitoring.

3.2 X-ray Radiography

By weekly radiographic monitoring, external callus around the fracture site was observed since week 1 post-treatment in both control and vibration groups. The fracture gap fused gradually during the healing process. Compared with the control groups, vibration group showed a faster bridging rate of fracture gaps in the digitized radiographies than controls. With regard to the quantitative measurements, both callus width (CW) (Figure 3.2-1) and callus area (CA) (Figure 3.2-2) increased and reached the peak at week 3. After that, the callus size began to decrease gradually. At the early phase of fracture healing, the vibration groups had better callus formation than the corresponding control groups. Both CW and CA in OVX-C were lower than in Sham-C, but this trend reversed at week 8. OVX-V had a comparable callus size with the one in Sham-V. For CW, significant increases were demonstrated in OVX-V as compared with in OVX-C at week 2 ($p=0.019$) and week 3 ($p=0.001$). For CA, OVX-V was significantly higher than OVX-C (week 1: $p=0.006$; week 2: $p<0.001$; week 3: $p=0.001$). Significantly higher CA was also detected in Sham-C than in OVX-C at week 2 ($p=0.038$) and week 3 ($p=0.045$). During the stage of callus formation, the increased percentage of CW after LMHFV treatment in osteoporotic group (week 1: +5.0%; week 2: +6.3%; week 3: +10.6%) was higher than the normal group (week 1: +2.3%; week 2: +3.1%; week 3: +4.0%). Similarly, OVX-V showed a higher increase rate of CA (week 1: +9.1%; week 2: +11.5%; week 3: +10.7%) as compared with Sham-V (week 1: +4.0%; week 2: +4.3%; week 3: +6.9%).
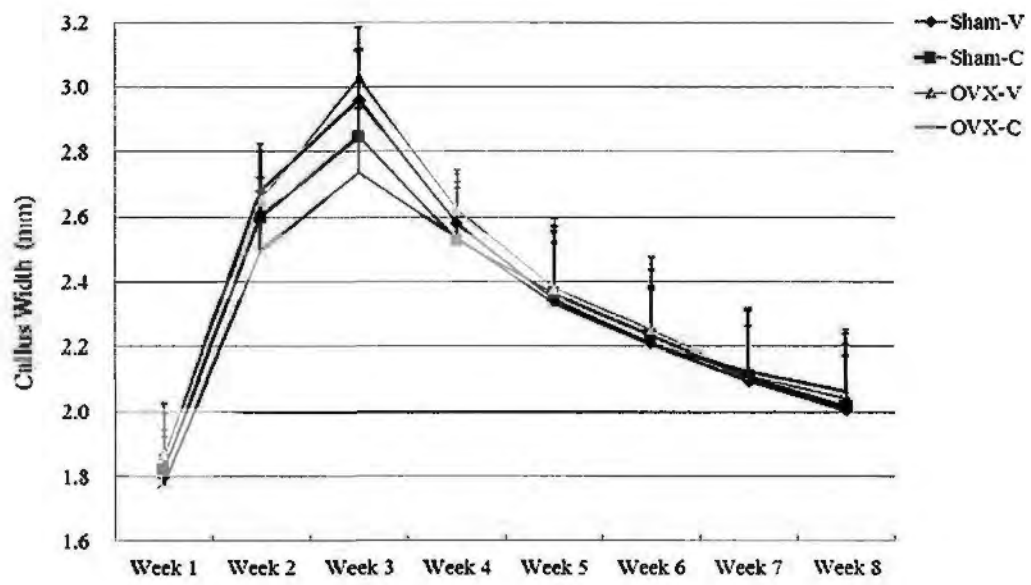
Figure 3.2-1 Radiographic analysis of callus width (CW) among 4 groups at different time points
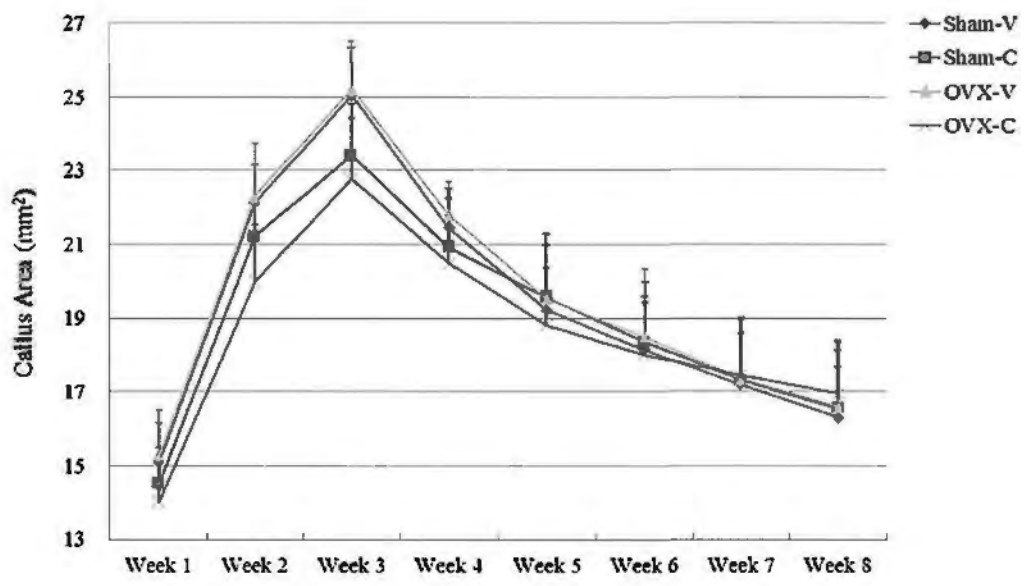
Figure 3.2-2 Radiographic analysis of callus area (CA) among 4 groups at different time points.

3.3 Pulsed-wave Doppler Ultrasonography

The blood flow velocity of injured femoral artery was measured at week 2, 4 and 8 after treatment. In general, the blood flow velocity increased gradually from weeks 2 to 8 (Figure 3.3). At each time point, higher blood flow velocity was shown in vibration groups as compared with control groups. Significant differences were found at week 2 and week 4 (week 2: OVX-V > OVX-C, $p=0.030$; week 4: Sham-V > Sham-C, $p=0.020$; OVX-V > OVX-C, $p=0.012$). Inferior level of blood flow velocity was indicated in osteoporotic rats as compared with corresponding normal ones. Difference between the two groups was significant at week 8 post-treatment (Sham-V> OVX-V, $p=0.006$; Sham-C > OVX-C, $p=0.005$).
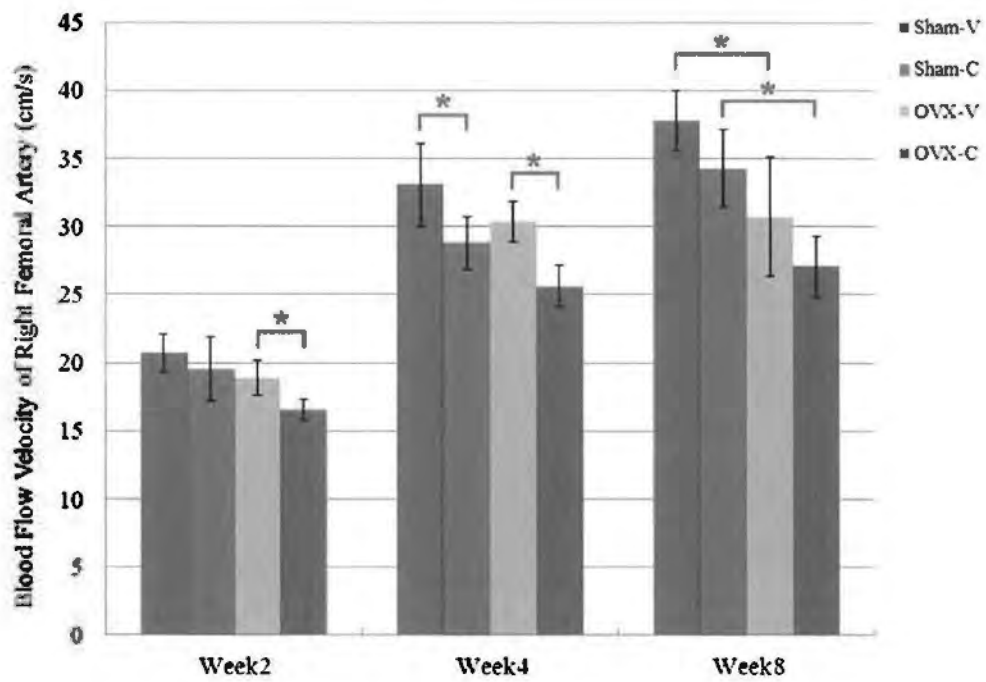
Figure 3.3 The blood flow velocity of injured femoral artery assessed by pulsed-wave Doppler among 4 groups at different time points

3.4 3D High Frequency Power Doppler Ultrasonography

In 3D-HR-PDU examinations, blood flow signals (colored in red and yellow) were present in the callus, periosteum and peripheral soft tissues (Figure 3.4-1). From the blood volume assessment (Figure 3.4-2), in general, a declining trend was found from weeks 2 to 8. At week 2 and 4, vibration groups showed a higher level of blood volume as compared with the control groups with significant difference at week 2 (Sham-V > Sham-C, p=0.021; OVX-V > OVX-C, p=0.077). However, the trend reversed at week 8 with no significance. The volume values in OVX groups were lower than the corresponding Sham ones, yet without significant difference found.

| **Sagittal** | **Horizontal** | **Coronal** |
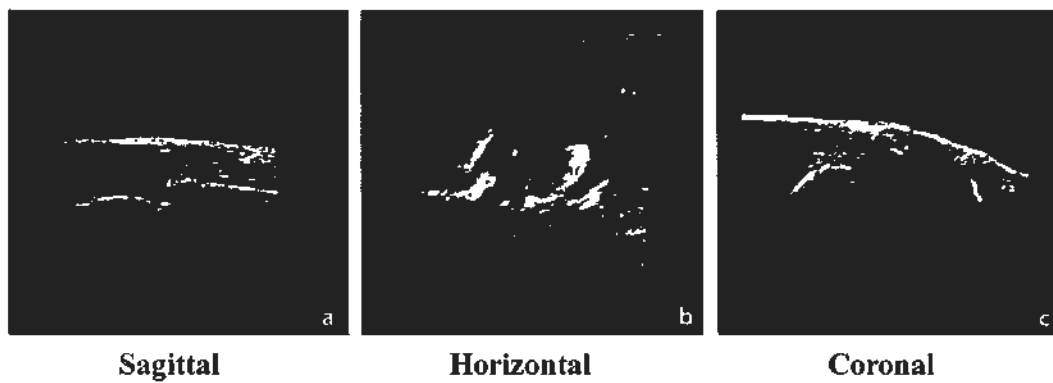
Figure 3.4-1 Images of fractured rat femur in sagittal (a), coronal (b) and horizontal (c) planes by 3D-HF-PDU reconstruction. The color signals represented the microvasculature at the peri-fracture region.
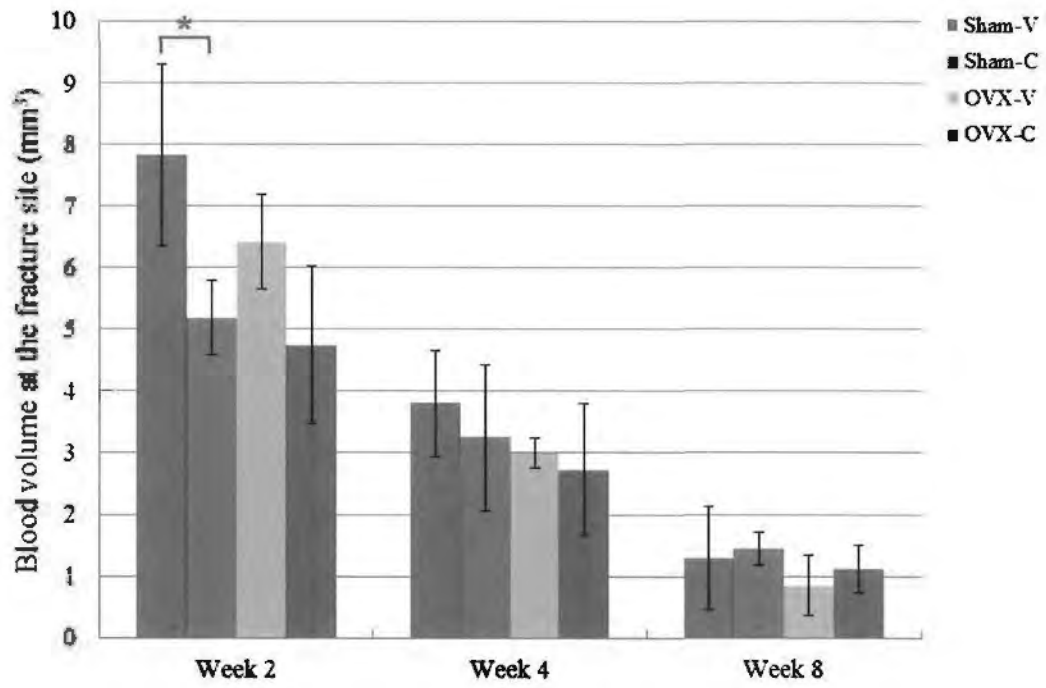
Figure 3.4-2 3D-HF-PDU analysis of the blood volume at the fracture site among 4 groups at different time points.

3.5 MicroCT-based Microangiography

After 3D reconstruction from microCT-based microangiography, the images showed osteoporotic groups had notably less neovasculature within the callus compared to non-osteoporotic groups. The angiogenesis in vibration groups was more and denser than the corresponding controls, which were more remarkable between OVX-V and OVX-C groups. At week 8, the neovasculature regeneration across the fracture gap was observed better in OVX-V group than OVX-C group (Figure 3.5-1). Quantitative analysis indicated the vessel volume decreased gradually from week 2 onwards. The vascular volume in the non-osteoporotic group was higher than the osteoporotic group at each time point, with significant differences in week 2 (Sham-V > OVX-V, p=0.014; Sham-C > OVX-C, p=0.014) and week 4 (Sham-C > OVX-C, p=0.027). Vibration groups had larger microvasculature volume than the control groups. Statistical significances were found at week 2 (OVX-V > OVX-C, p=0.009) and marginally at week 4 (OVX-V > OVX-C, p=0.034) (Figure 3.5-2 A). The ratio of vessel volume to total tissue volume (VV/TV) (Figure 3.5-2 B) and the ratio of vessel volume to bone volume (VV/BV) (Figure 3.5-2 C) showed similar trends as the vessel volume at each time point, with significant difference at week 2 (VV/TV: Sham-C > OVX-C, p=0.014; OVX-V>OVX-C, p=0.047; VV/BV: Sham-C > OVX-C, p=0.050) and week 4 (VV/TV: Sham-C>OVX-C, p=0.027; OVX-V>OVX-C, p=0.034). Interestingly, the percentage of increase in vessel volume promoted by LMHFV on osteoporotic fracture healing was higher than normal rats in week2 (Sham: +13.2%; OVX: +25.7%) and week4 (Sham: +2.2%; OVX: +57.1%).
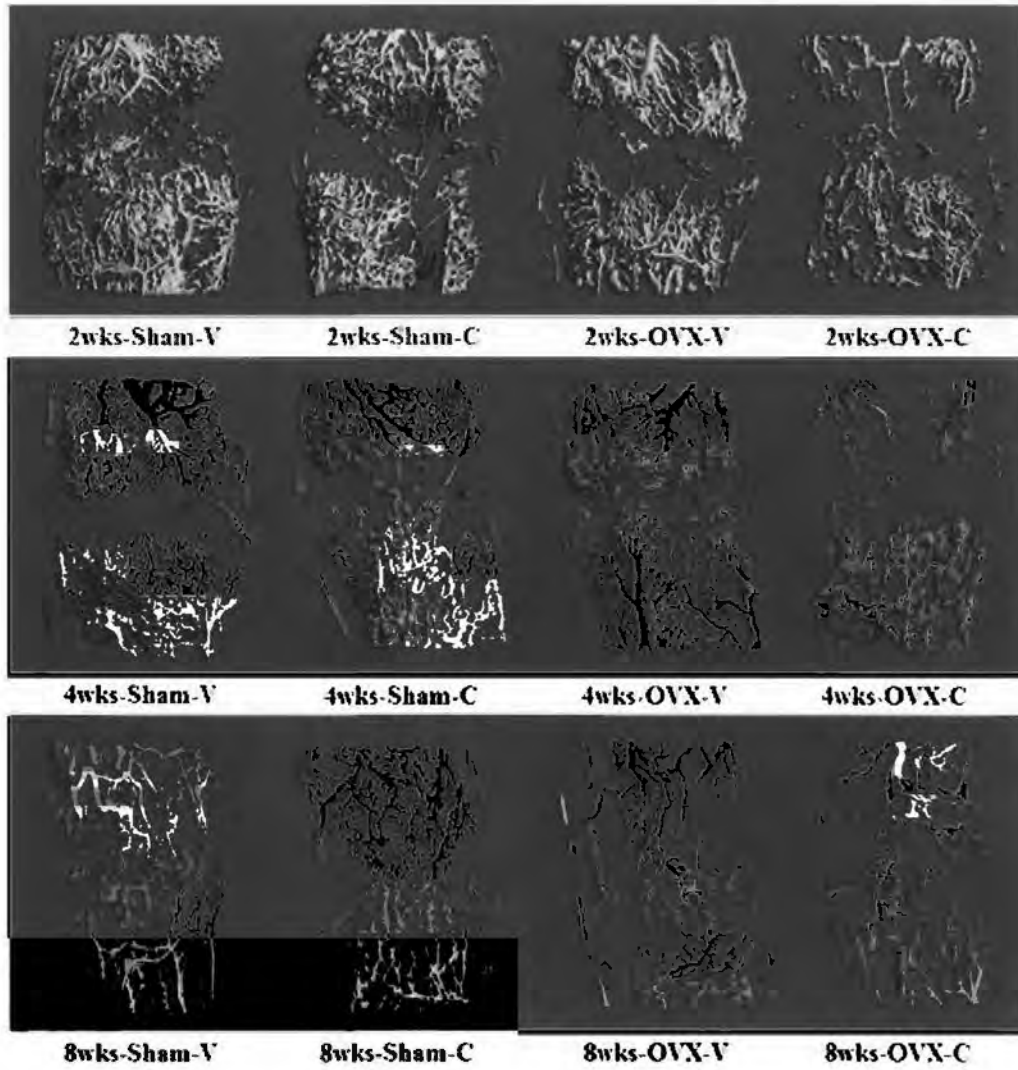
Figure 3.5-1 3D reconstruction of the vessels at the fracture site by microCT-based microangiography among 4 groups at different time points.
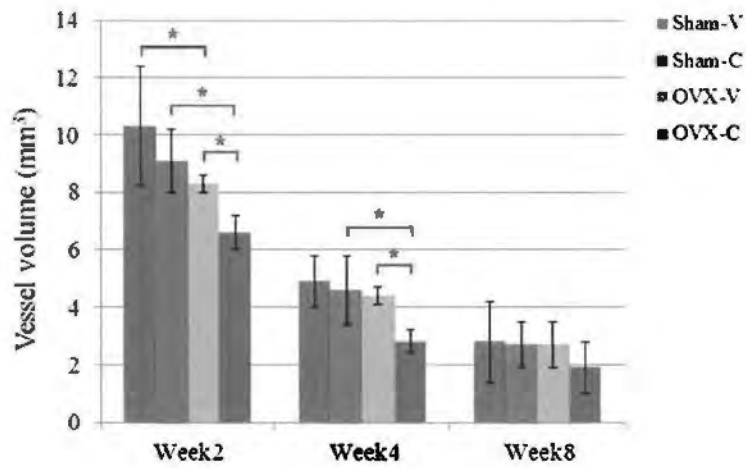
A. Vessel volume of fracture site
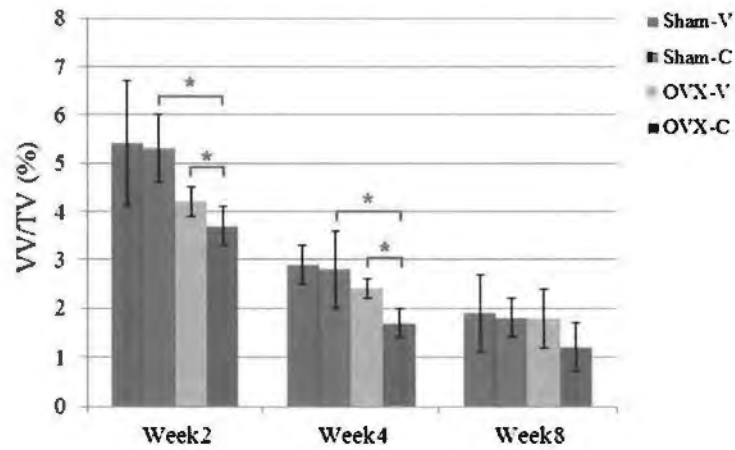
B. Vessel volume / total tissue volume
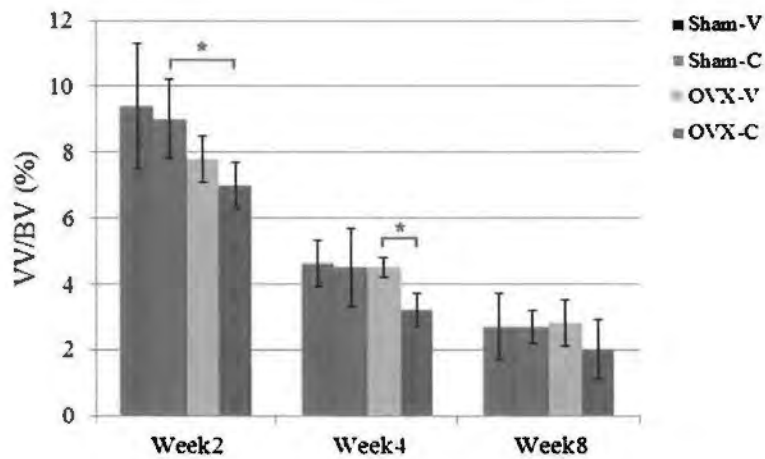
C. Vessel volume / bone volume

Figure 3.5-2 MicroCT analysis of vessel volumes of fracture site among 4 groups at different time points

3.6 MicroCT Analysis (Osseous Tissue)

The micro-CT images showed femoral cortices and mineralized calluses in the peri-fracture regions from week 2 (Figure 3.6). The vibration groups demonstrated more and larger callus formation than the controls. At week 4, the fracture gap in the peri-fracture regions started to fuse with smaller gap shown in the vibration groups as compared with the controls. The fusion in OVX-C group was slower with larger fracture gap than Sham-C group. At week 8, images showed the rats from the vibration groups had regular, symmetrical and well-connected calluses around fracture site, while the callus gap was still obvious in the controls, especially in the OVX group.

From the quantitative analysis of the osseous tissue at the fracture site (Table 3.6), it demonstrated a significant increase in OVX-V than OVX-C group, in terms of TV (week 2: $p=0.009$; week 4: $p=0.034$), BV (week 2: $p=0.016$), BV_h (week 2: $p=0.047$) and BV_l (week 2: $p=0.028$), however, there was no significant difference detected between Sham-V and Sham-C. TV in OVX-V group increased 13.4% at week 2 and 6.6% at week 4 as compared to OVX-C group, while in Sham-V, it was 9.1% and 3.8% higher than Sham-C at week 2 and week 4, respectively. BV/TV and BV_h/TV in each group increased from weeks 2 to 8. It also indicated higher value in vibration groups than in controls. BV_l showed a declining trend from week 2 on ward. At week 2, vibration groups had larger BV_l and BV_l/TV as compared to controls. From week 4, this trend reversed. BV_l and BV_l/TV in vibration groups were lower than the ones in corresponding controls. Significant difference was found in BV_l/TV at week 4

(OVX-V < OVX-C, p=0.034).

Compared Sham groups with OVX groups, Sham-C had larger callus size (by TV) than OVX-C at week 2 and 4, while it reversed at week 8. TV in Sham-V was smaller than the one in OVX-V. However, BV, BV_h, BV/TV and BV_h/TV in Sham groups were always higher than in OVX ones. Significant differences were detected in BV (week 4: Sham-C > OVX-C, p=0.020), BV_h (week 2: Sham-C > OVX-C, p=0.027; week 4: Sham-V > OVX-V, p=0.033; Sham-C > OVX-C, p=0.020; week 8: Sham-V > OVX-V, p=0.030), BV/TV (week 2: Sham-C > OVX-C, p=0.050; week 8: Sham-C > OVX-C, p=0.008), and BV_h/TV (week 2: Sham-V > OVX-V, p=0.050, Sham-C > OVX-C, p=0.014; week 4: Sham-V > OVX-V, p=0.019, Sham-C > OVX-C, p=0.020; week 8: Sham-C > OVX-C, p=0.008).

2wks-Sham-V **2wks-Sham-C** **2wks-OVX-V** **2wks-OVX-C**

4wks-Sham-V **4wks-Sham-C** **4wks-OVX-V** **4wks-OVX-C**

8wks-Sham-V **8wks-Sham-C** **8wks-OVX-V** **8wks-OVX-C**
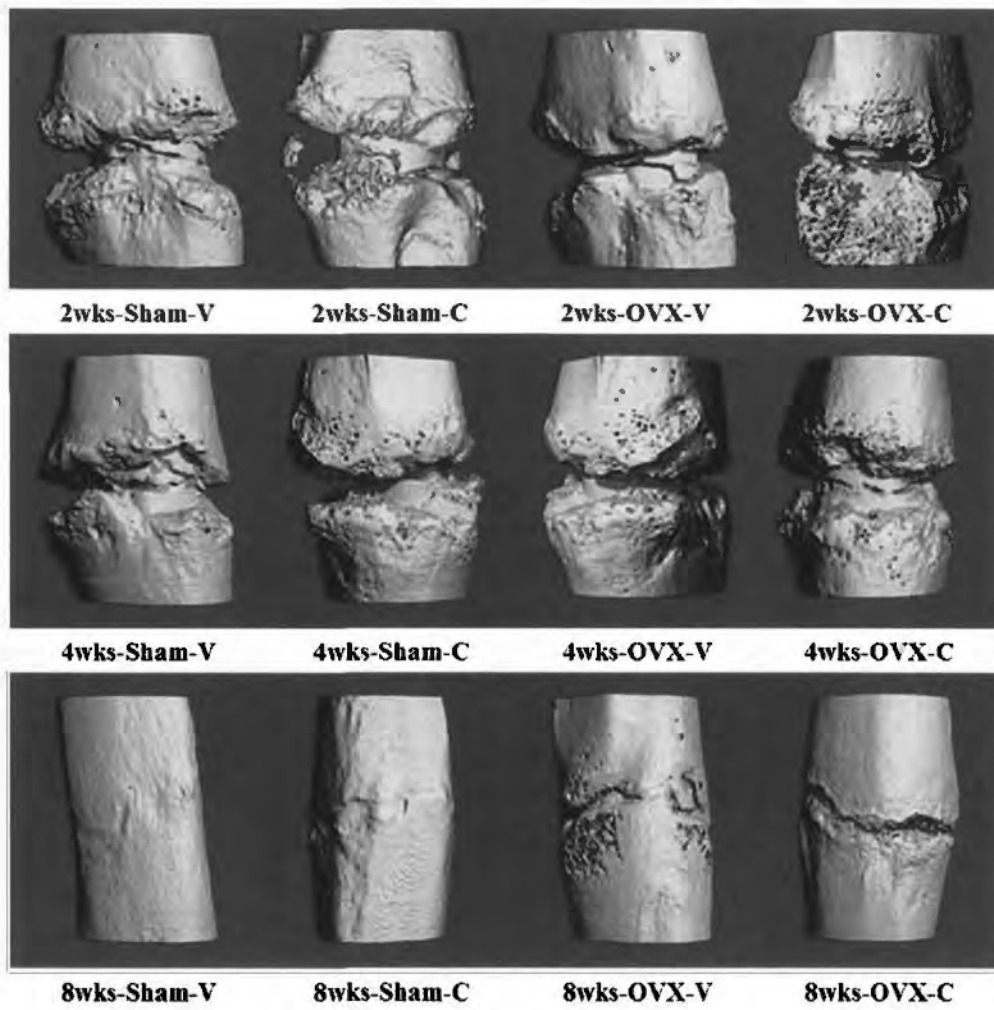
Figure 3.6 3D reconstruction of fracture site by microCT among 4 groups at different time points

Table 3.6 Micro-CT assessments of osseous tissue compared among 4 groups at different tim

	Week 2				Week 4				S
	Sham-V	Sham-C	OVX-V	OVX-C	Sham-V	Sham-C	OVX-V	OVX-C	
TV (mm^3)	194.0=21.0	177.9±11.8	198.3±13.9	174.9±6.5 [a]	177.3±20.1	170.8±14.8	184.5±3.0	173.0±6.0 [a]	1
BV (mm^3)	110.3±9.4	102.7±9.6	107.1±9.4	93.9±4.1 [a]	105.0±8.2	103.4±4.2	95.7±5.4	92.2±2.4 [c]	1
BV_h (mm^3)	53.4±2.4	52.2±3.0	50.5±4.6	44.6±3.6 [a,c]	62.2=5.1	59.1=4.3	53.1±5.7 [b]	46.9±4.0 [c]	
BV_l (mm^3)	56.9=7.6	50.5±8.5	56.6=5.1	49.2±3.2 [a]	42.9÷3.7	44.3±4.6	42.5±1.4	45.3±2.3	
BV/TV(%)	57.0=2.3	57.8±4.4	54.0=2.0	53.7±2.8 [c]	59.6±5.0	60.8±4.1	56.9±2.5	55.3±1.6	
BV_h/TV(%)	27.7±1.9	29.4±0.7	25.5±0.7 [b]	25.5±1.7 [c]	35.3±3.5	34.8±4.4	28.8±2.8 [b]	27.1±1.5 [c]	5
BV_l/TV(%)	29.3±2.1	28.4±4.4	28.5±1.6	28.2±2.5	24.3+1.7	26.0+2.0	23.1+0.8	26.2±2.3 [a]	

Note: a: $p<0.05$ between OVX-V and OVX-C;
b: $p<0.05$ between Sham-V and OVX-V;
c: $p<0.05$ between Sham-C and OVX-C.

3.7 Correlation of Angiogenesis and Osteogenesis

The association of the microvasculature and the osseous tissue at the fracture site was analyzed. It was demonstrated that both TV and BV had a positive linear correlation to the vessel volume (Figure 3.7 A, B). Significant correlation was found between BV_l and vessel volume ($R=0.7738$, $p<0.01$) (Figure 3.7 D). To the contrary, BV_h had a negative linear correlation to the vessel volume, yet without significance. (Figure 3.7 C)
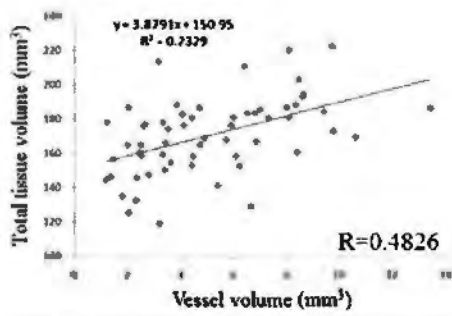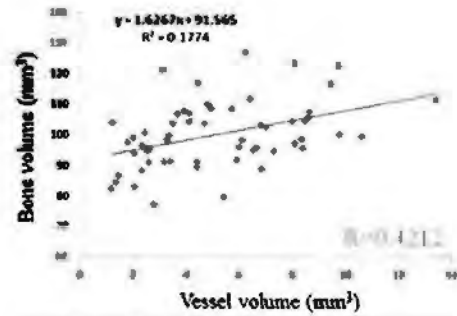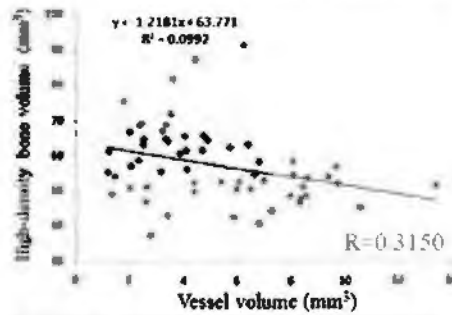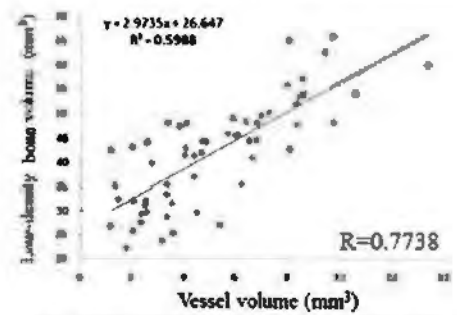
Figure 3.7 Correlation of the volume between osseous tissue and microvasculature at the fracture site. There was a linear positive correlation between TV and VV, as well as BV and BV_l. Significant correlation was indicated between BV_l and VV (r=0.7738, p<0.01). BV_h was negatively correlated to VV without significance.

3.8 Immunohistochemistry

Microscopic images (magnification: ×200) showed the features with immunohistochemical staining at the frontier of the endochondral ossification in external callus (Figure 3.8). VEGF signals could be mostly observed at the boundary of endothelial cells, as well as around the woven bone-trapped osteoblasts and hypertrophic chondrocytes. The expression of VEGF in OVX groups, in terms of immunostained area, was inferior to normal groups, and an increase of VEGF expression was detected in external callus after vibration treatment at week 2 and 4. Quantitative analyses were summarized in Table 1. In general, the area of VEGF expression at the fracture site declined from weeks 2 to 8. At weeks 2 and 4, the vibration groups had a higher ratio of VEGF.Ar/Cl.Ar as compared to controls. Statistical difference was noted between OVX-V and OVX-C at week 2 (p=0.034). At week 8, VEGF.Ar/Cl.Ar in vibration group was lower than in corresponding control group. OVX groups showed lower percentage of VEGF expression than normal ones at week 2 and 4, significant difference was found between Sham-C and OVX-C in VEGF.Ar/Cl.Ar at week 2 (p=0.031) (Table 3.8).
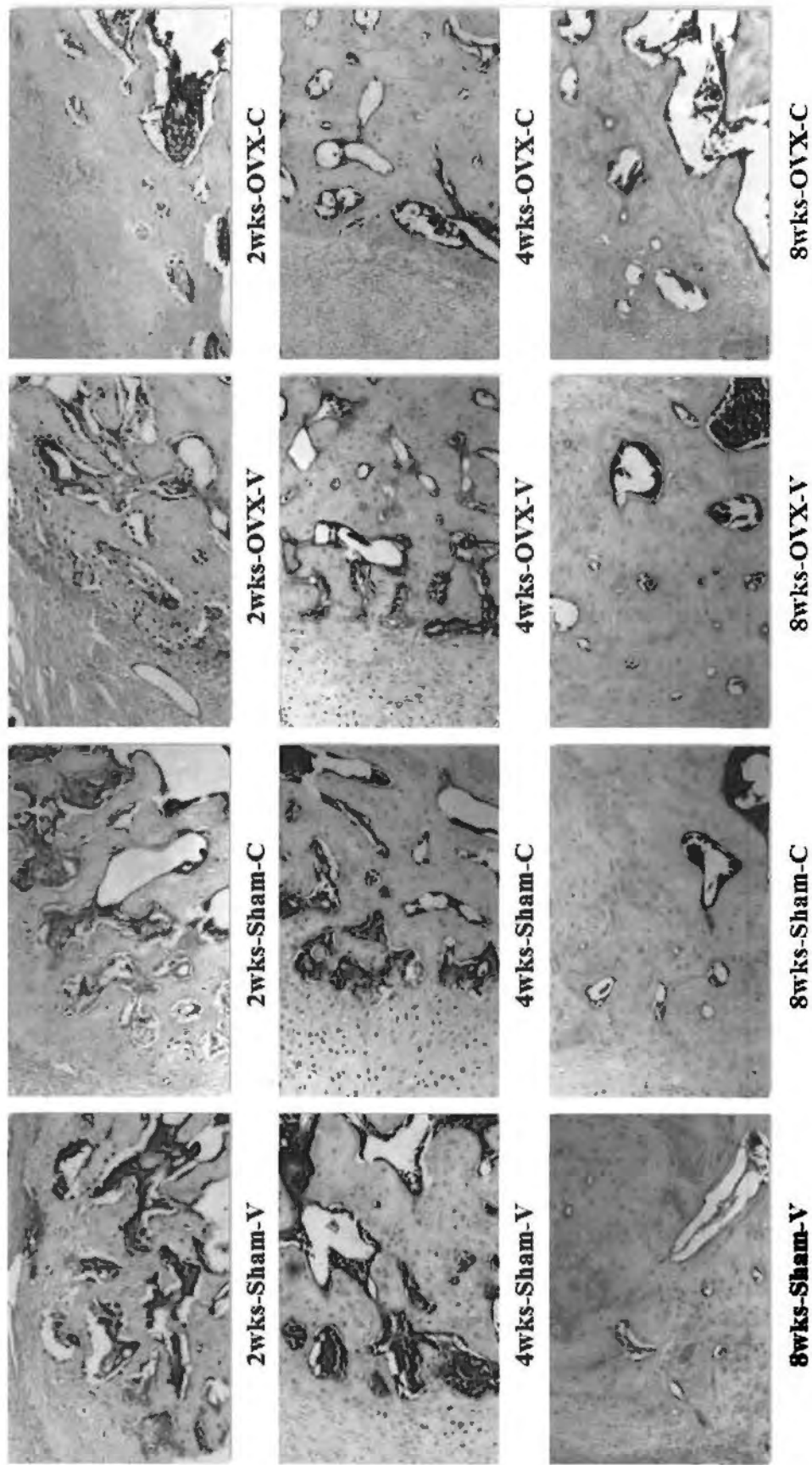
Figure 3.8 Immunohistochemical staining of VEGF at the frontier of endochondral ossification in the external callus among 4 groups at different time points (200×).

2wks-OVX-C
4wks-OVX-C
8wks-OVX-C
2wks-OVX-V
4wks-OVX-V
8wks-OVX-V
2wks-Sham-C
4wks-Sham-C
8wks-Sham-C
2wks-Sham-V
4wks-Sham-V
8wks-Sham-V

Table 3.8 Immunohistochemistry assessment of VEGF compared among 4 groups at different t

	Week 2				Week 4				
	Sham-V	Sham-C	OVX-V	OVX-C	Sham-V	Sham-C	OVX-V	OVX-C	S
VEGF Ar (mm^2)	0.5±0.2	0.4±0.1	0.4±0.2	0.2±0.1	0.4±0.1	0 3±0.1	0.4±0 2	0 3±0.1	(
Cl.Ar (mm^2)	9.2±0.8	8.9±0.7	9 0±1 0	7.8±0.9	9 0±0 7	8.6±0.8	8 8±0.8	8 2±0 6	(
VEGF.Ar / Cl.Ar (%)	5 1±0.5	4.5±0.4	4.1±0.7	2.6±0.5 [a b]	4 3±0 6	3 7±0 5	4 5±0 6	3 6±0 5	(

Note:a: p<0.05 between OVX-V and OVX-C;
b: p<0.05 between Sham-C and OVX-C.

VEGF. Ar: the area of positive VEGF stainings within external callus.
Cl Ar: the area of external callus.
VEGF.Ar / Cl.Ar (%): the ratio of VEGF. Ar to Cl.Ar.

89

3.9 Feasibility and Reproducibility of 3D-HF-PDU

3.9.1 3D-HF-PDU Analysis

From the vascular volume assessment, in general, a declining trend was found from weeks 2 to 8. In each time point, Sham group had a larger vascular volume than the corresponding osteoporotic group. Quantitative analysis demonstrated a significantly larger value in Sham group than OVX group at week 4 (p = 0.050). (Table 3.9-1)

For reproducibility testing, we calculated the intra- and inter-observer intra-class correlation coefficient. Results showed all ICCs > 0.75 (Table 3.9-2), indicating the microvasculature assessment by 3D-HF-PDU had good reproducibility.

3.9.2 MicroCT-based Microangiography

Results from microCT-based microangiography indicated the vascular volume decreased gradually from week 2 onwards. The vascular volume in the Sham group was also larger than the OVX group at each time point. Statistical significances were found at week 2 and week 4 (p = 0.014 and 0.028, respectively). (Table 3.9-1)

3.9.3 Correlation

The images with 3D reconstruction of power Doppler at the fracture site and microCT-based microangiography within callus (Figure 3.9-1) confirmed that 3D-HF-PDU provided accurate assessments into the anatomical structure of microvasculature at the fracture site, which was similar as the images from

microangiography. Compared the vascular volumes obtained from 3D-HF-PDU and the ones from microCT-based microangiography, we found a significant positive linear correlation between the outcomes of the two methodologies (r = 0.867, p < 0.001). (Figure 3.9-2)

Table 3.9-1 Vascular volume evaluated by 3D-HF-PDU and microCT-based microangiography at (

Vascular volume	Week 2		p	Week 4		p	
(mm^3)	Sham	OVX		Sham	OVX		
3D-HF-PDU	5.48±0.21	4.74±1.28	0.386	4.27±0.93	2.36±0.61	0.050*	
Microangiography	9.10±1.13	6.59±0.63	0.014*	4.61±1.21	2.89±0.35	0.028*	:

Note: * p < 0.05 between Sham and OVX.

Table 3.9-2 Intra- and inter-observer reproducibility of volume acquisition and ROI selection.

Vascularization parameters	Volume acquisition		ROI selection	
	Intra-ICC *	Inter-ICC **	Intra-ICC	Inter-ICC
Vascular volume	0.906	0.859	0.985	0.941
Mean intensity of blood signals	0.859	0.826	0.998	0.963

Note:

* Intra-ICC indicates intraobserver intra-class correlation coefficient;

** Inter-ICC indicates interobserver intra-class correlation coefficient.
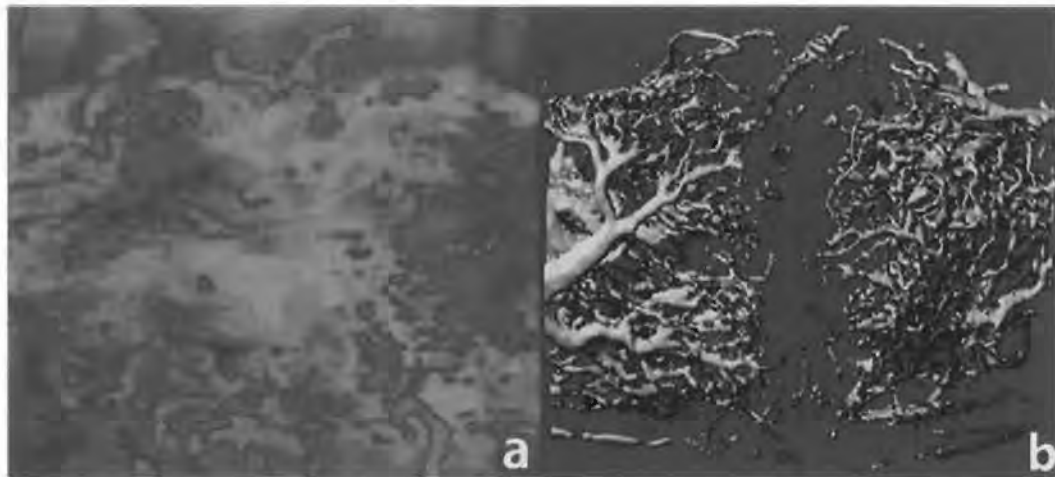
Figure 3.9-1 Comparison of 3D images by 3D-HF-PDU and microCT-based microangiography. **a:** The 3D reconstruction of power Doppler images at the fracture site (blood vessels colored in red, osseous tissues in green and surrounding soft tissues in blue). **b:** MicroCT-based microangiography within callus. Both the two methodologies showed the similar anatomic structures of microvasculature at the fracture site. At both proximal and distal sides of peri-fracture region, the neovessels regenerated towards the fracture gap.
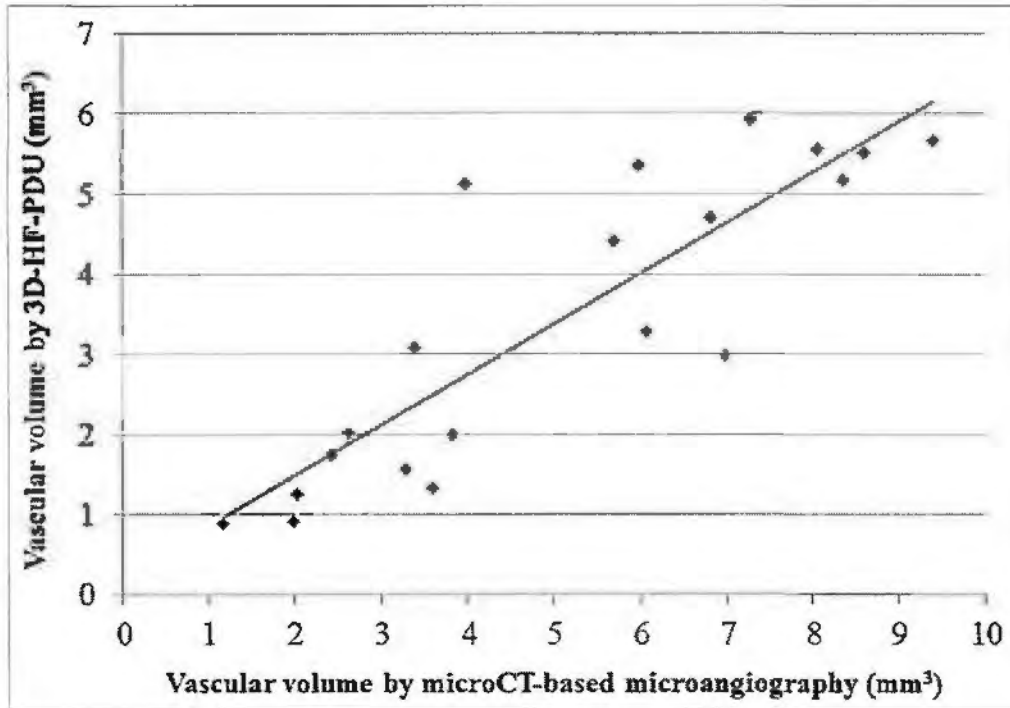
Figure 3.9-2. Correlation of the vascular volumes between 3D-HF-PDU and microCT-based microangiography at the fracture site. A significant positive linear correlation was found (r = 0.867, p<0.001).

CHAPTER 4
DISCUSSION

Fracture healing is a complex phenomenon that involves a well-characterized cascade in chronological order of haematoma formation, inflammation, intramembranous bone formation, endochondral ossification and callus modeling (256-258). In the population of postmenopausal women and elderly, osteoporosis is a major health problem characterized by decreased bone strength that leads to an increased risk of fragility fracture (259), which was recognized with an impaired capacity and prolonged process to heal (78,260). Poor bone repair status gives a pressing need for orthopaedic surgeons to develop effective, safe, convenient and economic therapeutic approaches to accelerate the osteoporotic fractures.

Bone fracture disrupts its blood circulation and leads to hypoxia and acute necrosis of bone, marrow and surrounding soft tissue. An adequate blood supply to the fracture site is prerequisite for bone repair, whereas the insufficient blood supply is likely to result in delayed, mal-union or non-union (58,60,197). Angiogenesis, or neovascularization, was defined as endothelium sprouts from the pre-existing vascularity (187,198,199). The neovasculature can recover oxygen homeostasis, deliver nutrients, remove metabolic and regenerative wastes, transport necessitous mesenchyme cells, growth factors and other biological cytokines to the peri-fracture region (60). Blood vessels also provide systemically circulating factors that may modify fracture healing such as PTH and Vitamin D (60). Furthermore, angiogenesis is pivotal during intramembranous and endocondral ossifications. During endochondral ossification, the avascular environment of cartilage is invaded by blood vessels fronted by chondroclastic cells with osteoblast progenitors which will deposit

new bone on the surface of cartilage islands. Intramembranous bone formation also requires vascularization, presumably to provide ingress for osteoblast progenitors (59). Ischemia of fracture significantly decreased callus formation (197,261). By using inhibitors of angiogenesis, the fracture healing was found completely prevented (208). Therefore, angiogenesis plays a pivotal role in multiple stages of fracture healing.

In osteoporotic condition, blood perfusion of bone is reduced (239). In addition, Strehlow et al. indicated the reendothelialization of injured vessel segments by bone marrow-derived endothelial progenitor cells (EPCs) was decreased in ovariectomized mice (262). In regard to the importance of blood supply in bone repair, it shows that the impaired capacity of osteoporotic fracture healing may closely relate to the poor revascularization and perfusion at fracture site.

Low magnitude, high frequency vibration (LMHFV), a biophysical modality that provides noninvasive, systemic, cyclic mechanical strain stimulation, has been reported to be effective in promoting osteogenesis, maintaining bone mineral density (BMD) (142,179,263-266), enhancing muscle strength and augmenting peripheral blood circulation in many studies of animals and humans (143,146,267). Our previous studies were the first to demonstrate that LMHFV (magnitude=0.3g, frequency =35Hz) accelerated fracture healing in both normal and osteoporotic fractures (10,11) and enhanced bone remodeling in rat model (180). The mechanism of the beneficial effects of LMHFV on fracture healing, however, remains uncertain.

Currently, the effects of whole body vibration on blood circulation have increasingly attracted a major concern. Kerschan-Schindl et al. demonstrated that the

mean blood velocity of participants' quadriceps and gastrocnemius muscles was doubled after vibration (magnitude=3mm, frequency=26Hz) (145). Stewart et al. provided additional evidence that whole body vibration (magnitude=0.2g, frequency=15&45Hz) increased blood flow to the lower extremities in perimenopausal women (146). Lythgo et al also reported the similar improvement in leg blood flow by vibration (magnitude=2.5mm & 4.5mm, frequency=5-30Hz with 5Hz increments) (143). An appropriate load to the fracture site was considered beneficial for angiogenesis and osteogenesis, because micro-motion actually increased blood flow to the fracture site (268,269).

Based on the scientific supports above, the application of LMHFV may have special properties in enhancing revascularization and blood perfusion at the peri-fracture region, thus to accelerate the fracture healing (*see chapter 1.6*). The present study was designed to examine the effects of LMHFV treatment (magnitude=0.3g, frequency=35Hz) on angiogenesis and blood flow in both non-osteoporotic and osteoporotic fractures, whilst to investigate the possible causes of delayed fracture healing in osteoporotic bones as compared with non-osteoporotic ones. The results shown in *chapter 3* demonstrated a few positive findings that would be discussed in the following sections.

4.1 Blood Flow Changes of Fractured Hind Limb

The results assessed by pulsed-wave Doppler indicated a gradual increase of blood flow velocity of femoral artery from weeks 2 to 8, which represented a recovery of blood supply to the distal hind limb. In blunt trauma, the high amount of energy that is typically absorbed causes severe damage to skeletal structures and soft tissues, and frequently produces almost complete distal ischemia, because of the crushing injury and soft tissue swelling (270). The endothelium injury might lead to the generation of thrombus and endotheliosis in the femoral artery, which resulted in arteriostenosis. Therefore, the distal blood flow of hind limb decreased at the beginning of arterial injury. Subsequently, recanalization provided capillary-sized channels through the thrombus for continuity of blood flow, and dissolution occured when fibrinolytic mechanisms broke up the thrombus and blood flow was then restored to the vessel (271,272).

4.1.1 Beneficial Effect of LMHFV on Blood Flow

In this study, LMHFV at 0.3g, 35Hz was confirmed to increase the blood flow velocity of hind limb in each time point compared to the control subjects, with significant improvements found at week 2 and week 4. This was substantiated by Stewart's study that reported a significantly improved leg fluid flow in 18 peri-menopausal women by plantar vibration at 45Hz, 0.2g point-to-point, as assessed by strain-gauge plethysmography (146). Lythgo et al. confirmed a four-fold increase of mean blood cell velocity by whole-body vibration (2.5 & 4.5mm magnitude,

5-30Hz with 5Hz increments) (143). McDonald et al. demonstrated that an important effect of mechanical loading was the significant alteration of blood flow in bone (273).

The explanation of blood flow enhancing effect might be that the blood had the feature of shear thinning that was the effect where the viscosity decreased with increase rate of shear stress by vibration (145). Also, vibration could widen small vessels in muscles to reduce the peripheral resistance, heighten muscle activity and muscle metabolic demand by activating muscle spindle, and hence increase the blood flow velocity (274).

Clinically, combined arterial and skeletal extremity trauma imparts a substantially higher risk of limb loss and limb morbidity than do isolated skeletal and arterial injuries. The lower extremities are involved in two thirds of all patients with vascular injuries. Our results showed an enhanced blood flow of ischemic lower extremity after vibration treatment, which might provide a potential modality to help a better recovery of blood perfusion and to reduce the clinical amputation rate.

To the contrary, some studies showed that high-frequency vibration would restrict blood flow (275-277) and even caused hypertrophy of the smooth vascular muscle cells (278). However, these findings were often encountered by operators of power tools with much higher frequency (above 80 Hz). From previous studies and our parameter, the frequency of vibration was distributed within a modest range (5-60 Hz) which indicated no damage to the organism. Therefore, the dosage of physiological safety should also be well considered and investigated for vibration

treatment.

4.1.2 Comparison of Blood Flow in Non-osteoporotic and Osteoporotic Conditions

In each time point, the blood flow velocity of femoral artery showed a higher level in sham-OVX group than corresponding OVX group, significant differences were found at week 8. A number of in vivo studies in animals (279,280) and human (281-289) indicated a decreased blood flow and increased peripheral resistance in various vascular beds after spontaneous or surgical menopause. It might result from the estrogen deficiency after ovariectomy, which increased the blood viscosity, and thus decreased the blood flow velocity (290,291). On the other hand, estrogens was proven to increase the production of nitric oxide (NO) and to reduce the production of reactive oxygen species, which in turn were putatively important for growth-stimulatory and antiapoptotic effects on the endothelium (292-294). Consequently, experiments in several animal models revealed that estrogen accelerated reendothelialization processes after injury (295). Strehlow et al. found that estrogen increased EPCs numbers which accelerated the vascular repair and decreased neointima formation (262). Combined previous studies with our findings, it was presumed the ovariectomized rats had higher peripheral blood viscosity and impaired capacity of artery repair due to the estrogen deficiency, which resulted in compromised hemodynamics of hind limb as compared with the ones of non-osteoporotic rats.

102

4.2 Angiogenesis at the Fracture Site

From the results of local angiogenesis assessments (microCT-based microangiography and 3D-HF-PDU), generally, a decline trend of neovasculature volume at the fracture site was shown from week 2 to week 8 post-treatment. Some previous studies looking into the neovascularization in bone repair showed similar findings. Raines et al. observed a decreasing trend of neovascular volume within the marrow cavity from the peak value at 14 days after bone drilling in tibial marrow ablation rats (296). Zeng et al.'s study found a high expression of vascular endothelial growth factor (VEGF) lasting from days 14 to 28 post femoral fracture in rats, then it decreased gradually until week 6 (297). The pathophysiology might be due to the changes of local oxygen concentration during fracture healing. Under the hypoxic condition after fracture, mesenchymal stem cells increased transcription of the gene encoding vascular endothelial growth factor (VEGF) in a HIF-1α dependent manner, and neovessels consequently sprouted from the pre-existing ones (298,299). According to the previous studies in rodents, the VEGF expression started from day 3-4 post-fracture and rose steadily to its peak concentration at about day 10-21 then declined thereafter (68,300). Due to the blood vessels ingrowth, the oxygen tension gradually rose, and the hypoxic condition relieved, hence the angiogenic response descended. In addition, during the mineralization and remodeling of callus, the microvasculature diminished with the callus resorption. Therefore, the amount of neovessels at the fracture site declined from week 2 to week 8.

Our observation showed that angiogenesis could be most important in the early

period of fracture healing. The temporal importance of angiogenesis in contributing to non-union development is considered by Brownlow et al., which demonstrated by immunocytochemistry that at 8 and 16 weeks post-fracture, established atrophic non-unions were well-vascularized in a rabbit tibia non-union model. Earlier time points, however, did show a discrepancy in vessel concentration between union and non-union groups, particularly at 1 week. (301) The fibrous tissue of non-unions may become revascularized eventually, but a critical window for fracture union has been missed, and some other manipulation of the fracture biology may be necessary to promote union. Our findings suggested that angiogenic stimulatory therapy for promoting healing might be required early rather than late.

4.2.1 Stimulatory Effect of Angiogenesis by LMHFV in Fracture Healing

The angiogenesis (VV, VV/TV, VV/BV by microangiography, blood volume by 3D-HF-PDU, VEGF.Ar./Cl.Ar. by IHC) at the peri-fracture region in vibration groups was demonstrated significantly enhanced as compared with controls, especially in week 2. This was consistent with Carvalho's study on mechanical stimulation, which reported the expression of angiogenic factors, such as hypoxia-induced factor-1α, neuropilin 1, and VEGF-A were induced in murine model of tibia distraction osteogenesis (302). Many previous reports substantiated that VEGF expression was induced in osteoblasts by various stimuli including mechanical loading (203,302,303). In turn, VEGF regulated recruitment, survival and activity of osteoclasts, endothelial cells and osteoblasts. Strong VEGF expression of osteoprogenitors had been found in

early stage of fracture healing (304). Furthermore, VEGF has been shown to play a major role in cartilage maturation and resorption, which initiate the endochondral ossification cascade by attracting osteoblasts and by recruiting and differentiating osteoclastic cells that resorb cartilage (305-310).

The LMHFV-induced angiogenic stimulatory effect could be explained by the reasons shown below: (1) Biomechanical forces generated by blood flow and blood pressure can regulate vascular functions. Flowing blood constantly exerts a frictional force, shear stress, on the endothelial cells (ECs) lining blood vessel walls, and the ECs respond to shear stress by changing their morphology, function, and gene expression, including angiogenesis (311), vascular remodeling (312), and atherosclerosis (313). Numerous studies have been devoted to clarify the mechanism of shear stress mechanotransduction (314-317), however, it is not yet fully understood. Abumiya et al. found increased the blood flow shear force at vascular endothelium, due to the inertia of blood, augmented the functions of VEGF by up-regulating VEGFR-2 (318). Vibration might enhance the angiogenesis through increasing the blood flow shear stress at the ECs underwent the same mechanism. (2) Besides around the endothelial cells, we also observed more positive VEGF expression than controls in the osteoblasts and hypertrophic chondrocytes, especially at the front of endochondral ossification. Osteoblasts were confirmed to synthesize VEGF in response to mechanical stimuli such as distraction osteogenesis (319,320) and shockwave (203). Wong et al. indicated cyclic shear stress up-regulated VEGF expression of hypertrophic chondrocyte *in vitro* (321). These studies imply LMHFV

might stimulate osseous cells to synthesize VEGF to provide important functions in endochondral ossification, which included the breakdown of calcified cartilage matrix, inducing invasion of endothelial and osteoblast-regulating mineralization. (3) LMHFV could increase skeletal muscle activity, which elevated the muscle blood flow several-fold as a result of metabolic vasodilation of resistance arterioles. As a consequence, there is enhanced capillary perfusion with significant increases in the velocity of red blood cells (322) and increased capillary pressure. It would increase the shear stress to which endothelial cells were exposed and hence enhance the angiogenesis in the soft tissue surrounding the fracture site. Brown's study partially supports our deduction (323). They demonstrated that VEGF protein was elevated at capillary sites due to the increase of shear by muscle activity stimulation. It was concluded that the most likely stimuli for angiogenesis could be increased blood flow and shear forces to vessel supplying the active muscle fibres, probably linked with metabolic factors.

Our osteogenesis results of this study further confirmed that LMHFV had positive effects on accelerating both normal and osteoporotic fracture healing. Both radiographic and microCT assessments indicated better callus formation and mineralization at the fracture site in LMHFV groups than control ones, where the enhancements were observed in the early phase at week 2 and 4. With the consistent findings between angiogenesis and osteogenesis and the significant correlation between neovascular volume and BV_1, it is believed angiogenesis plays a critical role in osteogenesis of fracture healing process. Colleran et al. also indicated that

decreased lower limb perfusion resulted in decreased cancellous bone formation as well as reduced periosteal bone (324). Therefore, LMHFV may accelerate the fracture healing through enhancing angiogenesis and hence osteogenesis.

Our results also demonstrated the early phase of healing was the most influential period for LMHFV treatment, which suggested that LMHFV should be applied at the beginning of fracture healing to obtain better angiogenic and osteogenic effectiveness.

4.2.2 Comparison of Angiogenesis in Normal and Osteoporotic Fracture Healing

The findings of the present study confirmed that osteoporotic fractures had lower level of angiogenesis at the peri-fracture site than the one of non-osteoporotic fractures, as reflected by lower microvascular volume, blood volume and expressions of VEGF. Consistently, in terms of osteogenesis, osteoporotic bones demonstrated a poorer callus formation, intramembranous ossification and fracture healing than the controls, as proven by lower CW, CA, BV and TV at week 2 and week 4. This was further supported by another report that histologically showed a delayed callus formation with poor development of mature bone in osteoporotic bone (325). Jesmin S et al also found a reduced VEGF expression level in ovariectomized rat model (326). Estrogen plays an important role in fracture healing. In animals with estrogen deficiency, delayed fracture healing and slowed muscle recovery after inactivity have been observed (325,327). As estrogen plays a potential role in angiogenesis (328), it is postulated that estrogen deficiency might cause impaired angiogenic capacity in osteoporotic bones, resulting in delayed fracture healing.

Interestingly, despite the generally lower angiogenic response than non-osteoporotic fractures, osteoporotic fractures were more sensitive than age-matched non-osteoporotic ones in response to LMHFV by higher percentage increase of blood flow and angiogenesis (week 2: Sham-V +13.2% vs. OVX-V +25.7%; week 4: Sham-V +2.2% vs. OVX-V +57.1%). This phenomenon was consistently observed in osteogenic responses as reported in this and our previous study (11), which further justify the close relationship between angiogenesis and osteogenesis. Shi et al. demonstrated that the OVX-V rats had a larger percentage of callus size increase during fracture healing. In Sham-V group, TV increased 11.2% at week 2 and 2.2% at week 4 by LMHFV, while OVX-V group improved 17.5% and 11.8% at week 2 and 4 respectively (11).The higher sensitivity of osteoporotic bones to LMHFV than sham-OVX ones might be explained by some evidences that ovariectomy induced higher extent of decline in estrogen receptor β (ERβ) than in ERα mRNA, thus altering the ratio of ERα/ERβ (329), where ER is well-known mechanosensitive and estrogen acts as a negative modulator of mechanotransduction via ERβ signaling (330-333). However, further investigations are required to verify the interactive effects of ERα and ERβ on angiogenesis by mechanical stimulation.

4.3 Effects of LMHFV on Fracture Healing in Normal and Osteoporotic Bones

4.3.1 Normal and Osteoporotic Fracture Healing

OVX-induced osteoporotic and age-matched non-osteoporotic fracture healing was compared. From our results, fracture healing in OVX-C group was poorer than that in Sham-C ones with less callus formation and slower intramembranous/endocondral ossification reflected by lower CW, CA, BV_l and BV_h. Other studies also showed impaired fracture healing in osteoporotic conditions with regard to BMD and microarchitecture at different stages (11,334). The reasons might include impaired capacity of angiogenesis (335,336), decreased growth hormone secretion The effect of growth hormone on fracture healing in old rats and reduced osteoinductive capacity of demineralized bone matrix.

4.3.2 Effect of LMHFV in Normal and Osteoporotic Fracture Healing

In our study, LMHFV was proven effective in accelerating fracture healing in both normal and OVX bones, especially in the early phase of the healing process, as indicated by most of the parameters (CW, CA, TV, BV, BV_h, B_h/TV) with significantly higher values by radiography and micro-CT analysis. This was consistent with previous studies which proved vibration had a positive effect in promoting osteogenesis. It also matched with other mechanical stimulation therapies like low-intensity pulsed ultrasound, of which the positive effect on fracture healing was remarkable in the early stages before mineralization (337).

Enhanced callus formation was confirmed by increased CW, CA, BVand BV_l.

Faster mineralization and remodeling were demonstrated respectively by significantly increased BV_h, BV_h/TV and faster decline of CW, BV_l in vibration groups as compared with controls. These findings revealed that LMHFV enhanced intramembranous ossification and endochondral ossification, which might imply the positive effects of mechanical stimulations on osteoprogenitor cells differentiation.

Interestingly, in this study, OVX-V group also showed a higher percentage of increase in CW, CA, TV and BV as compared with Sham-V in the early phase of fracture healing. It implied that the bones after ovariectomy might be more sensitive to mechanical stimuli, which echo with our previous findings (11). This is consistent with Rubinacci's study that found ovariectomy could sensitize the cortical bone to whole body vibration (176). As mentioned above, our angiogenesis assessments of fracture site also showed a more sensitive angiogenic response to LMHFV in osteoporotic fractures, which might partially explain why osteoporotic bone had a more osteogenic response to mechanical stimulation.

4.4 Newly Established *in vivo* Imaging Methodology for Assessing Microvasculature by 3D-HF-PDU

To understand revascularization and local blood perfusion in both normal and osteoporotic fracture healing, 3D high frequency power Doppler ultrasonography (3D-HF-PDU) was utilized and compared with microCT-based microangiography that is the gold standard to assess angiogenesis in small animals. The aim was to determine the application of 3D-HF-PDU imaging. This might serve as an *in vivo* platform for assessing the microcirculation in small animals both qualitatively and quantitatively.

4.4.1 Similarities with microCT-based microangiography

From the results, the vascular volume calculated by 3D-HF-PDU showed a similar decline as that from microangiography from weeks 2 to 8 in both Sham and OVX groups. An impaired angiogenic response in osteoporotic fracture healing was detected in our study. Microangiography data and other reports also confirmed impaired revascularizaion in osteoporotic fracture healing as compared to normal healing (31).

A significantly positive linear correlation of vascular volumes between 3D-HF-PDU and microCT-based microangiography was found. All the findings indicate 3D-HF-PDU is comparable to microCT-based microangiography and the results are consistent with other previous studies. Also, it is sensitive in distinguishing between normal and impaired angiogenic responses. To our knowledge, this is the first study to assess the changes in microvasculature and local blood flow during

111

fracture healing in rats using 3D-HF-PDU. Currently, despite conventional microCT-based microangiography being the gold standard assessment for microvasculature studies in fracture healing (226), it is not feasible for longitudinal analyses in the same animal as the animal need to be euthanized for such purpose. In addition, the results cannot provide the flow information and can be affected by the quality of capillary perfusion due to fluctuations variables such as blood flush, perfusion pressure and threshold value chosen of the vascular tree during CT analysis (59). Therefore, it is advantageous to use 3D-HF-PDU imaging because it is non-invasive, real-time and can be used for longitudinal follow-up for both vascularization and blood flow quantifications.

4.4.2 Other Parameters of 3D Power Doppler

The mean signal intensity of blood flow is a mean of amplitude value of the color voxels within VOI, which has been demonstrated to be positively correlated to the concentration of moving blood cells (338). The relative number of erythrocytes is calculated as the product of signal intensity and vascular volume, which combines the information of blood vessels and blood cells to evaluate the local circulation (339). These parameters can provide us more quantitative information of hemodynamics in microcirculation.

4.4.3 Advantages of Using 3D-HF-PDU

In other previous *in vivo* studies, some investigators adopted power Doppler

ultrasound to assess neovasculature at the fracture site in humans and large animals, i.e. detecting the existence of vascularity, evaluating the vessel area, vessel density or blood flow intensity from 2D images (340). However, since each 2D slice would give a different percentage of color pixels, it would be necessary to measure many parallel slices throughout the total volume in order to reach a reliable result. Since 3D geometric evaluation can provide the spatial vascular tree, the value of vascular volume and blood flow within VOI, 3D-HF-PDU measurement will certainly improve the accuracy, objectivity, and integrity of the microcirculation information. Conventional frequency (2-15 MHz) ultrasound in clinical examinations has difficulties in detecting small vessels (5-100 μm) and low flow velocities (~0-50 mm/s) of the microcirculation. One possible method is to increase the operating frequency to above 20 MHz range (237). Goertz et al.'s *in vivo* experiments confirmed that, at a center frequency of 50 MHz, the detection of vessels could be improved to 15-20μm in diameter in the mouse ear and demonstrated flow imaging in assessing a wide range of velocities (1-25 mm/s) present in superficial mouse tumors (238). Therefore, we chose the transducer with the center-frequency at 55 MHz, which was sensitive in detecting and assessing neovascularization around the fracture site.

4.4.4 Imaging Optimization and Other Technical Precautions

There are some technical precautions for 3D-HF-PDU. Firstly, it is necessary to reduce and filter the image noises during the scanning. Power Doppler is highly sensitive to motion artifacts which can be created by artery pulsations, breathing or

113

muscles contractions, etc. An overly high Doppler gain, increasing the scan speed and vibration of the motor used in motor-steered probes, may also generate such disturbances. In order to reduce these artifacts, animals should be anesthetized with the extremities fixed, and a hand-free stand was utilized to mount the transducer for scanning. In addition, it is appropriate to set the gain by up-regulating its value until random noise is encountered, then down-regulating until the noise disappears (341). The noise and low frequency flash artifacts could also be avoided by means of wall filters (342). Low filter settings can improve sensitivity but may easily generate flash artifacts, whereas high filters can reduce the artifacts but will filter out flow in low levels. In our study, we found wall filter setting at about 2.5 mm/s was suitable for scanning around the rat femur. Secondly, when dealing with the signals to assess the microcirculation, appropriate imaging programs need to be used to discriminate and filter large vessel signals, which has been indicated in the methods section. Finally, since anesthesia will affect the peripheral blood circulation, each animal should be anesthetized with the same dose strictly according to its body weight and placed at a set room temperature and positioned on a warming plate at the set room temperature to avoid the variations in anesthesia effect. Complete scanning should be finished within a short time.

In summary, our newly-established technique using 3D-HF-PDU improved power Doppler 2D imaging to a 3D spatial view. The results demonstrated the feasibility and reproducibility of 3D-HF-PDU for detecting and quantifying angiogenesis in fractured femur of rats. Being non-invasive, while offering

high-resolution anatomical visualization and allowing objective data analysis, 3D-HF-PDU provides a robust approach for the evaluation of neovascular networks in the fracture healing of small animals, especially for a longitudinal follow up *in vivo*.

4.5 Limitations

This study has some limitations. Due to the low resolution of pulsed-wave Doppler (16MHz) for small animals and the continuous pulsations of the femoral artery, it was difficult to measure the internal diameter of the artery (<0.8mm) accurately and objectively. We, therefore, used the blood flow velocity to represent the blood supply of the hind limb.

The application of 3D-HF-PDU also has its limitations. The detection of flow signals is limited by the penetration depth. With higher Doppler frequency, only lower penetration depths can be reached, so researchers need to compromise between the accuracy and the detection depth. We measured the muscle thickness at both lateral and medial sides of the fracture site in rats, which were shown 2.47 ± 0.33mm and 4.06 ± 0.42mm respectively. The focal length of our transducer was 4.5 mm from the transducer surface in soft tissues of rats. Therefore, both the resolution and the penetration depth were adequate for our study. Moreover, most sound waves were reflected as soon as it reached hard callus or cortical bone surfaces, so some vasculatures in the medullary cavity could not be detected, which explained why the absolute volume values detected by 3D-HF-PDU were consistently smaller than those of microangiography.

Due to the advantages of small size (2-3 μm) and high backscatter that enhance the intensity of the ultrasound signal, contrast agents have been developed to visualize the vasculature at the capillary level, which allow a more sensitive measure of microcirculation (343). In this study, we aimed to explore and determine the

feasibility of 3D-HF-PDU for assessing the microvasculature, so we did not use contrast agents. However, for further improvement of the image quality and more precise quantification, contrast agents are recommended for angiogenesis assessment at the fracture site in small animals.

Platelet endothelial cell adhesion molecule-1 (PECAM-1) is a molecule expressed on all cells within the vascular compartment, which is good for identifying blood vessels in immunohistochemistry assessment. Further investigation on PECAM-1 expression at the fracture site should be performed to verify whether the results can correlate with the findings demonstrated by microCT-based microangiography.

This study focused on diaphysial fracture healing and the effects of LMHFV on fracture repair at metaphysial region is still under investigation now at femoral neck in human. Our explanation of ER for impaired angiogenesis has also being studied in our laboratory.

4.6 Future Study

The present study has testified, through a translational approach, the stimulatory effects of LMHFV on angiogenesis and blood flow to accelerate fracture healing in normal and osteoporotic bones, which provides basis and evidences for the future studies on upstream mechanisms and downstream clinical applications.

Mechanical stimuli simultaneously affect other tissues through mechanotransduction, and this could be manipulated to improve bone regeneration. Indeed, it is feasible to use mechanical stimuli to promote bone regeneration, although this will occur only if there is a timely nutrient supply and waste cleaning. This suggests that angiogenesis is needed to facilitate the bone regeneration induced by mechanical stimuli. A study of the chorioallantoic membrane revealed mechanical strain could elicit angiogenic features (344). Moreover, osteoblasts responded in vitro to mechanical stimulation by increasing matrix production and regulating angiogenesis (203). Current research hypothesized that induction of matrix metalloproteinases after mechanical strain enhances attraction and penetration of blood vessels through which osteoblasts could reach the chondroosseous junction and promote ossification (345,346). Future research examining whether mechanical stimulus-induced bone regeneration can be improved by simultaneously activating mechanotransduction pathways that promote angiogenesis would be of considerable clinical interest.

4.6.1 Hypoxia-inducible Factor-1α Signaling Pathway Coupling Angiogenesis

and Osteogenesis Associated with LMHFV

Hypoxia-inducible factors (HIFs), which belong to the Per/Anrt/Sim subfamily of basic helix-loop-helix transcription factors (347), are major regulators of the gene programs that orchestrate angiogenic-osteogenic coupling. HIF-1α protein expression is regulated by an oxygen-sensitive proteolytic mechanism. Under normal conditions, HIF-1α is rapidly degraded, but, when oxygen levels drop below 5%, expression is stabilized and its activity progressively increases with additional decreases in the oxygen tension (348).When a fracture occurs, the abrupt interruption of oxygen and nutrient supply with consequential upregulation of HIF-1α has been proposed as a primary stimulus for new bone formation (60). Hypoxia is a major driving force for angiogenesis during endochondral bone formation. HIF-1α stimulates VEGF production in this microenvironment to initiate blood vessel invasion into cartilage. It is suggested that VEGF production by hypertrophic chondrocytes may be regulated by HIF-1α-dependent mechanism (349).

In addition to low oxygen levels, mechanical stimuli can also upregulate HIF-1α expression. Carvalho et al. found the activation of the distraction device induced the expression of HIF-1α and VEGF-A which were the major regulators of the angiogenic process. Inactivation of HIF-1α impairs both angiogenesis and bone regeneration as the distraction gap in these animals develop fewer blood vessels and accumulate less bone (302). The essential roles of HIF-1α during fracture repair suggest that this pathway could be targeted in mechanical stimuli interventions to accelerate bone healing, which may lead to further investigation on the mechanism of angiogenic–

osteogenic effect of LMHFV in cellular and molecular levels.

4.6.2 Role of LMHFV on Mesenchymal Stem Cells (MSCs) during Fracture Healing

Previous research indicated that low-level whole body vibration had osteogenic effect. It was proven angiogenesis could be enhanced as a result of applied mechanical load *in vitro*. Our study also demonstrated LMHFV could enhance both angiogenesis and osteogenesis during fracture healing in rats. However, the mechanism on the effects of mechanical stimulation (e.g. LMHFV) in a cellular level remains poorly understood.

In fracture and bone defect healing, MSCs largely drive tissue regeneration. MSCs have proangiogenic properties and harbor a great expansion potential (350). These cells are able to differentiate not only into mesenchymal cells, such as osteoblasts and chondrocytes, but also into non-mesenchymal cells, such as endothelial cells (ECs) (350). To date, there is clear evidence for a complex interplay between MSCs and ECs. MSCs seem to be able to promote angiogenesis, and the presence of ECs appears to promote osteogenic differentiation of MSCs (351). Mechanical boundary conditions are known to alter the gene expression pattern and consequently the functional behavior of MSCs. Osteogenic differentiation and proliferation of MSCs can be stimulated by mechanical loading (352). In other previous studies, the influence of mechanical loading on the paracrine stimulation of angiogenesis by MSCs was investigated. MSCs are capable of angiogenesis induction

in an *in vivo* model (353). Based on these findings, we predict LMHFV may have the capacity of MSCs recruitment through mechanotransductional pathways and can promote the differentiation of MSCs into osteoblasts, chondrocytes and endothelial cells, hence to accelerate the fracture healing.

Therefore, further insight into these interactions and the influence of mechanical stimulations is vital for an understanding of the physiological coordination of angiogenesis, progenitor cell differentiation, and regenerated osseous tissue formation. This understanding is in turn the foundation for a rational approach to the design and optimization of prevascularized tissue-engineered constructs and essential for predicting optimal mechanical stabilization conditions for successful bone regeneration.

4.6.3 Effects of LMHFV on Blood Circulation in Clinical Trials

4.6.3.1 Haemodynamic responses of Peripheral Circulation to LMHFV

To date, many effects of whole-body vibration have been reported in the literatures, including increased leg power, strength and flexibility (354,355), increased BMD and enhanced fracture healing in post-menopausal women (356), and improved postural control and mobility in adults with multiple sclerosis (357). However, only few studies investigated the effect of whole-body vibration on peripheral blood flow. Kerschan-Schindl et al. found vibrations delivered by a rotary type platform with a frequency of 26 Hz and amplitude of 3 mm doubled leg blood flow after 9 min of vibration (145). Zhang et al. similarly found increased leg blood flow after direct

transmission of vibration to the foot of subjects (358). The results suggest that vibration serves to significantly enhance peripheral and systemic blood flow, peripheral lymphatic flow, and venous drainage.

Improvements in blood flow by vibration may be beneficial in the bone mass, muscle functions, therapeutic alleviation of pain or other symptoms (e.g. hyperlipemia, stroke) resulting from acute or chronic musculoskeletal injuries. The clinical goal should focus on the effects of different parameters of vibration (magnitude, frequency, duration of treatment, etc.) to provide evidence for a more optimized treatment regime.

4.6.3.2 Angiogenic Effect of LMHFV on the Therapy of Wound Healing and Avascular Diseases

The current study has proven positive effects of LMHFV on blood flow and angiogenesis in both normal and osteoporotic fractures. Based on these findings, clinical trials should be carried out to further testify the efficacy in fractured patients, especially in elderly, who may have high fall risk or long-term bedrest, hence have difficulty to get early functional exercise. Besides, the angiogenic enhancing effect may also be beneficial for the treatment of osteonecrosis, delayed union and non-union.

CHAPTER 5
CONCLUSIONS

In conclusion, osteoporotic fractures had lower level of blood flow and impaired angiogenesis than normal ones. LMHFV could enhance the blood flow velocity of hind limb and angiogenesis at the fracture site in both normal and osteoporotic groups, particularly in the early phase. Osteoporotic bones were also shown to be more sensitive in angiogenic and osteogenic responses to LMHFV than normal ones, which might partially explain the different extents of normal and osteoporotic fracture healing. Angiogenesis is one of the major mechanisms of LMHFV to accelerate fracture healing. The findings of this study help further understand the role of angiogenesis in the enhancement effect of LMHFV on fracture healing and in the impaired healing capacity of osteoporotic fracture. LMHFV has a great potential in clinical applications for fracture healing, wound healing and some other vascular diseases.

REFERENCES:

1. Schoenau E, Saggese G, Peter F, Baroncelli GI, Shaw NJ, Crabtree NJ, Zadik Z, Neu CM, Noordam C, Radetti G, Hochberg Z 2004 From bone biology to bone analysis. Horm Res **61**(6):257-69.

2. Bronner F 2002 Founding editorial--bone biology. ScientificWorldJournal **2**:787-90.

3. Marsell R, Einhorn TA 2011 The biology of fracture healing. Injury.

4. Einhorn TA 1998 The cell and molecular biology of fracture healing. Clin Orthop Relat Res (355 Suppl):S7-21.

5. Winters-Stone KM, Nail L, Bennett JA, Schwartz A 2009 Bone Health and Falls: Fracture Risk in Breast Cancer Survivors With Chemotherapy-Induced Amenorrhea. Oncol Nurs Forum **36**(3):315-325.

6. Forin V 2010 Genetic osteopathies in pediatry: imperfect osteogenesis and osteopetrosis. Correspondances En Metabolismes Hormones Diabetes Et Nutrition **14**(7):228-228.

7. Lewandrowski KU, Gresser JD, Wise DL, Trantol DJ 2000 Bioresorbable bone graft substitutes of different osteoconductivities: a histologic evaluation of osteointegration of poly(propylene glycol-co-fumaric acid)-based cement implants in rats. Biomaterials **21**(8):757-64.

8. Leung KS, Cheung WH, Yeung HY, Lee KM, Fung KP 2004 Effect of weightbearing on bone formation during distraction osteogenesis. Clin Orthop Relat Res (419):251-7.

9. Cheung WH, Chow SK, Sun MH, Qin L, Leung KS 2011 Low-intensity pulsed ultrasound accelerated callus formation, angiogenesis and callus remodeling in osteoporotic fracture healing. Ultrasound Med Biol **37**(2):231-8.

10. Leung KS, Shi HF, Cheung WH, Qin L, Ng WK, Tam KF, Tang N 2009 Low-magnitude high-frequency vibration accelerates callus formation, mineralization, and fracture healing in rats. J Orthop Res **27**(4):458-65.

11. Shi HF, Cheung WH, Qin L, Leung AH, Leung KS 2010 Low-magnitude

high-frequency vibration treatment augments fracture healing in ovariectomy-induced osteoporotic bone. Bone **46**(5):1299-305.

12. Xie L, Jacobson JM, Choi ES, Busa B, Donahue LR, Miller LM, Rubin CT, Judex S 2006 Low-level mechanical vibrations can influence bone resorption and bone formation in the growing skeleton. Bone **39**(5):1059-66.

13. Tzaphlidou M 2008 Bone architecture: collagen structure and calcium/phosphorus maps. J Biol Phys **34**(1-2):39-49.

14. Lanham SA, Roberts C, Perry MJ, Cooper C, Oreffo RO 2008 Intrauterine programming of bone. Part 2: alteration of skeletal structure. Osteoporos Int **19**(2):157-67.

15. Travlos GS 2006 Normal structure, function, and histology of the bone marrow. Toxicol Pathol **34**(5):548-65.

16. Klein-Nulend J, Nijweide PJ, Burger EH 2003 Osteocyte and bone structure. Curr Osteoporos Rep **1**(1):5-10.

17. McCarthy I 2006 The physiology of bone blood flow: a review. J Bone Joint Surg Am **88 Suppl 3**:4-9.

18. Shim SS 1986 Bone and joint circulation. Physiological basis for clinical practice. Yonsei Med J **27**(2):91-9.

19. Fleming JT, Barati MT, Beck DJ, Dodds JC, Malkani AL, Parameswaran D, Soukhova GK, Voor MJ, Feitelson JB 2001 Bone blood flow and vascular reactivity. Cells Tissues Organs **169**(3):279-84.

20. Iversen PO 1997 Blood flow to the haemopoietic bone marrow. Acta Physiol Scand **159**(4):269-76.

21. Hori Y, Tamai S, Okuda H, Sakamoto H, Takita T, Masuhara K 1979 Blood vessel transplantation to bone. J Hand Surg Am **4**(1):23-33.

22. Dawson JS, Martel AL, Davis TR 2001 Scaphoid blood flow and acute fracture healing. A dynamic MRI study with enhancement with gadolinium. J Bone Joint Surg Br **83**(6):809-14.

23. Grundnes O, Utvag SE, Reikeras O 1994 Effects of graded reaming on fracture healing. Blood flow and healing studied in rat femurs. Acta Orthop Scand

65(1):32-6.

24. Smith JW, Arnoczky SP, Hersh A 1992 The intraosseous blood supply of the fifth metatarsal: implications for proximal fracture healing. Foot Ankle 13(3):143-52.

25. Schumichen C, Mundriziewski L, Tischler E, Hoffmann G 1979 Relationship between blood flow and radiostrontium uptake in the healing bone fracture. Eur J Nucl Med 4(6):413-7.

26. Rhinelander FW 1974 Tibial blood supply in relation to fracture healing. Clin Orthop Relat Res (105):34-81.

27. Frost HM 1989 The biology of fracture healing. An overview for clinicians. Part II. Clin Orthop Relat Res (248):294-309.

28. Frost HM 1989 The biology of fracture healing. An overview for clinicians. Part I. Clin Orthop Relat Res (248):283-93.

29. Marsh DR, Li G 1999 The biology of fracture healing: optimising outcome. Br Med Bull 55(4):856-69.

30. Stein H, Perren SM, Mosheiff R 2004 New insights into the biology of fracture healing. Orthopedics 27(9):915-8.

31. Augat P, Simon U, Liedert A, Claes L 2005 Mechanics and mechano-biology of fracture healing in normal and osteoporotic bone. Osteoporos Int 16 Suppl 2:S36-43.

32. Perrien DS, Wahl EC, Hogue WR, Feige U, Aronson J, Ronis MJ, Badger TM, Lumpkin CK, Jr. 2004 IL-1 and TNF antagonists prevent inhibition of fracture healing by ethanol in rats. Toxicol Sci 82(2):656-60.

33. Wallace A, Cooney TE, Englund R, Lubahn JD 2011 Effects of Interleukin-6 Ablation on Fracture Healing in Mice. J Orthop Res.

34. Yang X, Ricciardi BF, Hernandez-Soria A, Shi Y, Pleshko Camacho N, Bostrom MP 2007 Callus mineralization and maturation are delayed during fracture healing in interleukin-6 knockout mice. Bone 41(6):928-36.

35. Kayal RA, Siqueira M, Alblowi J, McLean J, Krothapalli N, Faibish D, Einhorn TA, Gerstenfeld LC, Graves DT 2010 TNF-alpha mediates diabetes-enhanced chondrocyte apoptosis during fracture healing and stimulates

chondrocyte apoptosis through FOXO1. J Bone Miner Res **25**(7):1604-15.

36. Gerstenfeld LC, Cho TJ, Kon T, Aizawa T, Tsay A, Fitch J, Barnes GL, Graves DT, Einhorn TA 2003 Impaired fracture healing in the absence of TNF-alpha signaling: the role of TNF-alpha in endochondral cartilage resorption. J Bone Miner Res **18**(9):1584-92.

37. Schmidmaier G, Wildemann B, Ostapowicz D, Kandziora F, Stange R, Haas NP, Raschke M 2004 Long-term effects of local growth factor (IGF-I and TGF-beta 1) treatment on fracture healing. A safety study for using growth factors. J Orthop Res **22**(3):514-9.

38. Yu Y, Yang JL, Chapman-Sheath PJ, Walsh WR 2002 TGF-beta, BMPS, and their signal transducing mediators, Smads, in rat fracture healing. J Biomed Mater Res **60**(3):392-7.

39. Andrew JG, Hoyland J, Andrew SM, Freemont AJ, Marsh D 1993 Demonstration of TGF-beta 1 mRNA by in situ hybridization in normal human fracture healing. Calcif Tissue Int **52**(2):74-8.

40. Garrison KR, Shemilt I, Donell S, Ryder JJ, Mugford M, Harvey I, Song F, Alt V 2010 Bone morphogenetic protein (BMP) for fracture healing in adults. Cochrane Database Syst Rev (6):CD006950.

41. Cuenca-Lopez MD, Peris JL, Garcia-Rosello M, Atienza C, Prat J, Becerra J, Andrades JA 2010 Action of recombinant human BMP-2 on fracture healing in rabbits is dependent on the mechanical environment. J Tissue Eng Regen Med **4**(7):543-52.

42. Spiro AS, Beil FT, Baranowsky A, Barvencik F, Schilling AF, Nguyen K, Khadem S, Seitz S, Rueger JM, Schinke T, Amling M 2010 BMP-7-induced ectopic bone formation and fracture healing is impaired by systemic NSAID application in C57BL/6-mice. J Orthop Res **28**(6):785-91.

43. Chhabra A, Zijerdi D, Zhang J, Kline A, Balian G, Hurwitz S 2005 BMP-14 deficiency inhibits long bone fracture healing: a biochemical, histologic, and radiographic assessment. J Orthop Trauma **19**(9):629-34.

44. Southwood LL, Frisbie DD, Kawcak CE, Ghivizzani SC, Evans CH,

McIlwraith CW 2004 Evaluation of Ad-BMP-2 for enhancing fracture healing in an infected defect fracture rabbit model. J Orthop Res **22**(1):66-72.

45. Bouletreau PJ, Warren SM, Spector JA, Peled ZM, Gerrets RP, Greenwald JA, Longaker MT 2002 Hypoxia and VEGF up-regulate BMP-2 mRNA and protein expression in microvascular endothelial cells: implications for fracture healing. Plast Reconstr Surg **109**(7):2384-97.

46. Geris L, Sloten JV, Van Oosterwyck H 2010 Connecting biology and mechanics in fracture healing: an integrated mathematical modeling framework for the study of nonunions. Biomech Model Mechanobiol **9**(6):713-24.

47. Sakano S, Zhu Y, Sandell LJ 1999 Cartilage-derived retinoic acid-sensitive protein and type II collagen expression during fracture healing are potential targets for Sox9 regulation. J Bone Miner Res **14**(11):1891-901.

48. Hiltunen A, Metsaranta M, Virolainen P, Aro HT, Vuorio E 1994 Retarded chondrogenesis in transgenic mice with a type II collagen defect results in fracture healing abnormalities. Dev Dyn **200**(4):340-9.

49. Stogov MV, Luniova SN, Tkachuk EA 2010 Accumulation of calcium, phosphate, and collagen in bones and accumulation of creatine in muscles of mice with acute hepatic intoxication during shin fracture healing. Bull Exp Biol Med **149**(5):575-7.

50. Wigner NA, Luderer HF, Cox MK, Sooy K, Gerstenfeld LC, Demay MB 2010 Acute phosphate restriction leads to impaired fracture healing and resistance to BMP-2. J Bone Miner Res **25**(4):724-33.

51. Al-Zube L, Breitbart EA, O'Connor JP, Parsons JR, Bradica G, Hart CE, Lin SS 2009 Recombinant human platelet-derived growth factor BB (rhPDGF-BB) and beta-tricalcium phosphate/collagen matrix enhance fracture healing in a diabetic rat model. J Orthop Res **27**(8):1074-81.

52. Nakata E, Nakanishi T, Kawai A, Asaumi K, Yamaai T, Asano M, Nishida T, Mitani S, Inoue H, Takigawa M 2002 Expression of connective tissue growth factor/hypertrophic chondrocyte-specific gene product 24 (CTGF/Hcs24) during fracture healing. Bone **31**(4):441-7.

53. Jepsen KJ, Price C, Silkman LJ, Nicholls FH, Nasser P, Hu B, Hadi N, Alapatt M, Stapleton SN, Kakar S, Einhorn TA, Gerstenfeld LC 2008 Genetic variation in the patterns of skeletal progenitor cell differentiation and progression during endochondral bone formation affects the rate of fracture healing. J Bone Miner Res **23**(8):1204-16.

54. Lee FY, Choi YW, Behrens FF, DeFouw DO, Einhorn TA 1998 Programmed removal of chondrocytes during endochondral fracture healing. J Orthop Res **16**(1):144-50.

55. Beamer B, Hettrich C, Lane J 2009 Vascular Endothelial Growth Factor: An Essential Component of Angiogenesis and Fracture Healing. HSS J.

56. Chu T, Liu Y, Wang Z, Zhu P, Jiao W, Wen J, Gong S 2009 Sustained vascular endothelial growth factor blockade by antivascular endothelial growth factor antibodies results in nonunion in the process of fracture healing in rabbits. J Trauma **66**(4):1180-3.

57. Chu TW, Liu YG, Wang ZG, Zhu PF, Liu LD 2008 Vascular endothelial growth factor and its receptor expression during the process of fracture healing. Chin J Traumatol **11**(3):161-4.

58. Geris L, Gerisch A, Sloten JV, Weiner R, Oosterwyck HV 2008 Angiogenesis in bone fracture healing: a bioregulatory model. J Theor Biol **251**(1):137-58.

59. Lu C, Marcucio R, Miclau T 2006 Assessing angiogenesis during fracture healing. Iowa Orthop J **26**:17-26.

60. Glowacki J 1998 Angiogenesis in fracture repair. Clin Orthop Relat Res (355 Suppl):S82-9.

61. Luisetto G, Camozzi V 2009 Statins, fracture risk, and bone remodeling. J Endocrinol Invest **32**(4 Suppl):32-7.

62. Fazzalari NL 2008 Bone remodeling: A review of the bone microenvironment perspective for fragility fracture (osteoporosis) of the hip. Semin Cell Dev Biol **19**(5):467-72.

63. Schindeler A, McDonald MM, Bokko P, Little DG 2008 Bone remodeling

during fracture repair: The cellular picture. Semin Cell Dev Biol **19**(5):459-66.

64. Rizzo M, Rini GB 2006 Statins, fracture risk, and bone remodeling: What is true? Am J Med Sci **332**(2):55-60.

65. Blumsohn A 2003 Bone remodeling markers: assessment of fracture risk and fracture risk reduction. Curr Osteoporos Rep 1(3):91-7.

66. Sarahrudi K, Thomas A, Braunsteiner T, Wolf H, Vecsei V, Aharinejad S 2009 VEGF serum concentrations in patients with long bone fractures: a comparison between impaired and normal fracture healing. J Orthop Res **27**(10):1293-7.

67. Keramaris NC, Calori GM, Nikolaou VS, Schemitsch EH, Giannoudis PV 2008 Fracture vascularity and bone healing: a systematic review of the role of VEGF. Injury **39 Suppl 2**:S45-57.

68. Komatsu DE, Hadjiargyrou M 2004 Activation of the transcription factor HIF-1 and its target genes, VEGF, HO-1, iNOS, during fracture repair. Bone **34**(4):680-8.

69. Khodaparast O, Coberly DM, Mathey J, Rohrich RJ, Levin LS, Brown SA 2003 Effect of a transpositional muscle flap on VEGF mRNA expression in a canine fracture model. Plast Reconstr Surg **112**(1):171-6.

70. Kolar P, Gaber T, Perka C, Duda GN, Buttgereit F 2011 Human Early Fracture Hematoma Is Characterized by Inflammation and Hypoxia. Clin Orthop Relat Res.

71. Wei A, Leong A, Williams L, Chung S, Shen B, Bhargav D, Diwan AD 2010 BMP-7 in combination with estrogen enhances bone formation in a fracture callus explant culture. Tohoku J Exp Med **221**(1):61-8.

72. Yu YY, Lieu S, Lu C, Miclau T, Marcucio RS, Colnot C 2010 Immunolocalization of BMPs, BMP antagonists, receptors, and effectors during fracture repair. Bone **46**(3):841-51.

73. Kloen P, Di Paola M, Borens O, Richmond J, Perino G, Helfet DL, Goumans MJ 2003 BMP signaling components are expressed in human fracture callus. Bone **33**(3):362-71.

74. Kellum E, Starr H, Arounleut P, Immel D, Fulzele S, Wenger K, Hamrick

MW 2009 Myostatin (GDF-8) deficiency increases fracture callus size, Sox-5 expression, and callus bone volume. Bone **44**(1):17-23.

75. Rani S, Barbe MF, Barr AE, Litivn J 2010 Role of TNF alpha and PLF in bone remodeling in a rat model of repetitive reaching and grasping. J Cell Physiol **225**(1):152-67.

76. Lane JM 2011 Osteoporosis and fracture risk. Orthopedics **34**(5):368-9.

77. Rachner TD, Khosla S, Hofbauer LC 2011 Osteoporosis: now and the future. Lancet **377**(9773):1276-87.

78. Giannoudis P, Tzioupis C, Almalki T, Buckley R 2007 Fracture healing in osteoporotic fractures: is it really different? A basic science perspective. Injury **38 Suppl 1**:S90-9.

79. Reginster JY 2007 Calcium and vitamin D for osteoporotic fracture risk. Lancet **370**(9588):632-4.

80. Cummings SR, Melton LJ 2002 Epidemiology and outcomes of osteoporotic fractures. Lancet **359**(9319):1761-7.

81. Kanis JA 2002 Diagnosis of osteoporosis and assessment of fracture risk. Lancet **359**(9321):1929-36.

82. Lau EM, Lee JK, Suriwongpaisal P, Saw SM, Das De S, Khir A, Sambrook P 2001 The incidence of hip fracture in four Asian countries: the Asian Osteoporosis Study (AOS). Osteoporos Int **12**(3):239-43.

83. Ling X, Cummings SR, Mingwei Q, Xihe Z, Xioashu C, Nevitt M, Stone K 2000 Vertebral fractures in Beijing, China: the Beijing Osteoporosis Project. J Bone Miner Res **15**(10):2019-25.

84. Lloyd-Jones DM, Leip EP, Larson MG, D'Agostino RB, Beiser A, Wilson PW, Wolf PA, Levy D 2006 Prediction of lifetime risk for cardiovascular disease by risk factor burden at 50 years of age. Circulation **113**(6):791-8.

85. Shen B, Mu JX, Pei FX 2007 Relationship among bone mineral density, collagen composition, and biomechanical properties of callus in the healing of osteoporotic fracture. Chin J Traumatol **10**(6):360-5.

86. Hao YJ, Zhang G, Wang YS, Qin L, Hung WY, Leung K, Pei FX 2007

Changes of microstructure and mineralized tissue in the middle and late phase of osteoporotic fracture healing in rats. Bone **41**(4):631-8.

87. Wang JW, Li W, Xu SW, Yang DS, Wang Y, Lin M, Zhao GF 2005 Osteoporosis influences the middle and late periods of fracture healing in a rat osteoporotic model. Chin J Traumatol **8**(2):111-6.

88. Namkung-Matthai H, Appleyard R, Jansen J, Hao Lin J, Maastricht S, Swain M, Mason RS, Murrell GA, Diwan AD, Diamond T 2001 Osteoporosis influences the early period of fracture healing in a rat osteoporotic model. Bone **28**(1):80-6.

89. Nurmi-Luthje I, Luthje P, Kaukonen JP, Kataja M, Kuurne S, Naboulsi H, Karjalainen K 2009 Post-fracture prescribed calcium and vitamin D supplements alone or, in females, with concomitant anti-osteoporotic drugs is associated with lower mortality in elderly hip fracture patients: a prospective analysis. Drugs Aging **26**(5):409-21.

90. Carmona RJ, Adachi JD 2007 Calcium and vitamin D for osteoporotic fracture prevention. Pol Arch Med Wewn **117**(10):441-2.

91. Gennari L, Martini G 2008 Does calcium supplementation reduce the risk of osteoporotic fracture and bone loss? Nat Clin Pract Rheumatol **4**(2):70-1.

92. Klompmaker TR 2005 Lifetime high calcium intake increases osteoporotic fracture risk in old age. Med Hypotheses **65**(3):552-8.

93. Nurmi-Luthje I, Sund R, Juntunen M, Luthje P 2011 Post-hip fracture use of prescribed calcium plus vitamin D or vitamin D supplements and anti-osteoporotic drugs are associated with lower mortality. A nationwide study in Finland. J Bone Miner Res.

94. Moniz C, Dew T, Dixon T 2005 Prevalence of vitamin D inadequacy in osteoporotic hip fracture patients in London. Curr Med Res Opin **21**(12):1891-4.

95. Cooper C, Javaid K, Westlake S, Harvey N, Dennison E 2005 Developmental origins of osteoporotic fracture: the role of maternal vitamin D insufficiency. J Nutr **135**(11):2728S-34S.

96. Michaelsson K, Melhus H, Bellocco R, Wolk A 2003 Dietary calcium and vitamin D intake in relation to osteoporotic fracture risk. Bone **32**(6):694-703.

97. Hollinger JO, Onikepe AO, MacKrell J, Einhorn T, Bradica G, Lynch S, Hart CE 2008 Accelerated fracture healing in the geriatric, osteoporotic rat with recombinant human platelet-derived growth factor-BB and an injectable beta-tricalcium phosphate/collagen matrix. J Orthop Res 26(1):83-90.

98.Bak B, Andreassen TT 1989 The effect of aging on fracture healing in the rat. Calcif Tissue Int 45(5):292-7.

99. Tucci M, Lancaster R, Wingerter S, Woodall J, Jr., Russell G, Benghuzzi H 2009 Comparison of segmental fracture healing in young and old rats that were treated with bone stimulators - biomed 2009. Biomed Sci Instrum 45:407-12.

100. Meyer RA, Jr., Desai BR, Heiner DE, Fiechtl J, Porter S, Meyer MH 2006 Young, adult, and old rats have similar changes in mRNA expression of many skeletal genes after fracture despite delayed healing with age. J Orthop Res 24(10):1933-44.

101. Bak B, Andreassen TT 1991 The effect of growth hormone on fracture healing in old rats. Bone 12(3):151-4.

102. Foppiani L, Cella A, Carrara P, Balocco M, Forzano F, Leone D, Ivaldi G, Bacigalupo L, Del Monte P 2011 Osteoporosis in an elderly man as interplay of multiple diseases. Geriatr Gerontol Int 11(1):123-6.

103. Katz S, Weinerman S 2010 Osteoporosis and gastrointestinal disease. Gastroenterol Hepatol (N Y) 6(8):506-17.

104. Baldini M, Forti S, Marcon A, Ulivieri FM, Orsatti A, Tampieri B, Airaghi L, Zanaboni L, Cappellini MD 2010 Endocrine and bone disease in appropriately treated adult patients with beta-thalassemia major. Ann Hematol 89(12):1207-13.

105. Meczekalski B, Podfigurna-Stopa A, Genazzani AR 2010 Hypoestrogenism in young women and its influence on bone mass density. Gynecol Endocrinol 26(9):652-7.

106. Yoon J, Kwon SR, Lim MJ, Joo K, Moon CG, Jang J, Park W 2010 A comparison of three different guidelines for osteoporosis treatment in patients with rheumatoid arthritis in Korea. Korean J Intern Med 25(4):436-46.

107. Huusko TM, Korpela M, Karppi P, Avikainen V, Kautiainen H, Sulkava R 2001 Threefold increased risk of hip fractures with rheumatoid arthritis in Central Finland. Ann Rheum Dis **60**(5):521-2.

108. Gennari L, Becherini L, Falchetti A, Masi L, Massart F, Brandi ML 2002 Genetics of osteoporosis: role of steroid hormone receptor gene polymorphisms. J Steroid Biochem Mol Biol **81**(1):1-24.

109. Gyulai L, Bauer M, Garcia-Espana F, Hierholzer J, Baumgartner A, Berghofer A, Whybrow PC 2001 Bone mineral density in pre-and post-menopausal women with affective disorder treated with long-term L-thyroxine augmentation. J Affect Disord **66**(2-3):185-91.

110. Leung KS 2001 Practical Manual for Musculoskeletal Trauma. Springer.

111. Carr JB, Williams D, Richards M 2009 Lateral decubitus positioning for intramedullary nailing of the femur without the use of a fracture table. Orthopedics **32**(10).

112. Godley DR 1997 Nonunited carpal scaphoid fracture in a child: treatment with pulsed electromagnetic field stimulation. Orthopedics **20**(8):718-9.

113. Tsai CL, Chang WH, Liu TK, Wu KH 1991 Additive effects of prostaglandin E2 and pulsed electromagnetic fields on fracture healing. Chin J Physiol **34**(2):201-11.

114. Mundi R, Petis S, Kaloty R, Shetty V, Bhandari M 2009 Low-intensity pulsed ultrasound: Fracture healing. Indian J Orthop **43**(2):132-40.

115. Pounder NM, Harrison AJ 2008 Low intensity pulsed ultrasound for fracture healing: a review of the clinical evidence and the associated biological mechanism of action. Ultrasonics **48**(4):330-8.

116. Siska PA, Gruen GS, Pape HC 2008 External adjuncts to enhance fracture healing: what is the role of ultrasound? Injury **39**(10):1095-105.

117. Azuma Y, Ito M, Harada Y, Takagi H, Ohta T, Jingushi S 2001 Low-intensity pulsed ultrasound accelerates rat femoral fracture healing by acting on the various cellular reactions in the fracture callus. J Bone Miner Res **16**(4):671-80.

118. Hsu RW, Tai CL, Chen CY, Hsu WH, Hsueh S 2003 Enhancing

mechanical strength during early fracture healing via shockwave treatment: an animal study. Clin Biomech (Bristol, Avon) **18**(6):S33-9.

119.   Goldberg VM 2003 The biology of bone grafts. Orthopedics **26**(9):923-4.

120.   Stevenson S 1999 Biology of bone grafts. Orthop Clin North Am **30**(4):543-52.

121.   Fowler BL, Dall BE, Rowe DE 1995 Complications associated with harvesting autogenous iliac bone graft. Am J Orthop (Belle Mead NJ) **24**(12):895-903.

122.   Goulet JA, Senunas LE, DeSilva GL, Greenfield ML 1997 Autogenous iliac crest bone graft. Complications and functional assessment. Clin Orthop Relat Res (339):76-81.

123.   Rutten S, Nolte PA, Korstjens CM, van Duin MA, Klein-Nulend J 2008 Low-intensity pulsed ultrasound increases bone volume, osteoid thickness and mineral apposition rate in the area of fracture healing in patients with a delayed union of the osteotomized fibula. Bone **43**(2):348-54.

124.   Stein H, Lerner A 2005 How does pulsed low-intensity ultrasound enhance fracture healing? Orthopedics **28**(10):1161-3.

125.   McAlinden MM 2002 Fracture healing using low-intensity pulsed ultrasound. CMAJ **167**(2):128; author reply 128.

126.   Romano CL, Romano D, Logoluso N 2009 Low-intensity pulsed ultrasound for the treatment of bone delayed union or nonunion: a review. Ultrasound Med Biol **35**(4):529-36.

127.   Jingushi S, Mizuno K, Matsushita T, Itoman M 2007 Low-intensity pulsed ultrasound treatment for postoperative delayed union or nonunion of long bone fractures. J Orthop Sci **12**(1):35-41.

128.   Takikawa S, Matsui N, Kokubu T, Tsunoda M, Fujioka H, Mizuno K, Azuma Y 2001 Low-intensity pulsed ultrasound initiates bone healing in rat nonunion fracture model. J Ultrasound Med **20**(3):197-205.

129.   Lavandier B, Gleizal A, Bera JC 2009 Experimental assessment of

calvarial bone defect re-ossification stimulation using low-intensity pulsed ultrasound. Ultrasound Med Biol **35**(4):585-94.

130.   Walsh WR, Langdown AJ, Auld JW, Stephens P, Yu Y, Vizesi F, Bruce WJ, Pounder N 2008 Effect of low intensity pulsed ultrasound on healing of an ulna defect filled with a bone graft substitute. J Biomed Mater Res B Appl Biomater **86**(1):74-81.

131.   Ibiwoye MO, Powell KA, Grabiner MD, Patterson TE, Sakai Y, Zborowski M, Wolfman A, Midura RJ 2004 Bone mass is preserved in a critical-sized osteotomy by low energy pulsed electromagnetic fields as quantitated by in vivo micro-computed tomography. J Orthop Res **22**(5):1086-93.

132.   Inoue N, Ohnishi I, Chen D, Deitz LW, Schwardt JD, Chao EY 2002 Effect of pulsed electromagnetic fields (PEMF) on late-phase osteotomy gap healing in a canine tibial model. J Orthop Res **20**(5):1106-14.

133.   Fredericks DC, Nepola JV, Baker JT, Abbott J, Simon B 2000 Effects of pulsed electromagnetic fields on bone healing in a rabbit tibial osteotomy model. J Orthop Trauma **14**(2):93-100.

134.   Mackenzie D, Veninga FD 2004 Reversal of delayed union of anterior cervical fusion treated with pulsed electromagnetic field stimulation: case report. South Med J **97**(5):519-24.

135.   Sharrard WJ 1990 A double-blind trial of pulsed electromagnetic fields for delayed union of tibial fractures. J Bone Joint Surg Br **72**(3):347-55.

136.   Brighton CT 1984 The semi-invasive method of treating nonunion with direct current. Orthop Clin North Am **15**(1):33-45.

137.   Schaden W, Fischer A, Sailler A 2001 Extracorporeal shock wave therapy of nonunion or delayed osseous union. Clin Orthop Relat Res (387):90-4.

138.   Davis R, Sanborn C, Nichols D, Bazett-Jones DM, Dugan EL 2010 The effects of whole body vibration on bone mineral density for a person with a spinal cord injury: a case study. Adapt Phys Activ Q **27**(1):60-72.

139.   Humphries B, Fenning A, Dugan E, Guinane J, MacRae K 2009 Whole-body vibration effects on bone mineral density in women with or without

137

resistance training. Aviat Space Environ Med **80**(12):1025-31.

140.   Totosy de Zepetnek JO, Giangregorio LM, Craven BC 2009 Whole-body vibration as potential intervention for people with low bone mineral density and osteoporosis: a review. J Rehabil Res Dev **46**(4):529-42.

141.   Ezenwa B, Burns E, Wilson C 2008 Multiple vibration intensities and frequencies for bone mineral density improvement. Conf Proc IEEE Eng Med Biol Soc **2008**:4186-9.

142.   Iwamoto J, Takeda T, Sato Y, Uzawa M 2005 Effect of whole-body vibration exercise on lumbar bone mineral density, bone turnover, and chronic back pain in post-menopausal osteoporotic women treated with alendronate. Aging Clin Exp Res **17**(2):157-63.

143.   Lythgo N, Eser P, de Groot P, Galea M 2009 Whole-body vibration dosage alters leg blood flow. Clin Physiol Funct Imaging **29**(1):53-9.

144.   Nakagami G, Sanada H, Matsui N, Kitagawa A, Yokogawa H, Sekiya N, Ichioka S, Sugama J, Shibata M 2007 Effect of vibration on skin blood flow in an in vivo microcirculatory model. Biosci Trends **1**(3):161-6.

145.   Kerschan-Schindl K, Grampp S, Henk C, Resch H, Preisinger E, Fialka-Moser V, Imhof H 2001 Whole-body vibration exercise leads to alterations in muscle blood volume. Clin Physiol **21**(3):377-82.

146.   Stewart JM, Karman C, Montgomery LD, McLeod KJ 2005 Plantar vibration improves leg fluid flow in perimenopausal women. Am J Physiol Regul Integr Comp Physiol **288**(3):R623-9.

147.   Roelants M, Verschueren SM, Delecluse C, Levin O, Stijnen V 2006 Whole-body-vibration-induced increase in leg muscle activity during different squat exercises. J Strength Cond Res **20**(1):124-9.

148.   Rietschel E, van Koningsbruggen S, Fricke O, Semler O, Schoenau E 2008 Whole body vibration: a new therapeutic approach to improve muscle function in cystic fibrosis? Int J Rehabil Res **31**(3):253-6.

149.   Kawanabe K, Kawashima A, Sashimoto I, Takeda T, Sato Y, Iwamoto J 2007 Effect of whole-body vibration exercise and muscle strengthening, balance, and

walking exercises on walking ability in the elderly. Keio J Med **56**(1):28-33.

150.   Feltham MG, van Dieen JH, Coppieters MW, Hodges PW 2006 Changes in joint stability with muscle contraction measured from transmission of mechanical vibration. J Biomech **39**(15):2850-6.

151.   Cormie P, Deane RS, Triplett NT, McBride JM 2006 Acute effects of whole-body vibration on muscle activity, strength, and power. J Strength Cond Res **20**(2):257-61.

152.   Ahlborg L, Andersson C, Julin P 2006 Whole-body vibration training compared with resistance training: effect on spasticity, muscle strength and motor performance in adults with cerebral palsy. J Rehabil Med **38**(5):302-8.

153.   Luo J, McNamara B, Moran K 2005 The use of vibration training to enhance muscle strength and power. Sports Med **35**(1):23-41.

154.   Von Stengel S, Kemmler W, Engelke K, Kalender WA 2010 Effect of whole-body vibration on neuromuscular performance and body composition for females 65 years and older: a randomized-controlled trial. Scand J Med Sci Sports.

155.   Pujari AN, Neilson RD, Cardinale M 2009 A novel vibration device for neuromuscular stimulation for sports and rehabilitation applications. Conf Proc IEEE Eng Med Biol Soc **2009**:839-44.

156.   Marin PJ, Bunker D, Rhea MR, Ayllon FN 2009 Neuromuscular activity during whole-body vibration of different amplitudes and footwear conditions: implications for prescription of vibratory stimulation. J Strength Cond Res **23**(8):2311-6.

157.   Furness TP, Maschette WE 2009 Influence of whole body vibration platform frequency on neuromuscular performance of community-dwelling older adults. J Strength Cond Res **23**(5):1508-13.

158.   Luo J, Clarke M, McNamara B, Moran K 2009 Influence of resistance load on neuromuscular response to vibration training. J Strength Cond Res **23**(2):420-6.

159.   Luo J, McNamara B, Moran K 2008 Effect of vibration training on neuromuscular output with ballistic knee extensions. J Sports Sci **26**(12):1365-73.

160.   Abercromby AF, Amonette WE, Layne CS, McFarlin BK, Hinman MR, Paloski WH 2007 Variation in neuromuscular responses during acute whole-body vibration exercise. Med Sci Sports Exerc **39**(9):1642-50.

161.   Erskine J, Smillie I, Leiper J, Ball D, Cardinale M 2007 Neuromuscular and hormonal responses to a single session of whole body vibration exercise in healthy young men. Clin Physiol Funct Imaging **27**(4):242-8.

162.   Gosselink KL, Roy RR, Zhong H, Grindeland RE, Bigbee AJ, Edgerton VR 2004 Vibration-induced activation of muscle afferents modulates bioassayable growth hormone release. J Appl Physiol **96**(6):2097-102.

163.   Stein H, D'Ambrosia R 2008 Wolff's law decoded. Orthopedics **31**(3):213.

164.   Mullender MG, Huiskes R 1995 Proposal for the regulatory mechanism of Wolff's law. J Orthop Res **13**(4):503-12.

165.   Greer RB, 3rd 1993 Wolff's Law. Orthop Rev **22**(10):1087-8.

166.   Ebersbach G, Edler D, Kaufhold O, Wissel J 2008 Whole body vibration versus conventional physiotherapy to improve balance and gait in Parkinson's disease. Arch Phys Med Rehabil **89**(3):399-403.

167.   van Nes IJ, Latour H, Schils F, Meijer R, van Kuijk A, Geurts AC 2006 Long-term effects of 6-week whole-body vibration on balance recovery and activities of daily living in the postacute phase of stroke: a randomized, controlled trial. Stroke **37**(9):2331-5.

168.   Bautmans I, Van Hees E, Lemper JC, Mets T 2005 The feasibility of Whole Body Vibration in institutionalised elderly persons and its influence on muscle performance, balance and mobility: a randomised controlled trial [ISRCTN62535013]. BMC Geriatr **5**:17.

169.   Ozdurak RH, Sezgin OC, Akn S, Korkusuz F 2006 Vibration analysis of the human radius of elderly men. Clin Orthop Relat Res **443**:94-100.

170.   von Stengel S, Kemmler W, Engelke K, Kalender WA 2011 Effects of whole body vibration on bone mineral density and falls: results of the randomized controlled ELVIS study with postmenopausal women. Osteoporos Int **22**(1):317-25.

171. Ruan XY, Jin FY, Liu YL, Peng ZL, Sun YG 2008 Effects of vibration therapy on bone mineral density in postmenopausal women with osteoporosis. Chin Med J (Engl) **121**(13):1155-8.

172. Verschueren SM, Roelants M, Delecluse C, Swinnen S, Vanderschueren D, Boonen S 2004 Effect of 6-month whole body vibration training on hip density, muscle strength, and postural control in postmenopausal women: a randomized controlled pilot study. J Bone Miner Res **19**(3):352-9.

173. Wahlstrom J, Burstrom L, Hagberg M, Lundstrom R, Nilsson T 2008 Musculoskeletal symptoms among young male workers and associations with exposure to hand-arm vibration and ergonomic stressors. Int Arch Occup Environ Health **81**(5):595-602.

174. Rubin C, Turner AS, Mallinckrodt C, Jerome C, McLeod K, Bain S 2002 Mechanical strain, induced noninvasively in the high-frequency domain, is anabolic to cancellous bone, but not cortical bone. Bone **30**(3):445-52.

175. Flieger J, Karachalios T, Khaldi L, Raptou P, Lyritis G 1998 Mechanical stimulation in the form of vibration prevents postmenopausal bone loss in ovariectomized rats. Calcif Tissue Int **63**(6):510-4.

176. Rubinacci A, Marenzana M, Cavani F, Colasante F, Villa I, Willnecker J, Moro GL, Spreafico LP, Ferretti M, Guidobono F, Marotti G 2008 Ovariectomy sensitizes rat cortical bone to whole-body vibration. Calcif Tissue Int **82**(4):316-26.

177. Oxlund BS, Ortoft G, Andreassen TT, Oxlund H 2003 Low-intensity, high-frequency vibration appears to prevent the decrease in strength of the femur and tibia associated with ovariectomy of adult rats. Bone **32**(1):69-77.

178. Judex S, Lei X, Han D, Rubin C 2007 Low-magnitude mechanical signals that stimulate bone formation in the ovariectomized rat are dependent on the applied frequency but not on the strain magnitude. J Biomech **40**(6):1333-9.

179. Gilsanz V, Wren TA, Sanchez M, Dorey F, Judex S, Rubin C 2006 Low-level, high-frequency mechanical signals enhance musculoskeletal development of young women with low BMD. J Bone Miner Res **21**(9):1464-74.

180. Chow DH, Leung KS, Qin L, Leung AH, Cheung WH 2010

Low-magnitude high-frequency vibration (LMHFV) enhances bone remodeling in osteoporotic rat femoral fracture healing. J Orthop Res.

181.   Helmkamp JC, Talbott EO, Marsh GM 1984 Whole body vibration--a critical review. Am Ind Hyg Assoc J **45**(3):162-7.

182.   Zhang Q, Ericson K, Styf J 2003 Blood flow in the tibialis anterior muscle by photoplethysmography during foot-transmitted vibration. Eur J Appl Physiol **90**(5-6):464-9.

183.   Fong GH 2009 Regulation of angiogenesis by oxygen sensing mechanisms. J Mol Med **87**(6):549-60.

184.   Karamysheva AF 2008 Mechanisms of angiogenesis. Biochemistry (Mosc) **73**(7):751-62.

185.   Fong GH 2008 Mechanisms of adaptive angiogenesis to tissue hypoxia. Angiogenesis **11**(2):121-40.

186.   Carmeliet P 2000 Mechanisms of angiogenesis and arteriogenesis. Nat Med **6**(4):389-95.

187.   Risau W 1997 Mechanisms of angiogenesis. Nature **386**(6626):671-4.

188.   Bauer SM, Bauer RJ, Velazquez OC 2005 Angiogenesis, vasculogenesis, and induction of healing in chronic wounds. Vasc Endovascular Surg **39**(4):293-306.

189.   Shim WS, Ho IA, Wong PE 2007 Angiopoietin: a TIE(d) balance in tumor angiogenesis. Mol Cancer Res **5**(7):655-65.

190.   Zhu Y, Shwe Y, Du R, Chen Y, Shen FX, Young WL, Yang GY 2006 Effects of angiopoietin-1 on vascular endothelial growth factor-induced angiogenesis in the mouse brain. Acta Neurochir Suppl **96**:438-43.

191.   Giuliani N, Colla S, Morandi F, Rizzoli V 2005 Angiopoietin-1 and myeloma-induced angiogenesis. Leuk Lymphoma **46**(1):29-33.

192.   Oliner J, Min H, Leal J, Yu D, Rao S, You E, Tang X, Kim H, Meyer S, Han SJ, Hawkins N, Rosenfeld R, Davy E, Graham K, Jacobsen F, Stevenson S, Ho J, Chen Q, Hartmann T, Michaels M, Kelley M, Li L, Sitney K, Martin F, Sun JR, Zhang N, Lu J, Estrada J, Kumar R, Coxon A, Kaufman S, Pretorius J, Scully S, Cattley R, Payton M, Coats S, Nguyen L, Desilva B, Ndifor A, Hayward I, Radinsky

R, Boone T, Kendall R 2004 Suppression of angiogenesis and tumor growth by selective inhibition of angiopoietin-2. Cancer Cell **6**(5):507-16.

193.   Przybylski M 2009 A review of the current research on the role of bFGF and VEGF in angiogenesis. J Wound Care **18**(12):516-9.

194.   Liu Y, Sun L, Huan Y, Zhao H, Deng J 2006 Application of bFGF and BDNF to improve angiogenesis and cardiac function. J Surg Res **136**(1):85-91.

195.   Rak J, Kerbel RS 1997 bFGF and tumor angiogenesis--back in the limelight? Nat Med **3**(10):1083-4.

196.   Walgenbach KJ, Gratas C, Shestak KC, Becker D 1995 Ischaemia-induced expression of bFGF in normal skeletal muscle: a potential paracrine mechanism for mediating angiogenesis in ischaemic skeletal muscle. Nat Med **1**(5):453-9.

197.   Carano RA, Filvaroff EH 2003 Angiogenesis and bone repair. Drug Discov Today **8**(21):980-9.

198.   Folkman J, Shing Y 1992 Angiogenesis. J Biol Chem **267**(16):10931-4.

199.   Costa C, Incio J, Soares R 2007 Angiogenesis and chronic inflammation: cause or consequence? Angiogenesis **10**(3):149-66.

200.   Armulik A, Lindblom P, Norlin J, Betsholtz C 2009 A gain-of-function approach to analyze the role of PDGF-B in pericyte recruitment to microvessels. Journal of the Neurological Sciences **283**(1-2):289.

201.   Abramsson A, Lindblom P, Betsholtz C 2003 Endothelial and nonendothelial sources of PDGF-B regulate pericyte recruitment and influence vascular pattern formation in tumors. Journal of Clinical Investigation **112**(8):1142-51.

202.   Hammes HP, Renner O, Breier G, Lin J, Alt A, Betzholtz C, Bretzel RG 1999 Pericyte recruitment and angiogenesis are altered in heterozygous PDGF-BB knockout mice. Diabetologia **42**:A316.

203.   Wang CJ, Huang KE, Sun YC, Yang YJ, Ko JY, Weng LH, Wang FS 2010 VEGF Modulates Angiogenesis and Osteogenesis in Shockwave-Promoted Fracture Healing in Rabbits. J Surg Res.

204.   Gong ZY, Zhou SX, Gu XM, Li DC, Sun ML 2003 Effect of recombinant human basic fibroblast growth factor on angiogenesis during mandible fracture healing in rabbits. Chin J Traumatol **6**(4):242-4.

205.   Yang QL, McHugh KP, Patntirapong S, Gu XS, Wunderlich L, Hauschka PV 2008 VEGF enhancement of osteoclast survival and bone resorption involves VEGF receptor-2 signaling and beta(3)-integrin. Matrix Biology **27**(7):589-99.

206.   Kaku M, Kohno S, Kawata T, Tanne K 2003 Vegf stimulates bone remodeling by enhancing osteoclast differentiation. Journal of Dental Research **82**:403.

207.   Amano H, Suzuki K, Niida S, Yamada S 2003 Effect of VEGF on osteoclastogenesis and activation of osteoclast. Journal of Pharmacological Sciences **91**:165p.

208.   Hausman MR, Schaffler MB, Majeska RJ 2001 Prevention of fracture healing in rats by an inhibitor of angiogenesis. Bone **29**(6):560-4.

209.   Iversen N, Krustrup P, Rasmussen HN, Rasmussen UF, Saltin B, Pilegaard H 2011 Mitochondrial biogenesis and angiogenesis in skeletal muscle of the elderly. Exp Gerontol.

210.   Edelberg JM, Reed MJ 2003 Aging and angiogenesis. Front Biosci **8**:s1199-209.

211.   Francis MK, Appel S, Meyer C, Balin SJ, Balin AK, Cristofalo VJ 2004 Loss of EPC-1/PEDF expression during skin aging in vivo. J Invest Dermatol **122**(5):1096-105.

212.   Shiu YT, Weiss JA, Hoying JB, Iwamoto MN, Joung IS, Quam CT 2005 The role of mechanical stresses in angiogenesis. Crit Rev Biomed Eng **33**(5):431-510.

213.   Baker AB, Sanders JE 2000 Angiogenesis stimulated by mechanical loading. Microvasc Res **60**(2):177-81.

214.   Tomanek RJ 1994 Exercise-induced coronary angiogenesis: a review. Med Sci Sports Exerc **26**(10):1245-51.

215.   Rivilis I, Milkiewicz M, Boyd P, Goldstein J, Brown MD, Egginton S,

Hansen FM, Hudlicka O, Haas TL 2002 Differential involvement of MMP-2 and VEGF during muscle stretch- versus shear stress-induced angiogenesis. Am J Physiol Heart Circ Physiol **283**(4):H1430-8.

216.   Hansen-Smith F, Egginton S, Zhou AL, Hudlicka O 2001 Growth of arterioles precedes that of capillaries in stretch-induced angiogenesis in skeletal muscle. Microvasc Res **62**(1):1-14.

217.   Zheng W, Seftor EA, Meininger CJ, Hendrix MJ, Tomanek RJ 2001 Mechanisms of coronary angiogenesis in response to stretch: role of VEGF and TGF-beta. Am J Physiol Heart Circ Physiol **280**(2):H909-17.

218.   Muratore CS, Nguyen HT, Ziegler MM, Wilson JM 2000 Stretch-induced upregulation of VEGF gene expression in murine pulmonary culture: a role for angiogenesis in lung development. J Pediatr Surg **35**(6):906-12; discussion 912-3.

219.   Vailhe B, Ronot X, Tracqui P, Usson Y, Tranqui L 1997 In vitro angiogenesis is modulated by the mechanical properties of fibrin gels and is related to alpha(v)beta3 integrin localization. In Vitro Cell Dev Biol Anim **33**(10):763-73.

220.   Tranqui L, Tracqui P 2000 Mechanical signalling and angiogenesis. The integration of cell-extracellular matrix couplings. C R Acad Sci III **323**(1):31-47.

221.   Baum O, Da Silva-Azevedo L, Willerding G, Wockel A, Planitzer G, Gossrau R, Pries AR, Zakrzewicz A 2004 Endothelial NOS is main mediator for shear stress-dependent angiogenesis in skeletal muscle after prazosin administration. American Journal of Physiology-Heart and Circulatory Physiology **287**(5):H2300-08.

222.   Fernandes T, Hashimoto NY, Cachofeiro V, Lahera V, Krieger J, Oliveira EM 2008 Aerobic exercise training promotes angiogenesis through of angiotensin II and ACE 2 and ang-(1-7) can activates vasodilatation pathways in the skeletal muscle. Journal of Hypertension **26**:S529.

223.   Lu CY, Zhou YF, Wang HY, Huang CC, Piao LS, Yang SH, Liu SY, Wang Z 2003 [Mechanism of percutaneous myocardial laser revascularization in the treatment of experimental cardiac ischemia]. Zhonghua Yi Xue Za Zhi **83**(23):2083-6.

224.   Milkiewicz M, Brown MD, Egginton S, Hudlicka O 2001 Association

between shear stress, angiogenesis, and VEGF in skeletal muscles in vivo. Microcirculation **8**(4):229-41.

225.   Wietholt C, Roerig DL, Gordon JB, Haworth ST, Molthen RC, Clough AV 2008 Bronchial circulation angiogenesis in the rat quantified with SPECT and micro-CT. Eur J Nucl Med Mol Imaging **35**(6):1124-32.

226.   Qin L, Zhang G, Sheng H, Yeung KW, Yeung HY, Chan CW, Cheung WH, Griffith J, Chiu KH, Leung KS 2006 Multiple bioimaging modalities in evaluation of an experimental osteonecrosis induced by a combination of lipopolysaccharide and methylprednisolone. Bone **39**(4):863-71.

227.   Deshpande N, Pysz MA, Willmann JK 2010 Molecular ultrasound assessment of tumor angiogenesis. Angiogenesis **13**(2):175-88.

228.   Eisenbrey JR, Forsberg F 2010 Contrast-enhanced ultrasound for molecular imaging of angiogenesis. Eur J Nucl Med Mol Imaging **37 Suppl 1**:S138-46.

229.   Cosgrove D 2003 Angiogenesis imaging--ultrasound. Br J Radiol **76 Spec No 1**:S43-9.

230.   Forsberg F, Ro RJ, Potoczek M, Liu JB, Merritt CR, James KM, Dicker AP, Nazarian LN 2004 Assessment of angiogenesis: implications for ultrasound imaging. Ultrasonics **42**(1-9):325-30.

231.   Su MY, Cheung YC, Fruehauf JP, Yu H, Nalcioglu O, Mechetner E, Kyshtoobayeva A, Chen SC, Hsueh S, McLaren CE, Wan YL 2003 Correlation of dynamic contrast enhancement MRI parameters with microvessel density and VEGF for assessment of angiogenesis in breast cancer. J Magn Reson Imaging **18**(4):467-77.

232.   Principi M, Italiani M, Guiducci A, Aprile I, Muti M, Giulianelli G, Ottaviano P 2003 Perfusion MRI in the evaluation of the relationship between tumour growth, necrosis and angiogenesis in glioblastomas and grade 1 meningiomas. Neuroradiology **45**(4):205-11.

233.   Helbich TH, Roberts TP, Rollins MD, Shames DM, Turetschek K, Hopf HW, Muhler M, Hunt TK, Brasch RC 2002 Noninvasive assessment of wound-healing angiogenesis with contrast-enhanced MRI. Acad Radiol **9 Suppl**

1:S145-7.

234.   Tempel-Brami C, Neeman M 2002 Non-invasive analysis of rat ovarian angiogenesis by MRI. Mol Cell Endocrinol **187**(1-2):19-22.

235.   Niu G, Chen X 2009 PET Imaging of Angiogenesis. PET Clin **4**(1):17-38.

236.   Lijowski M, Caruthers S, Hu G, Zhang H, Scott MJ, Williams T, Erpelding T, Schmieder AH, Kiefer G, Gulyas G, Athey PS, Gaffney PJ, Wickline SA, Lanza GM 2009 High sensitivity: high-resolution SPECT-CT/MR molecular imaging of angiogenesis in the Vx2 model. Invest Radiol **44**(1):15-22.

237.   Goertz DE, Christopher DA, Yu JL, Kerbel RS, Burns PN, Foster FS 2000 High-frequency color flow imaging of the microcirculation. Ultrasound Med Biol **26**(1):63-71.

238.   Goertz DE, Yu JL, Kerbel RS, Burns PN, Foster FS 2003 High-frequency 3-D color-flow imaging of the microcirculation. Ultrasound Med Biol **29**(1):39-51.

239.   Griffith JF, Wang YX, Zhou H, Kwong WH, Wong WT, Sun YL, Huang Y, Yeung DK, Qin L, Ahuja AT 2010 Reduced bone perfusion in osteoporosis: likely causes in an ovariectomy rat model. Radiology **254**(3):739-46.

240.   Ding WG, Wei ZX, Liu JB 2011 Reduced local blood supply to the tibial metaphysis is associated with ovariectomy-induced osteoporosis in mice. Connect Tissue Res **52**(1):25-9.

241.   Meyer RA, Jr., Tsahakis PJ, Martin DF, Banks DM, Harrow ME, Kiebzak GM 2001 Age and ovariectomy impair both the normalization of mechanical properties and the accretion of mineral by the fracture callus in rats. J Orthop Res **19**(3):428-35.

242.   Ammann P, Bourrin S, Brunner F, Meyer JM, Clement-Lacroix P, Baron R, Gaillard M, Rizzoli R 2004 A new selective estrogen receptor modulator HMR-3339 fully corrects bone alterations induced by ovariectomy in adult rats. Bone **35**(1):153-61.

243.   Bonnarens F, Einhorn TA 1984 Production of a standard closed fracture

in laboratory animal bone. J Orthop Res **2**(1):97-101.

244.   Gembruch U, Baschat AA 1996 Demonstration of fetal coronary blood flow by color-coded and pulsed wave Doppler sonography: a possible indicator of severe compromise and impending demise in intrauterine growth retardation. Ultrasound Obstet Gynecol 7(1):10-6.

245.   Kirberger RM, van den Berg JS 1993 Pulsed wave Doppler echocardiographic evaluation of intracardiac blood flow in normal sheep. Res Vet Sci **55**(2):189-94.

246.   Tanaka K, Umesaki N 2010 Impact of three-dimensional (3D) ultrasonography and power Doppler angiography in the management of cervical cancer. Eur J Gynaecol Oncol **31**(1):10-7.

247.   Hsiao YH, Huang YL, Kuo SJ, Liang WM, Chen ST, Chen DR 2009 Characterization of benign and malignant solid breast masses in harmonic 3D power Doppler imaging. Eur J Radiol **71**(1):89-95.

248.   Kalmantis K, Papageorgiou T, Rodolakis A, Lymberopoulos E, Daskalakis G, Voulgaris Z, Antsaklis A 2007 The role of three-dimensional (3D) sonography and 3D power Doppler in the preoperative assessment of borderline ovarian tumors. Eur J Gynaecol Oncol **28**(5):381-5.

249.   Rebol J, Brkljacic B, Bumber Z, Psenicnik S, Povalej P 2007 3D power Doppler analysis of the vascularisation in tumours of the oral cavity. Ultraschall Med **28**(1):40-4.

250.   Sauvain JL, Palascak P, Bourscheid D, Chabi C, Atassi A, Bremon JM, Palascak R 2003 Value of power doppler and 3D vascular sonography as a method for diagnosis and staging of prostate cancer. Eur Urol **44**(1):21-30; discussion 30-1.

251.   Pan HA, Wu MH, Cheng YC, Li CH, Chang FM 2002 Quantification of Doppler signal in polycystic ovarian syndrome using 3D power Doppler ultrasonography. Hum Reprod **17**(9):2484.

252.   Duvall CL, Taylor WR, Weiss D, Guldberg RE 2004 Quantitative microcomputed tomography analysis of collateral vessel development after ischemic injury. Am J Physiol Heart Circ Physiol **287**(1):H302-10.

253. Gabet Y, Muller R, Regev E, Sela J, Shteyer A, Salisbury K, Chorev M, Bab I 2004 Osteogenic growth peptide modulates fracture callus structural and mechanical properties. Bone 35(1):65-73.

254. Rissanen TT, Markkanen JE, Gruchala M, Heikura T, Puranen A, Kettunen MI, Kholova I, Kauppinen RA, Achen MG, Stacker SA, Alitalo K, Yla-Herttuala S 2003 VEGF-D is the strongest angiogenic and lymphangiogenic effector among VEGFs delivered into skeletal muscle via adenoviruses. Circ Res 92(10):1098-106.

255. Geiger F, Bertram H, Berger I, Lorenz H, Wall O, Eckhardt C, Simank HG, Richter W 2005 Vascular endothelial growth factor gene-activated matrix (VEGF165-GAM) enhances osteogenesis and angiogenesis in large segmental bone defects. J Bone Miner Res 20(11):2028-35.

256. Phillips AM 2005 Overview of the fracture healing cascade. Injury 36 Suppl 3:S5-7.

257. Einhorn TA 2005 The science of fracture healing. Journal of Orthopaedic Trauma 19(10):S4-S6.

258. Giannoudis PV, Einhorn TA, Marsh D 2007 Fracture healing: the diamond concept. Injury 38 Suppl 4:S3-6.

259. Sambrook P, Cooper C 2006 Osteoporosis. Lancet 367(9527):2010-8.

260. Gruber R, Koch H, Doll BA, Tegtmeier F, Einhorn TA, Hollinger JO 2006 Fracture healing in the elderly patient. Exp Gerontol 41(11):1080-93.

261. Claes L, Eckert-Hubner K, Augat P 2002 The effect of mechanical stability on local vascularization and tissue differentiation in callus healing. J Orthop Res 20(5):1099-105.

262. Strehlow K, Werner N, Berweiler J, Link A, Dirnagl U, Priller J, Laufs K, Ghaeni L, Milosevic M, Bohm M, Nickenig G 2003 Estrogen increases bone marrow-derived endothelial progenitor cell production and diminishes neointima formation. Circulation 107(24):3059-65.

263. Rubin C, Judex S, Qin YX 2006 Low-level mechanical signals and their potential as a non-pharmacological intervention for osteoporosis. Age Ageing 35

Suppl 2:ii32-ii36.

264.   Xie LQ, Rubin C, Judex S 2008 Enhancement of the adolescent murine musculoskeletal system using low-level mechanical vibrations. Journal of Applied Physiology **104**(4):1056-1062.

265.   Rubin C, Recker R, Cullen D, Ryaby J, McCabe J, McLeod K 2004 Prevention of postmenopausal bone loss by a low-magnitude, high-frequency mechanical stimuli: a clinical trial assessing compliance, efficacy, and safety. J Bone Miner Res **19**(3):343-51.

266.   Ward K, Alsop C, Caulton J, Rubin C, Adams J, Mughal Z 2004 Low magnitude mechanical loading is osteogenic in children with disabling conditions. J Bone Miner Res **19**(3):360-9.

267.   Button C, Anderson N, Bradford C, Cotter JD, Ainslie PN 2007 The effect of multidirectional mechanical vibration on peripheral circulation of humans. Clin Physiol Funct Imaging **27**(4):211-6.

268.   Wallace AL, Draper ER, Strachan RK, McCarthy ID, Hughes SP 1994 The vascular response to fracture micromovement. Clin Orthop Relat Res (301):281-90.

269.   Kirchen ME, O'Connor KM, Gruber HE, Sweeney JR, Fras IA, Stover SJ, Sarmiento A, Marshall GJ 1995 Effects of microgravity on bone healing in a rat fibular osteotomy model. Clin Orthop Relat Res (318):231-42.

270.   Faris IB, Raptis S, Fitridge R 1997 Arterial injury in the lower limb from blunt trauma. Aust N Z J Surg **67**(1):25-30.

271.   Wootton DM, Ku DN 1999 Fluid mechanics of vascular systems, diseases, and thrombosis. Annu Rev Biomed Eng **1**:299-329.

272.   Kumar V, Chapman JR 2007 Whole blood thrombin: development of a process for intra-operative production of human thrombin. J Extra Corpor Technol **39**(1):18-23.

273.   McDonald F, Pitt Ford TR 1993 Blood flow changes in the tibia during external loading. J Orthop Res **11**(1):36-48.

274.   Cardinale M, Wakeling J 2005 Whole body vibration exercise: are

vibrations good for you? Br J Sports Med **39**(9):585-9.

275.   Greenstein D, Kester RC 1992 Acute vibration--its effect on digital blood flow by central and local mechanisms. Proc Inst Mech Eng H **206**(2):105-8.

276.   Bovenzi M, Hulshof CT 1999 An updated review of epidemiologic studies on the relationship between exposure to whole-body vibration and low back pain (1986-1997). Int Arch Occup Environ Health **72**(6):351-65.

277.   Bovenzi M, Lindsell CJ, Griffin MJ 1999 Magnitude of acute exposures to vibration and finger circulation. Scand J Work Environ Health **25**(3):278-84.

278.   Takeuchi T, Futatsuka M, Imanishi H, Yamada S 1986 Pathological changes observed in the finger biopsy of patients with vibration-induced white finger. Scand J Work Environ Health **12**(4 Spec No):280-3.

279.   Magness RR, Rosenfeld CR 1989 Local and systemic estradiol-17 beta: effects on uterine and systemic vasodilation. Am J Physiol **256**(4 Pt 1):E536-42.

280.   Miller VM, Vanhoutte PM 1990 17-Beta-Estradiol Augments Endothelium-Dependent Contractions to Arachidonic-Acid in Rabbit Aorta. American Journal of Physiology **258**(6):R1502-7.

281.   Bartelink ML, Wollersheim H, Theeuwes A, Vanduren D, Thien T 1990 Changes in Skin Blood-Flow during the Menstrual-Cycle - the Influence of the Menstrual-Cycle on the Peripheral-Circulation in Healthy Female Volunteers. Clinical Science **78**(5):527-32.

282.   Bourne T, Hillard TC, Whitehead MI, Crook D, Campbell S 1990 Oestrogens, arterial status, and postmenopausal women. Lancet **335**(8703):1470-1.

283.   Penotti M, Nencioni T, Gabrielli L, Farina M, Castiglioni E, Polvani F 1993 Blood-Flow Variations in Internal Carotid and Middle Cerebral-Arteries Induced by Postmenopausal Hormone Replacement Therapy. American Journal of Obstetrics and Gynecology **169**(5):1226-32.

284.   Manhem K, Brandin L, Ghanoum B, Rosengren A, Gustafsson H 2003 Acute effects of transdermal estrogen on hemodynamic and vascular reactivity in elderly postmenopausal healthy women. J Hypertens **21**(2):387-94.

285.   Gilligan DM, Badar DM, Panza JA, Quyyumi AA, Cannon RO, 3rd

1994 Acute vascular effects of estrogen in postmenopausal women. Circulation **90**(2):786-91.

286.   Hillard TC, Crayford TB, Bourne TH, Collins WP, Whitehead MI, Campbell S 1992 Differential-Effects of Transdermal Estradiol and Sequential Progestogens on Impedance to Flow within the Uterine Arteries of Postmenopausal Women. Fertility and Sterility **58**(5):959-63.

287.   Pirhonen JP, Vuento MH, Makinen JI, Salmi TA 1993 Long-term effects of hormone replacement therapy on the uterus and on uterine circulation. Am J Obstet Gynecol **168**(2):620-30.

288.   Reis SE, Gloth ST, Blumenthal RS, Resar JR, Zacur HA, Gerstenblith G, Brinker JA 1994 Ethinyl estradiol acutely attenuates abnormal coronary vasomotor responses to acetylcholine in postmenopausal women. Circulation **89**(1):52-60.

289.   Reis SE 1994 Oestrogens attenuate abnormal coronary vasoreactivity in postmenopausal women. Ann Med **26**(6):387-8.

290.   Krejza J, Mariak Z, Huba M, Wolczynski S, Lewko J 2001 Effect of endogenous estrogen on blood flow through carotid arteries. Stroke **32**(1):30-6.

291.   Woodward M, Rumley A, Tunstall-Pedoe H, Lowe GD 1999 Associations of blood rheology and interleukin-6 with cardiovascular risk factors and prevalent cardiovascular disease. Br J Haematol **104**(2):246-57.

292.   Gonzales RJ, Walker BR, Kanagy NL 2001 17beta-estradiol increases nitric oxide-dependent dilation in rat pulmonary arteries and thoracic aorta. Am J Physiol Lung Cell Mol Physiol **280**(3):L555-64.

293.   Tran CT, Leiper JM, Vallance P 2003 The DDAH/ADMA/NOS pathway. Atheroscler Suppl **4**(4):33-40.

294.   Azuma H, Sato J, Hamasaki H, Sugimoto A, Isotani E, Obayashi S 1995 Accumulation of endogenous inhibitors for nitric oxide synthesis and decreased content of L-arginine in regenerated endothelial cells. Br J Pharmacol **115**(6):1001-4.

295.   Beppu M, Obayashi S, Aso T, Goto M, Azuma H 2002 Endogenous nitric oxide synthase inhibitors in endothelial cells, endothelin-1 within the vessel wall, and intimal hyperplasia in perimenopausal human uterine arteries. Journal of

Cardiovascular Pharmacology 39(2):192-200.

296.   Raines AL, Olivares-Navarrete R, Wieland M, Cochran DL, Schwartz Z, Boyan BD 2010 Regulation of angiogenesis during osseointegration by titanium surface microstructure and energy. Biomaterials 31(18):4909-17.

297.   Zeng ZH, Luo BH, Gao YJ, Su CJ, He CC, Yi JJ, Li N, Lee RM 2004 Control of vascular changes by renin-angiotensin-aldosterone system in salt-sensitive hypertension. Eur J Pharmacol 503(1-3):129-33.

298.   Wang Y, Wan C, Gilbert SR, Clemens TL 2007 Oxygen sensing and osteogenesis. Ann N Y Acad Sci 1117:1-11.

299.   Riddle RC, Khatri R, Schipani E, Clemens TL 2009 Role of hypoxia-inducible factor-1alpha in angiogenic-osteogenic coupling. J Mol Med 87(6):583-90.

300.   Dimitriou R, Tsiridis E, Giannoudis PV 2005 Current concepts of molecular aspects of bone healing. Injury-International Journal of the Care of the Injured 36(12):1392-404.

301.   Brownlow HC, Reed A, Simpson AHRW 2002 The vascularity of atrophic non-unions. Injury-International Journal of the Care of the Injured 33(2):145-50.

302.   Carvalho RS, Einhorn TA, Lehmann W, Edgar C, Al-Yamani A, Apazidis A, Pacicca D, Clemens TL, Gerstenfeld LC 2004 The role of angiogenesis in a murine tibial model of distraction osteogenesis. Bone 34(5):849-61.

303.   Zheng LW, Ma L, Cheung LK 2011 Comparison of gene expression of osteogenic factors between continuous and intermittent distraction osteogenesis in rabbit mandibular lengthening (vol 108, pg 496, 2009). Oral Surgery Oral Medicine Oral Pathology Oral Radiology and Endodontology 111(5):668.

304.   Uchida S, Sakai A, Kudo H, Otomo H, Watanuki M, Tanaka M, Nagashima M, Nakamura T 2003 Vascular endothelial growth factor is expressed along with its receptors during the healing process of bone and bone marrow after drill-hole injury in rats. Bone 32(5):491-501.

305.   Gerber HP, Vu TH, Ryan AM, Kowalski J, Werb Z, Ferrara N 1999

VEGF couples hypertrophic cartilage remodeling, ossification and angiogenesis during endochondral bone formation. Nature Medicine **5**(6):623-28.

306.   Niida S, Kaku M, Amano H, Yoshida H, Kataoka H, Nishikawa S, Tanne K, Maeda N, Nishikawa SI, Kodama H 1999 Vascular endothelial growth factor can substitute for macrophage colony-stimulating factor in the support of osteoclastic bone resorption. Journal of Experimental Medicine **190**(2):293-98.

307.   Engsig MT, Chen QT, Vu TH, Pedersen AC, Therkidsen B, Lund LR, Henriksen K, Lenhard T, Foged NT, Werb Z, Delaisse JM 2001 Matrix metalloproteinase 9 and vascular endothelial growth factor are essential for osteoclast recruitment into developing long bones (vol 151, pg 879, 2000). Journal of Cell Biology **152**(2):419.

308.   Nakagawa M, Kaneda T, Arakawa T, Morita S, Sato T, Yomada T, Hanada K, Kumegawa M, Hakeda Y 2000 Vascular endothelial growth factor (VEGF) directly enhances osteoclastic bone resorption and survival of mature osteoclasts. Febs Letters **473**(2):161-4.

309.   Zelzer E, McLean W, Ng YS, Fulkai N, Reginato AM, Lovejoy S, D'Amore PA, Olsen BR 2002 Skeletal defects in VEGF(120/120) mice reveal multiple roles for VEGF in skeletogenesis. Development **129**(8):1893-904.

310.   Maes C, Moermans K, Stockmans I, Carmeliet P, D'Amore PA, Bouillon R, Carmeliet G 2000 Impaired angiogenesis and endochondral bone formation in mice lacking the vascular endothelial growth factor isoforms VEGF164 and VEGF188. Journal of Bone and Mineral Research **15**:S173.

311.   Dawson JM, Hudlicka O 1993 Can Changes in Microcirculation Explain Capillary Growth in Skeletal-Muscle. International Journal of Experimental Pathology **74**(1):65-71.

312.   Kamiya A, Togawa T 1980 Adaptive Regulation of Wall Shear-Stress to Flow Change in the Canine Carotid-Artery. American Journal of Physiology **239**(1):H14-21.

313.   Cunningham KS, Gotlieb AI 2005 The role of shear stress in the pathogenesis of atherosclerosis. Laboratory Investigation **85**(1):9-23.

314.   Meeson A, Palmer M, Calfon M, Lang R 1996 A relationship between apoptosis and flow during programmed capillary regression is revealed by vital analysis. Development **122**(12):3929-38.

315.   Meeson AP, Argilla M, Ko K, Witte L, Lang RA 1999 VEGF deprivation-induced apoptosis is a component of programmed capillary regression. Development **126**(7):1407-15.

316.   Dejana E, Lampugnani MG, Martinez-Estrada O, Bazzoni G 2000 The molecular organization of endothelial junctions and their functional role in vascular morphogenesis and permeability. International Journal of Developmental Biology **44**(6):743-8.

317.   Dejana E, Spagnuolo R, Bazzoni G 2001 Interendothelial junctions and their role in the control of angiogenesis, vascular permeability and leukocyte transmigration. Thrombosis and Haemostasis **86**(1):308-15.

318.   Abumiya T, Sasaguri T, Taba Y, Miwa Y, Miyagi M 2002 Shear stress induces expression of vascular endothelial growth factor receptor Flk-1/KDR through the CT-rich Sp1 binding site. Arteriosclerosis Thrombosis and Vascular Biology **22**(6):907-13.

319.   Choi IH, Chung CY, Cho TJ, Yoo WJ 2002 Angiogenesis and mineralization during distraction osteogenesis. Journal of Korean Medical Science **17**(4):435-47.

320.   Pacicca DM, Patel N, Lee C, Salisbury K, Lehmann W, Carvalho R, Gerstenfeld LC, Einhorn TA 2003 Expression of angiogenic factors during distraction osteogenesis. Bone **33**(6):889-98.

321.   Wong M, Siegrist M, Goodwin K 2003 Cyclic tensile strain and cyclic hydrostatic pressure differentially regulate expression of hypertrophic markers in primary chondrocytes. Bone **33**(4):685-93.

322.   Slaaf DW, Egbrink MGAO 2002 Capillaries and flow redistribution play an important role in muscle blood flow reserve capacity. Journal Des Maladies Vasculaires **27**(2):63-7.

323.   Brown MD, Hudlicka O 2003 Modulation of physiological angiogenesis

in skeletal muscle by mechanical forces: involvement of VEGF and metalloproteinases. Angiogenesis **6**(1):1-14.

324.   Colleran PN, Wilkerson MK, Bloomfield SA, Suva LJ, Turner RT, Delp MD 2000 Alterations in skeletal perfusion with simulated microgravity: a possible mechanism for bone remodeling. Journal of Applied Physiology **89**(3):1046-54.

325.   Namkung-Matthai H, Appleyard R, Jansen J, Lin JH, Maastricht S, Swain M, Mason RS, Murrell GAC, Diwan AD, Diamond T 2001 Osteoporosis influences the early period of fracture healing in a rat osteoporotic model. Bone **28**(1):80-6.

326.   Jesmin S, Sakuma I, Hattori Y, Kitabatake A 2002 In vivo estrogen manipulations on coronary capillary network and angiogenic molecule expression in middle-aged female rats. Arteriosclerosis Thrombosis and Vascular Biology **22**(10):1591-7.

327.   Sitnick M, Foley AM, Brown M, Spangenburg EE 2006 Ovariectomy prevents the recovery of atrophied gastrocnemius skeletal muscle mass. Journal of Applied Physiology **100**(1):286-93.

328.   Amant C, Holm P, Xu SH, Tritman N, Kearney M, Losordo DW 2001 Estrogen receptor-mediated, nitric oxide-dependent modulation of the immunologic barrier function of the endothelium - Regulation of Fas ligand expression by estradiol. Circulation **104**(21):2576-81.

329.   Jesmin S, Hattori Y, Sakuma I, Liu MY, Mowa CN, Kitabatake A 2003 Estrogen deprivation and replacement modulate cerebral capillary density with vascular expression of angiogenic molecules in middle-aged female rats. Journal of Cerebral Blood Flow and Metabolism **23**(2):181-9.

330.   Lim SK, Won YJ, Lee HC, Huh KB, Park YS 1999 A PCR analysis of ER alpha and ER beta mRNA abundance in rats and the effect of ovariectomy. Journal of Bone and Mineral Research **14**(7):1189-96.

331.   Zaman G, Cheng MZ, Jessop HL, White R, Lanyon LE 2000 Mechanical strain activates estrogen response elements in bone cells. Bone **27**(2):233-39.

332.   Jessop HL, Sjoberg M, Cheng MZ, Zaman G, Wheeler-Jones CPD,

Lanyon LE 2001 Mechanical strain and estrogen activate estrogen receptor alpha in bone cells. Journal of Bone and Mineral Research **16**(6):1045-55.

333.   Saxon LK, Turner CH 2005 Estrogen receptor beta: the antimechanostat? Bone **36**(2):185-92.

334.   Kubo T, Shiga T, Hashimoto J, Yoshioka M, Honjo H, Urabe M, Kitajima I, Semba I, Hirasawa Y 1999 Osteoporosis influences the late period of fracture healing in a rat model prepared by ovariectomy and low calcium diet. Journal of Steroid Biochemistry and Molecular Biology **68**(5-6):197-202.

335.   Reed MJ, Edelberg JM 2004 Impaired angiogenesis in the aged. Sci Aging Knowledge Environ **2004**(7):pe7.

336.   Swift ME, Kleinman HK, DiPietro LA 1999 Impaired wound repair and delayed angiogenesis in aged mice. Lab Invest **79**(12):1479-87.

337.   Pilla AA, Mont MA, Nasser PR, Khan SA, Figueiredo M, Kaufman JJ, Siffert RS 1990 Non-invasive low-intensity pulsed ultrasound accelerates bone healing in the rabbit. J Orthop Trauma **4**(3):246-53.

338.   Kollmann C, Turetschek K, Mostbeck G 1998 Amplitude-coded colour Doppler sonography: physical principles and technique. Eur Radiol **8**(4):649-56.

339.   Cossi A, Cheng J, Holalkere N, Katur A, Rana A, Tornetta P 2010 Quantifying Power Doppler Ultrasound Using ImageJ 3D Color Inspector/Color Histogram. American Journal of Roentgenology **194**(5):A237.

340.   Caruso G, Lagalla R, Derchi L, Iovane A, Sanfilippo A 2000 Monitoring of fracture calluses with color Doppler sonography. J Clin Ultrasound **28**(1):20-7.

341.   Martinoli C, Derchi LE 1997 Gain setting in power Doppler US. Radiology **202**(1):284-5.

342.   Bude RO, Rubin JM, Adler RS 1994 Power versus conventional color Doppler sonography: comparison in the depiction of normal intrarenal vasculature. Radiology **192**(3):777-80.

343.   Fleischer AC 2000 Sonographic depiction of tumor vascularity and flow: from in vivo models to clinical applications. J Ultrasound Med **19**(1):55-61.

344.   Herrmann U, Grevers G, Hammersen F 1986 Reactions of the Capillary

Plexus of the Chorioallantoic Membrane to Mechanical Stimulation. International Journal of Microcirculation-Clinical and Experimental 5(1):103.

345. Behonick DJ, Xing ZQ, Lieu S, Buckley JM, Lotz JC, Marcucio RS, Werb Z, Miclau T, Colnot C 2007 Role of Matrix Metalloproteinase 13 in Both Endochondral and Intramembranous Ossification during Skeletal Regeneration. PLoS One 2(11):e1150.

346. Wei L, Kanbe K, Lee M, Wei XC, Pei M, Sun XJ, Terek R, Chen Q 2010 Stimulation of chondrocyte hypertrophy by chemokine stromal cell-derived factor 1 in the chondro-osseous junction during endochondral bone formation. Developmental Biology 341(1):236-45.

347. Semenza GL 2000 HIF-1: Using two hands to flip the angiogenic switch. Cancer and Metastasis Reviews 19(1-2):59-65.

348. Pouyssegur J, Dayan F, Mazure NM 2006 Hypoxia signalling in cancer and approaches to enforce tumour regression. Nature 441(7092):437-43.

349. Schipani E, Ryan HE, Didrickson S, Kobayashi T, Knight M, Johnson RS 2001 Hypoxia in cartilage: HIF-1 alpha is essential for chondrocyte growth arrest and survival. Genes & Development 15(21):2865-76.

350. Mackay AM, Beck SC, Murphy JM, Barry FP, Chichester CO, Pittenger MF 1998 Chondrogenic differentiation of cultured human mesenchymal stem cells from marrow. Tissue Engineering 4(4):415-28.

351. Bordenave L, Georges A, Bareille R, Conrad V, Villars F, Amedee J 2002 Human bone marrow endothelial cells: a new identified source of B-type natriuretic peptide. Peptides 23(5):935-40.

352. Mauney JR, Sjostorm S, Blumberg J, Horan R, O'Leary JP, Vunjak-Novakovic G, Volloch V, Kaplan DL 2004 Mechanical stimulation promotes osteogenic differentiation of human bone marrow stromal cells on 3-D partially demineralized bone scaffolds in vitro. Calcified Tissue International 74(5):458-68.

353. Asahara T, Bauters C, Pastore C, Kearney M, Rossow S, Bunting S, Ferrara N, Symes JF, Isner JM 1995 Local-Delivery of Vascular Endothelial Growth-Factor Accelerates Reendothelialization and Attenuates Intimal Hyperplasia

in Balloon-Injured Rat Carotid-Artery. Circulation **91**(11):2793-801.

354.	Brooke-Wavell K, Mansfield NJ 2009 Risks and benefits of whole body vibration training in older people. Age and Ageing **38**(3):254-5.

355.	Mester J, Kleinoder H, Yue Z 2006 Vibration training: benefits and risks. Journal of Biomechanics **39**(6):1056-65.

356.	Russo CR, Lauretani F, Bandinelli S, Bartali B, Cavazzini C, Guralnik JM, Ferrucci L 2003 High-frequency vibration training increases muscle power in postmenopausal women. Archives of Physical Medicine and Rehabilitation **84**(12):1854-7.

357.	Schuhfried O, Vacariu G, Rochowanski H, Serek M, Fialka-Moser V 2005 The effects of low-dosed and high-dosed low-frequency electromagnetic fields on microcirculation and skin temperature in healthy subjects. International Journal of Sports Medicine **26**(10):886-90.

358.	Zhang QX, Ericson K, Styf J 2003 Blood flow in the tibialis anterior muscle by photoplethysmography during foot-transmitted vibration. European Journal of Applied Physiology **90**(5-6):464-9.

APPENDIX

Animal license: 08-237 in DH/HA&P/8/2.1 Pt.4

香港特別行政區政府
衛 生 署
香港灣仔皇后大道東 213 號
胡忠大廈 17 及 21 樓

THE GOVERNMENT OF THE HONG KONG
SPECIAL ADMINISTRATIVE REGION
DEPARTMENT OF HEALTH,
WU CHUNG HOUSE, 17TH & 21ST FLOORS,
213 QUEEN'S ROAD EAST, WAN CHAI,
HONG KONG

本署檔號 OUR REF.: (08-237) in DH/HA&P/8/2/1 Pt.4

來函檔號 YOUR REF

電   話 TEL.   2961 8645

圖文傳真 FAX   2127 7329

15 June 2009

SUN Minghui
Department of Orthopaedics and Traumatology
The Chinese University of Hong Kong

Dear Sir/Madam,

Animals (Control of Experiments) Ordinance
Chapter 340

I refer to your application we received on 12 September 2008 and the supplementary information of 12 June 2009.   I forward herewith the following licence(s) issued under the above Ordinance :-

Form 2   :   Licence to Conduct Experiments

Your attention is drawn to regulations 4 and 5 of the Animals (Control of Experiments) Regulations as excerpted below:-

"4 Records
Every licensee shall keep up-to-date a book in the form set out as Form 6 in the Schedule in which he shall record the particulars therein indicated of all experiments performed by him

5. Returns
Every licensee shall render to the Director of Health on or before the 1st day of January each year a return in the form set out as Form 7 in the Schedule of all experiments performed by him during the preceding twelve months."
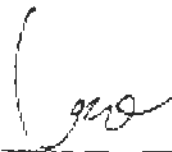
Copies of Form 6 and Form 7 are enclosed for your convenience.   Failure to comply with either regulation 4 or regulation 5 is an offence, each offence punishable by a fine of HK$500 and to imprisonment for 3 months.   Conviction of an offence against either regulation 4 or regulation 5 or failure to comply with either regulation may result in your licence being cancelled.

/P.2. .

We are committed to providing quality client-oriented service

- 2 -

Please also be reminded that if you wish to continue your experiments after the specified periods as stated on the above licence / endorsements / teaching permit, you should renew them at least two months before the end-dates   On the other hand, if you have completed or stopped your experiments before the specified periods, you should inform us immediately.

Yours sincerely,

(Dr Emily LEUNG)
for Director of Health

* *Remarks:-*

A "Code of Practice – Care and Use of Animals for Experimental Purposes" was prepared by the Agriculture, Fisheries and Conservation Department on the advice of the Animal Welfare Advisory Group.

Please visit the Agriculture, Fisheries and Conservation Department's website at <http://www.afcd.gov.hk/english/publications/publications_qua/files/code.pdf> for details of the Code of Practice.

Encl

We are committed to providing quality client-oriented service